THESIS APPROVAL

GRADUATE SCHOOL, KASETSART UNIVERSITY

Doctor of Engineering (Irrigation Engineering)

DEGREE

Irrigation Engineering — **FIELD**

Irrigation Engineering — **DEPARTMENT**

TITLE: Analysis of Land Use Change and Its Effects on Runoff and Sediment Yields in Fincha Watershed, Ethiopia

NAME: Mr Abdi Boru Ayana

THIS THESIS HAS BEEN ACCEPTED BY

______________________ **THESIS ADVISOR**

(Assistant Professor Ekasit Kositsakulchai, Dipl.Docteur)

______________________ **HEAD OF DEPARTMENT**

(Associate Professor Santi Tongpumnuk, M.Eng.)

APPROVED BY THE GRADUATE SCHOOL ON ______________________

______________________ **DEAN**

(Associate Professor Gunjana Theeragool, D.Agr.)

THESIS

ANALYSIS OF LAND USE CHANGE AND ITS EFFECTS ON RUNOFF AND SEDIMENT YIELDS IN FINCHA WATERSHED, ETHIOPIA

ABDI BORU AYANA

A Thesis Submitted in Partial Fulfillment of
the Requirement for the Degree of
Doctor of Engineering (Irrigation Engineering)
Graduate School, Kasetsart University
2012

Abdi Boru Ayana 2012: Analysis of Land Use Change and Its Effects on Runoff and Sediment Yields in Fincha Watershed, Ethiopia. Doctor of Engineering (Irrigation Engineering), Major Field: Irrigation Engineering, Department of Irrigation Engineering. Thesis Advisor: Assistant Professor Ekasit Kositsakulchai, Dipl. Docteur. 189 pages.

The land use change of Fincha watershed was analyzed using remote sensing, GIS and Markov modeling between 1985 and 2005. An attempt was also made to predict the effects of land use change and management practices on runoff and sediment yields using SWAT model. Analysis results showed that agricultural land and water bodies increased by 53.59 and 93.10%, respectively. In contrast, tremendous loss of forest, grazing and shrub lands were observed by as much as 50.48, 31.23, 51.37 and 24.81%, respectively.

SWAT model also adequately predicted runoff and sediment yields from the study watershed with R2 and ENS values ranging from 0.82 to 0.86 and 0.73 to 0.85, respectively. Simulation of various land use scenarios clearly indicated that average monthly runoff volumes and sediment yields increased between 2.24 to 17.86% and between 2.07 and 19.46%, respectively as the result of the increase under the area of agricultural land. Simulation of land management practices also showed that while runoff volumes remained almost unchanged, the average monthly sediment yields decreased between 20.82 and 24.41 t/ha due to interventions. This study demonstrated that SWAT model is capable of predicting the effects of land use change and management practices on the hydrological processes. Hence, it can be used as for land and water resources planning and management. Moreover, the use of remote sensing, GIS and Markov modeling was found to be beneficial in describing the direction, rate and spatial patterns of land use change.

________________________ ________________________ ___ / ___ / ___

Student's signature Thesis Advisor's signature

ACKNOWLEDGMENTS

First of all, I would like to thank God Almighty who has been with and for me, and who carried me through from the beginning, both during good and bad situations. He has been gracious to me and blessed me with health, audacity and wisdom. Without His aid, this work would have never come into fruition. He made my dream come true.

My sincere and special thanks go to my advisor Assistant Professor Dr. Ekasit Kositsakulchai for his continuous advice, encouragement, tremendous supervision, and guidance. Associate Professor Dr. Varawoot Vudhivanich, Dr. Chirakarn Sirivitmaitrie and Dr. Desalegn Chemeda are also thanked for their technical support. The Head of the Department, Associate Professor Santi Tongpumnak, and all the Staff of the Department of Irrigation Engineering, are thanked for the support they provided to me. I am also grateful to all PhD and Masters Degree students of the Department for their collegiality.

I would like to gratefully acknowledge the Rural Capacity Building Project, Ministry of Agriculture, for granting me full financial support for my study. Oromia Bureau of Agriculture is also thanked for giving me an opportunity to continue my study. Horro Guduru Wallaga Zone and district Agriculture Offices are also thanked for providing me important data for my research work.

My deepest gratitude go to all my family members especially to my wife, Sr. Dinke Belina; my children, Bikiltu, Bonika, and Robsan; my brothers Berhanu and Tariku; and my nieces Meti and Solane. I would also like to thank all my friends who were supporting me through their prayer and looking after my family in one way or another while I was abroad.

Last but not least, I would like to thank the staff of the Graduate Studies, International Studies Center, and the community of Kasetsart University as a whole for their help in many ways during my study.

Abdi Boru Ayana

February 2012

TABLE OF CONTENTS

LIST OF TABLES

LIST OF TABLES (Continued)

Table **Page**

Appendix Table

APPENDIX TABLES (Continued)

Appendix Table **Page**

LIST OF FIGURES

LIST OF FIGURES (Continued)

LIST OF FIGURES (Continued)

APPENDIX FIGURES (Continued)

LIST OF ABBREVIATIONS

ARDO	Agriculture and Rural Development Office
ARS	Agricultural Research Service
ASTER	Advanced Spaceborne Thermal Emission and Reflection Radiometer
DEM	Digital Elevation Model
cms	Cubic meter per second
CN	Curve Numbers
DA	Development Agents
EELPA	Ethiopian Electrical Light and Power Authority
EFAP	Ethiopian Forestry Action Program
EPCO	Plant evaporation compensation factor
ERDAS	Earth Resources Data Analysis System
ESCO	Soil evaporation compensation factor
ESRI	Environmental Systems Research Institute
ETM+	Enhanced Thematic Mapper plus
FAO	Food and Agriculture Organization
GDEM	Global Digital Elevation Model
GIS	Geographic Information System
GLF	Global Land Cover Facility
ha	Hectare
HRU	Hydrological response units
HSD	Hydrologic soil group
Km	Kilometer
LULC	Land use and land cover
m.a.s.l	Meter above sea level
mm	Millimeter
MoARD	Ministry of Agriculture and Rural Development
MoWR	Ministry of Water Resources
MSS	Multispectral Scanner
MUSLE	Modified Universal Soil Loss Equation
NGO	Non-governmental organizations

LIST OF ABBREVIATIONS (Continued)

MSS	Multispectral Scanner
MUSLE	Modified Universal Soil Loss Equation
NGO	Non-governmental organizations
NMSA	National Meteorological Service Agency
OADB	Oromia Agriculture and Development Bureau
PA	Peasant Association
PET	Potential Evapotranspiration
REVAPC	Re-evaporation coefficient for ground water
SCS	Soil Conservation Service
SPCON	Linear factor for calculating the maximum amount of sediment during channel sediment routing
SPEXP	Exponential factor for calculating the sediment in the channel sediment routing
SWAT	Soil and Water Assessment Tool
TM	Thematic Mapper
TP	Transition probabilities
USDA	United States Department of Agriculture
USGS	United States Geological Survey
USLE	Universal Soil Loss Equation
UTM	Universal Transverse Mercator Projection
WGS 84	World Geodetic System 84

ANALYSIS OF LAND USE CHANGE AND ITS EFFECTS ON RUNOFF AND SEDIMENT YIELDS IN FINCHA WATERSHED, ETHIOPIA

INTRODUCTION

Today, land use/cover change is perhaps the most prominent form of global environmental change since it occurs at spatial and temporal scales immediately relevant to our daily existence (Turner *et al*., 1995). It has been attracting increasing attention from both the environmental and socio-economic points of view. It is also one of the most important factors that have shaped the landscapes in many parts of the world (Black *et al.*, 1998; Correia, 2000; Bicik *et al.*, 2001; Burgi and Russel, 2001) and influencing the hydrological processes of a watershed. Due to anthropogenic activities, the Earth's surface is being significantly altered in some manner and man's presence on the Earth and his use of land has had a profound effect upon the natural environment thus resulting into an observable pattern in the land use/cover over time. The land use pattern of an area is directly related with the level of technological advancement and the nature and degree of civilization of its inhabitants. Land use is a dynamic phenomenon, and both its value and pattern changes with varying efficiencies, abilities, priorities, and needs (Bisht and Tiwari, 1996). This change, when coupled with climate change and variability is likely to affect natural resources and ecosystem in complex ways. It causes a multitude of environmental impacts such as changes in the hydrological balance, increase in the risk of floods and landslides, organic matter depletion, soil erosion, nutrient leaching, sedimentation, water pollution, and soil and groundwater contamination etc.

Land use and land cover change has become a central component in current strategies for managing natural resources and monitoring environmental changes. The degree and type of land cover influence the rate of infiltration and consequently the volume of runoff and sediment loads transported from a watershed. The effect of land use/cover change on the hydrological responses of a watershed is most likely where the change alters the surface characteristics of a watershed. Moreover, land use change has a direct impact on land management practices, economic health and social processes of concern at regional, national and global level (Ojima *et al*., 1994).

In the past, conversion of forest, shrub, and grass lands to agricultural land was prevalent in Ethiopia due to the lack of appropriate land use planning policy in the country. Ethiopian Forestry Action Program (EFAP, 1994) reported that over 97% of the forest cover of the country had been lost. Land is becoming a scarce resource due to immense agricultural and demographic pressure. The rapidly growing number of population, rising demand for food and agricultural land, increasing socio-economic necessities, and the short-term benefit derived from those newly opened productive forest lands created pressure on land and its resources. Bezuayehu (2006) reported that Fincha watershed is a typical example of many watersheds in the country that had undergone land use change and presently undergoing environmental degradation and causing serious problems. It is one of those highland areas of the country with severe soil erosion problem draining to the Nile River.

A study conducted by Assefa (1994) and Oromia Agriculture and Development Bureau OADB (1996) showed that after the construction of hydropower Reservoir Dam (1973) in Fincha watershed, the area has experienced a substantial land use change. Bezuayehu and Strek (2008) also reported that the backing water inundated large areas of temporarily wet lands (swamp areas), grazing, and agricultural lands. The gradual expansion of agricultural land from gently sloping land onto the steeper slopes of neighboring mountains on the one hand, and into the flat swampy plains of the plateau on the other accelerated soil erosion (Hurni, 1990). The transformation of marginal lands from forests, shrubs, and grazing lands to agricultural land is basically to fulfill the ever increasing demand for food, fuel wood, fodder, and timber.

At present, of the many resources at risk in the Ethiopian highlands including the Fincha watershed, soil and water are unarguably the most critical, as nearly 85% of the population depend on subsistence agriculture. One process that severely threatens these resources is soil erosion and its associated effects. In Fincha watershed, the majority of the watershed is under intensive cultivation of annual crops that encourage erosion. These include cultivation of cereal crops such as *teff* (Ergrotis tef) and wheat (*Triticum sativum*) which require the preparation of a fine-tilth seedbed. Erosion generated from such intensively cultivated areas had resulted to soil nutrient depletion or soil fertility reduction (Bezuayehu *et al*., 2002; Ella, 2005). The eroded sediment may also adsorb and transport agricultural contaminants such as fertilizers and pesticides posing serious threat to those living downstream. Moreover, the socio-political situation, especially insecurity of land and tree tenure has greatly discouraged farmers from investing in soil and water conservation practices (Bezuayehu, 2006). These processes combined with the lack of appropriate soil and water conservation strategies accelerated soil erosion and increased the amounts of sediment loads entering streams, rivers, reservoir, and irrigation structures.

Statement of the Problem

After the construction of hydropower Reservoir Dam (1973) in the Fincha watershed, the backing water inundated large areas of swamp, grazing, agricultural, forest, and shrub lands and caused major land use change and evicted several people from their original places**.** Consequently, the displaced farmers moved to the surrounding upland steep areas of the watershed and open up new farm lands on the expenses of marginal forest land, shrub land, and grasslands that had brought about fundamental changes in the land use/cover pattern of the study watershed. In 1975, Fincha valley (downstream of the Fincha Reservoir) was selected as state farm for producing food and commercial crops. Few years later the same area was again chosen for large scale plantation of sugar-cane for the newly established sugar factory. Following this pronounced forest clearance (deforestation) was observed in the area leading to land degradation.

The process of rapid land transformation has not only brought about an ecological crisis in the area but has also threatened the agricultural economy of the watershed through accelerated soil erosion, and deforestation. The watershed had gradually been encroached by agricultural activities and forests, shrubs and grazing lands have been converted to crop lands. As the result, nutrient-rich soil particles have continuously been detached and transported by erosion leading to the decline of soil fertility. Moreover, ragged topography of the area combined with poor farming system greatly contributed to the loss of huge amounts of fertile and productive soil from farm lands with multiple on-site soil erosion and off-site heavy sedimentation. This process coupled with the ever increasing number of population and climate variability caused major land use change and aggravated degradation of the area. Soil erosion and its consequent effects are the most important environmental problems in Fincha watershed and will continue to be the most severe threat to the area unless urgent measures will be taken.

Significance of the Study

In Fincha watershed land use change occurred at faster rate than expected and information about the magnitude and rate of these change, resources degradation, and loss is urgently needed. The present status of soil erosion found in Fincha watershed will lead to further degradation of the area and in the long run aggravate the poverty of farmers living in the watershed. In order to design efficient conservation strategies for the sustainable development, it is essential to know the patterns of land use change of the area over time and space and to quantify the extent to which these changes influence the hydrological processes of the watershed. In the past, the lack of decision support tools and limitations of data were the main factors that significantly hindered research and development in the study area. Moreover, the reliable estimates of the various hydrological processes of a watershed are tedious and time consuming by the use of conventional methods especially in remote and inaccessible areas like in Fincha watershed. Therefore, there is an urgent need for developing integrated watershed management plan based on hydrological simulation studies using suitable modeling techniques. Considering the hydrological behavior of the watershed and applicability of the existing models for the solutions of aforementioned problems, this study was undertaken using the Soil and Water Assessment Tool (SWAT) model, GIS, and Markov modeling.

OBJECTIVES

The main objective of this study is to analyze the land use/cover changes of the Fincha watershed, measure the rate of these changes, and relate the overall changes to the hydrological processes and physical features of the watershed.

The specific objectives of the study are:

1. To analyze the land use change of the study area from 1985 to 2005 using the technologies of satellite remote sensing, GIS, and Markov modeling;

2. To examine the applicability of the Soil and Water Assessment Tool (SWAT) model in estimating runoff and sediment yields; and

3. To predict the effects of land use change and management practices on runoff and sediment yields.

Research Questions

The objectives of this study are reflected in the following research questions:

1. What is the extent of the past and present land use/cover change in Fincha watershed over time and space?

2. How these changes have been affecting the hydrological processes of the watershed especially runoff and sediment yields?

3. Can we use information from the past to project the patterns of land use/cover change about 30 to 50 years in to the future?

Expected Outputs

Information on land use /cover of an area and possibilities for their optimal use is essential for the selection, planning, and implementation of land use schemes to meet the increasing demands for basic human needs and welfare. Analyzing land use/cover change and its impacts on the hydrological processes of a watershed is used to derive basic information for appropriate decision-making. The information obtained also assists in monitoring the dynamics of land use resulting out of changing demands of increasing population.

In general, the information obtained on the rate and extent of land use/cover change and its environmental impacts will help policy makers at local, national and international levels for designing appropriate strategies for the sustainable development of the watershed. Therefore, by looking at long and short-term rates of change and its spatial distribution, land use analysis provides a way to discriminate the role of different variables and their importance at different scales.

At watershed scale, the information obtained from this study will help the local government and private organizations for further assessment of the land and water resources degradation of the area and for designing cost-effective soil and water conservation strategies. It is also used for designing suitable strategies that can reduce the total sediment loads entering the hydropower reservoir.

At national level, the result of this study enables policy makers to formulate and implement appropriate land use and water resources management policies, design strategies for the optimum utilization and management of these precious resources in a sustainable way, and design effective and appropriate conservation strategies that can minimize the undesirable effects of future land use changes.

At international level, the information obtained from this study will help the concerned body for designing sound land and water resources management policies which are environmentally friendly. As Nile River is transboundary (because Fincha watershed is the tributary of Blue Nile River which contributes about 85% flow to the main Nile River), the result of this study enhances all national and international efforts towards the efficient, equitable and optimum utilization of the available water resource of the area on sustainable basis.

Scope of the Study

The bio-physical and climatic characteristics of a watershed are different at different scales. The scientific study of the determinants and impacts of land use change cannot be limited or confined to a single scale. Variations in explanatory variables of land use change analysis with scale follow a consistent pattern: at farm scale, mostly social and accessibility variables do influence land use, at landscape scale, topography and agro-climatic factors are the key determinants, while at regional to national scale, climatic variables as well as macro-economic and demographic factors seem to drive land use. The larger the scale of assessment, the higher is the physical and meteorological heterogeneity and the smaller the scale of assessment, the higher is the physical and meteorological homogeneity.

Changes in the uses of land occurring at various spatial levels and within various time periods are the material expressions, among others, of environmental and human dynamics and of their interactions which are mediated by land. The magnitude of land use change varies with the time period being examined as well as with the geographical area. Moreover, assessments of these changes depend on the source, the definitions of land use types, the spatial groupings, and the data sets used.

In this study, analysis was carried out at watershed scale to describe the land use change of the study area over time, measure the rate of change, and relate these changes to the hydrologic processes of the watershed.

Definition of Terms

Backflow: The backing up of water in the direction opposite to normal flow. Also referred to as backwater as in water surface profiles.

Basin: An extent or an area of land where surface water from rain converges to a single point, usually the exit of the basin. It is an area having a common outlet to which surface runoff flows.

Calibration: The process of using historical data to estimate parameters in a hydrologic forecast technique.

Digital Elevation Model (DEM): A digital model with an array of uniformly spaced elevation data in raster format.

Drainage Basin: A part of the surface of the Earth that is occupied by a drainage system, which consists of a surface or a body of impounded surface water together with all tributary surface streams and bodies of impounded surface water. A geographical area or region containing one or more drainage areas that discharge runoff to a single point.

Geographic Information system (GIS): A computer based system for the input, storage, retrieval, analysis and display of interpreted geographic data. The database is typically composed of map-like spatial representations, often called coverage or layers.

Land cover: Refers to the kinds of vegetation that blanket the Earth's surface, or the kinds of physical materials that form the surface where vegetation is absent. It implies the physical or natural state of the Earth’s surface like grass, asphalt, trees, bare ground, water, etc.

Hydrologic model: A conceptual or physical-based procedure for numerically simulating a process or processes, which occur in a watershed.

Land use: Refers to the functional roles that the land plays in human economic activities such as for agricultural, industrial, residential, recreational and other purposes. This is the manner in which human beings employ the land and its resources.

Remote sensing: The technique of obtaining information about objects through the analysis of data collected by special instruments that are not in physical contact with the objects of investigation. As such, remote sensing can be regarded as *"reconnaissance from a distance," "teledetection,"* or a form of the common adage *"look but don't touch."*

Simulation: The manipulation of a model in such a way that it operates on time or space to compress it, thus enabling one to perceive the interactions that would not otherwise be apparent because of their separation in time or space.

Surface runoff: The runoff that travels overland to the stream channel. Rain that falls on the stream channel is often lumped with this quantity.

Watershed: An area of land that contains a common set of streams and rivers that all drain toward a common watercourse or point. It is a basin-like landform defined by highpoints and ridgelines that descend into lower elevations and stream valleys. It can cover a small or large land area.

Structure of the Thesis

The organization of the thesis is as follows:

1. Chapter one contains Introduction, Statement of the Problem, Significance of the Study, Objectives, Research questions, Expected Outputs, and Scope of the Study.

2. Chapter two contains Literature Reviews which includes land use/cover change analysis, simulation of hydrological processes of a watershed using SWAT model, and effect of land use/cover changes and management practices on the hydrological processes of a watershed.

3. Chapter three contains Descriptions of the study area such as location, topography, climate, and socio economic situations; Analytical background of Markov modeling; Description of SWAT model; Input data used; methods for analyzing land use/cover change, Markovian analysis of land use/cover change process; Simulation of hydrological processes of a watershed by SWAT model; and Effects of land use change and management practices on the hydrological processes of the study watershed.

4. Chapter four contains Results and Discussions that summarizes the main findings of the research work. It is subdivided into three parts. The first part deals with Analysis of land use/cover change. The second part deals with Simulation of hydrological processes in the study watershed; and the third part deals with Effects of land use change and management practices on the hydrological processes of a watershed. It includes prediction of the hydrological processes, effects of land use changes and management practices on runoff and sediment yields.

5. Chapter five contains the conclusion and recommendation that summarizes the whole research work.

LITERATURE REVIEWS

Land Use and Land Cover Change Analysis

Land use and land cover of an area is continuously changing, both under the influence of humans and nature, resulting in various kinds of impacts on the ecosystem (Rajan *et al*., 1997a). These impacts at local, regional and global levels have the potential to major human life supporting systems. Turner *et al*. (1993) reported that the most important factor in the modification of the land cover and its conversion is the human use component rather than the natural changes. Land use and land cover changes cannot be understood without a better knowledge of the external forces that drive them and their links to human causes. Rajan *et al*. (1997b) stated that the linkages between human and biophysical causes or drivers to land management and land cover are not sufficiently understood. This arises from the complexity in dealing with the considerable variations in the land use change drivers at various levels - local, regional and global.

A study conducted by Munasinghe and Shearer (1995) showed that land clearing, agricultural intensification, and urbanization are currently the most consequential components of land use changes caused by human intervention. Agarwal *et al*. (2000) stated that on a global scale, forest, woodland, and grassland have been converted to other uses during the last three centuries in one way or another, to support and satisfy the increasing demands of the society and economy. Mustard *et al*. (2005) also reported that of the challenges facing the earth over the next century, land use and land cover changes are likely to be the most significant.

Turner *et al*. (1995) showed that land use and land cover changes have occurred primarily in response to population growth, technological advances, and economic opportunity. They are the results of natural processes such as climatic variations, volcanic eruptions, changes in river channels or the sea level, etc. However, most of the land use and land cover changes of the present and the recent past are due to human actions – i.e. to uses of land for production or settlement. More specifically, Meyer and Turner (1996) suggested that land use alters land cover in three ways: *converting* the land cover, or changing it to a qualitatively different state; *modifying* it, or quantitatively changing its condition without full conversion; and *maintaining* it in its condition against natural agents of change.

It was reported by Turner *et al*. (1995) that understanding the implication of past, present and future patterns of human land use for biodiversity and ecosystem function is increasingly important. They added that historical land use and cover change patterns are a means to evaluate the complex causes and responses in order to better project future trends of human activities and land use and land cover changes. Gete (2000) stated that if land use and land cover changes are not carried out based on scientific knowledge, the negative impacts on both the environment and the socio-economic settings are not easily measurable. Belay (2002) reported that a study of land use and land cover changes gives valuable information for analyzing the environmental impacts of human activities, climate change, and other driving forces.

Land use change and its hydrological consequences have received a considerable amount of interest in hydrology, both from the perspective of field monitoring (Stednick, 1996; Bowling *et al*., 2000) and from a modeling perspective (Fohrer *et al*., 2001; Niehoff *et al*., 2002; Binder *et al*., 2003). It was reported by Skole and Tucker (1993) that land use changes often have significant effects on the surrounding environment and consequently on the hydrological cycle. Therefore, understanding the patterns of land use changes of a watershed in relation to its driving factors provides essential information for land use planning and sustainable management of resources (Verburg *et al*., 1999).

It was stated by Lambin (2001) that the knowledge of spatial dynamics of the magnitudes of different land use types, factors driving the changes and implications of those changes are very important for managers and decision makers. Jianchu *et al*. (2005) showed that in many countries the study of land use and land cover changes have been extensively researched due to its key role in environmental goods and services. It was reported by Mesfin (1985), EFAP (1994) and Ritler (1997) that the land use studies that were carried in the past in Ethiopia emphasized to estimation of only forest cover and deforestation rates at national level. Studies of land use and land cover dynamics and its consequence impacts have not been carried out widely in the country. However, few studies showed that there has been an increase in croplands at the expenses of forest, grassland and bush lands (Solomon, 1994; Gete, 2000; Woldeamlak, 2003).

Bezuayehu (2006) reported that the factors of land use changes have been interacting in a very complicated ways, whose overall implication could be onsite soil erosion and offsite sedimentation, which in turn affects the lively hood of the community. Soil erosion, which is resulted from the combined influence of factors such as climate, topography, soil type, and land use (Molnar and Julien, 1998), is one of the most chronic environmental and economic problems of the present situation.

Meyer and Turner (1996) reported that land use changes impacts are the cause to another class of environmental changes that can be regarded as global in reach, when their occurrence in many places adds up. Deforestation, wetland drainage, and grassland degradation have all amounted to a globally significant alteration of the land cover class. They stated that large scale environmental phenomena like land degradation and desertification, biodiversity loss, habitat destruction and species transfer fall in the same category as all of them are caused by land use changes.

According to Meyer (1995) every parcel of land on the Earth's surface is unique in the cover it possesses. Land use and land cover are distinct yet closely linked characteristics of the Earth's surface. The use to which we put land could be grazing, agriculture, urban development, logging, and mining among many others. While land cover categories could be cropland, forest, wetland, pasture, roads, urban areas among others. The term land cover originally referred to the kind and state of vegetation, such as forest or grass cover but it has broadened in subsequent usage to include other things such as human structures, soil type, biodiversity, surface and ground water (Meyer, 1995).

Assefa (1994) stated that when the construction of the Fincha dam was completed in 1973, approximately 100 km^2 of the swamp area was submerged and few years later, the submerged area had increased to about 149 km^2. A study by OADB (1996) showed that the total swamp area submerged by the reservoir had increased to 431 km^2 and it is still increasing in volume, mainly due to continuous sedimentation originated from the upstream agricultural land induced by land use changes. Bezuayehu (2006) reported that significant land use changes were observed in Fincha watershed and the reservoir inundated about 100, 120, 18 and 1.2 km^2 of grazing land, swamp, crop land, and forest lands respectively. Significant differences were observed in amounts of runoff, soil loss and nutrient loss due to land use changes and types of management (Thomas *et al*., 1992). Although soil erosion is an important process influencing nutrient loss (Fu and Chen, 2000), land use change accelerates the process that resulted to the irreversible nutrient loss (Ripl, 1995).

Shifting land use patterns driven by a variety of social causes, result in land use/cover changes that affects biodiversity, water and radiation budgets, trace gas emissions and other processes that come together to affect climate and biosphere (Riebsame *et al*., 1994). Land cover can be altered by forces other than anthropogenic. Natural events such as weather, flooding, fire, climate fluctuations, and ecosystem dynamics may also initiate modifications upon land cover. Globally, land cover today is altered principally by direct human use: by agriculture and livestock raising, forest harvesting and management and urban and suburban construction and development.

Hence, in order to use land optimally, it is not only necessary to have the information on existing land use/cover but also the capability to monitor the dynamics of land use resulting out of both changing demands of increasing population and forces of nature acting to shape the landscape.

Conventional ground methods of land use mapping are labor intensive, time consuming and are done relatively infrequently. Olorunfemi (1983) stated that monitoring changes and time series analysis is quite difficult with traditional method of surveying. In recent years, satellite remote sensing techniques have been developed, which have proved to be of immense value for preparing accurate land use/cover maps and monitoring changes at regular intervals of time. In case of inaccessible region, this technique is perhaps the only method of obtaining the required data on a cost and time – effective basis.

The generation of remotely sensed data/images by various types of sensor flown aboard different platforms at varying heights above the terrain and at different times of the day and the year does not lead to a simple classification system. It is often believed that no single classification could be used with all types of imagery and all scales. To date, the most successful attempt in developing a general purpose classification scheme compatible with remote sensing data has been by Anderson *et al* (1976) which is also referred to as USGS classification scheme. Other classification schemes available for use with remotely sensed data are basically modification of the above classification scheme.

Xiaomei and Rong Qing (1999) noted that information about change is necessary for updating land cover maps and the management of natural resources. The information may be obtained by visiting sites on the ground and or extracting it from remotely sensed data. Singh (1989) stated that change detection is the process of identifying differences in the state of an object or phenomenon by observing it at different times. It is an important process in monitoring and managing natural resources and urban development because it provides quantitative analysis of the spatial distribution of the population of interest. The basis of using remote sensing data for change detection is that changes in land cover result in changes in radiance values which can be remotely sensed. Techniques to perform change detection with satellite imagery have become numerous as a result of increasing versatility in manipulating digital data and increasing computer power.

According to the study conducted by Moshen (1999), in some instances, land use/cover change may result in environmental, social and economic impacts of greater damage than benefit to the area. Therefore data on land use change are of great importance to planners in monitoring the consequences of land use change on the area. Such data are of value to resources management and agencies that plan and assess land use patterns and in modeling and predicting future changes.

Shosheng and Kutiel (1994) investigated the advantages of remote sensing techniques in relation to field surveys in providing a regional description of vegetation cover. The results of their research were used to produce four vegetation cover maps that provided new information on spatial and temporal distributions of vegetation in this area and allowed regional quantitative assessment of the vegetation cover.

Arvind *et al*. (2006) carried out a study on land use/cover mapping of Panchkula, Ambala and Yamunanger districts, Hangana State in India. They observed that the heterogeneous climate and physiographic conditions in these districts has resulted in the development of different land use/cover in these districts. An evaluation by digital analysis of satellite data indicated that the majority areas in these districts were used for agricultural purpose. The hilly regions exhibit fair development of reserved forests. It is inferred that land use/cover pattern in the area are generally controlled by agro-climatic conditions, ground water potential and a host of other factors.

A study conducted by Ehlers *et al*. (1990), Meaille and Wald (1990), Treitz *et al*. (1992), Westmoreland and Stow (1992), Harris and Ventura (1995), and Weng (2001) showed that satellite remote sensing, in conjunction with geographic information systems (GIS) has been widely applied and is recognized as a powerful and effective tool in detecting land use/cover change and it. An analysis of land use/cover changes conducted by Dimyati (1995) using the combination of MSS Landsat and land use map of Indonesia also revealed that index of land use/cover changes were evaluated by using remote sensing.

Satellite imagery has been used to monitor discrete land cover types by spectral classification or to estimate biophysical characteristics of land surfaces via linear relationships with spectral reflectances or indices (Steininger, 1996). Jensen (1996) stated that post-classification comparison and multi-date composite image change detection are the two most commonly used methods in the change detection. A study conducted by Dai *et al*. (1996), Yeh and Li (1999), and Chen *et al*. (2000) showed that the techniques of satellite remote sensing and GIS have been increasingly used to examine the spatial and temporal patterns of land use/cover change in China, especially related to urban growth. Verburg and Chen (2000) also showed that scale-dependent relationships between Chinese land uses and driving forces have also been examined using correlation and regression analyses.

Remote sensing and GIS based change detection studies have predominantly focused on providing the knowledge of how much, where, what type of land use and land cover change has occurred. Only a few models have been developed to address how and why the changes occurred. The models of land use/cover change process fall into two groups: regression-based and spatial transition-based models. The majority of research utilizes regression-based approach, which relates the locations of land use and land cover change to a set of spatially explicit variables, and uses models such as logistic (Landis, 1994; Turner *et al*., 1996; Wear *et al*., 1998), and hedonic price models (Geohegan *et al*., 1997). Spatial transition-based models often refer to cellular automaton simulation models, which allow for predicting future land development based on probabilistic estimates with Monte Carlo or other methods (Clarke *et al*., 1997; Clarke and Gaydos, 1998). One crucial limit to the development of the process models is, however, the deficiency of explicit modeling tools for change processes in the current generation of remote sensing and GIS systems. Equally important is the issue of data availability (Baker, 1989). Moreover, few studies have attempted to link satellite remote sensing and GIS to stochastic modeling methods in land use and land cover change studies, in spite of the fact that the techniques for such linkages have become mature in recent years due to advances in the technology of GIS and its integration with remote sensing.

Markov chains have been used to model changes in land use and land cover at a variety of spatial scales. Changes in land use were often separated from changes in land cover/vegetation type, in spite of similarities in method and approach. Markov analysis of vegetation types tends to focus on a small area of less than a few hectares or on a single small plot. Markov modelling of land use and land cover changes have not been substantial by the use of satellite imagery and digital image processing technique. Previous studies mostly utilize data sampled from field surveys, existing maps, or aerial photography (Drewett, 1969; Bourne, 1971; Bell, 1974; Bell and Hinojosa, 1977; Robinson, 1978; Jahan, 1986; Muller and Middleton, 1994). Data uncertainty in these studies remains relatively high, because only a certain amount of sites was sampled. The use of satellite imagery would create an opportunity for improved analysis. Moreover, the Markov models have been mostly employed for studies around a city or a slightly larger area, with a regional concentration in North America.

Land use/cover changes play a major role in the study of global change. Many studies showed that land use/cover change and human and/or natural modifications have largely resulted in deforestation, biodiversity loss, global warming and increase of natural disaster-flooding (Dwivedi *et al*., 2005; Mas *et al*., 2004; and Zhao *et al*., 2004). These environmental problems are often related to land use/cover changes. Therefore, available data on land use/cover changes can provide critical input to decision-making of environmental management and planning the future (Fan *et al*., 2007; Prenzel, 2004).

The growing population and increasing socio-economic necessities creates a pressure on land. Seto (2002) stated that the pressure on land resulted in unplanned and uncontrolled changes in land use/cover. The land use/cover alterations are generally caused by mismanagement of agricultural, urban, range and forest lands which lead to severe environmental problems such as landslides, floods etc.

Remote sensing and GIS are powerful tools to derive accurate and timely information on the spatial distribution of land use/cover changes over large areas (Carlson and Azofeifa, 1999; Guerschman, 2003; Rogana and Chen, 2004; and Zsuzsanna, 2005). Past and present studies conducted by organizations and institutions around the world have concentrated on the application of land use/cover changes. GIS provides a flexible environment for collecting, storing, displaying and analyzing digital data necessary for change detection (Demers, 2005; Wu *et al*., 2006).

Remote sensing imagery is the most important data resources of GIS. Ulbricht and Heckendorf (1998) showed that satellite imagery can be used for recognition of synoptic data of earth's surface. Campbell (2007) also showed in his study that Landsat Multispectral Scanner (MSS), Thematic Mapper (TM) and Enhanced Thematic Mapper Plus (ETM+) data have been broadly employed in studies towards the determination of land cover since 1972, the starting year of Landsat program, mainly in forest and agricultural areas. The rich archive and spectral resolution of satellite images are the most important reasons for their use.

The aim of change detection process is to recognize land use/cover on digital images that change features of interest between two or more dates (Muttitanon and Tripathi, 2005). There are many techniques developed in literature using post classification comparison, conventional image differentiation, using image ratio, image regression, and manual on-screen digitization of change principal components analysis and multi date image classification (Lu *et al*., 2005). A variety of studies have addressed that post-classification comparison was found to be the most accurate procedure and presented the advantage of indicating the nature of the changes (Mas, 1999; Yuan *et al*., 2005). In this study, change detection comparison (pixel by pixel) technique was applied to the Land use\land cover maps derived from satellite imagery.

Simulation of Runoff and Sediment Yields Using SWAT Model

Currently SWAT model is being applied worldwide successfully. Several studies showed the robustness of SWAT model in predicting sediment yields at different watershed scales. Recently, SWAT model is used worldwide and considered as a versatile model that can be used to integrate multiple environmental processes, which support more effective watershed management and the development of better informed policy decision (Gassman *et al*., 2005). The model has been widely applied for simulation of runoff, sediment yield, and total phosphorus losses from watersheds in different geographical locations, conditions and management practices (Saleh *et al*., 2000; Spruill *et al*., 2000; Santhi *et al*., 2001; Kirsch *et al*., 2002; Van Liew *et al*., 2003; White *et al*., 2004; Qi and Grunwald, 2005; White and Chaubery, 2005; Wang *et al*., 2006; Jha *et al*., 2007; Gassman *et al*., 2007; Parajuli *et al*., 2007), and extensively used across US for flow and sediment yield modeling (Arnold and Allen, 1999). But few studies have been conducted on the applicability of SWAT model in Ethiopia particularly in Nile Basin (Chekol *et al*., 2007; Tadele and Forch, 2007; Zeray *et al*., 2007).

Chu *et al.* (2004) evaluated SWAT sediment prediction from a 346 ha watershed and reported that a strong agreement was observed between yearly measured and SWAT simulated sediment load but simulation of monthly sediment loading was poor. Jha *et al.* (2007) found that the sediment loads predicted by SWAT were consistent with sediment loads measured for the Raccon River Watershed in west central Iowa, as evidenced by monthly and annual N_{SE} values of 0.78 and 0.79, respectively. Bracmort *et al.* (2006) reported satisfactory SWAT sediment simulation results for two small watersheds in Indiana. Benaman & Shoemaker (2005) found that SWAT underestimated observed load by 29% for the Cannonsville Reservoir Watershed in New York, primarily because of underestimation of surface runoff during snow melt events. Cotter *et al.* (2003) reported a calibrated NSE value of 0.48 for monthly SWAT predictions for the Moores Creek Watershed in Arkansas, while White and Chaubey (2005) reported NSE values of 0.43 to 0.76 for three Beaver Reservoir watershed sites in northeast Arkansas. Muleta and Nicklow (2005) calibrated daily SWAT sediment yield with observed sediment yield data from the Big Creek Watershed in southern Illinois and concluded that sediment fitted seems reasonable with an R^2 of 0.42.

Shimelis *et al*. (2007) applied SWAT model in order to test the performance and feasibility of the model in predicting stream flow from the Lake Tana Basin of Ethiopia. It was reported that the model accurately tracked the measured stream flows and simulated well. Xue-song *et al*., (2003) also applied the SWAT model in the Huanghe yellow river basin of China in order to examine the applicability of the model in simulating runoff volumes and sediment yields. They reported that the model successfully predicted both runoff volumes and sediment yields with coefficient of determination (R^2) and Nash Sutcliffe efficiency (N_{SE}) above 0.7. They also concluded that SWAT model is a useful tool for water resources and soil conservation planning in the study basin.

Saleh *et al*. (2000) conducted a comprehensive SWAT evaluation for the 932.5 km^2 Upper North Bosque River Watershed, north central Texas and found that predicted monthly sediment losses matched measured data well but that SWAT daily output was poor. Srinivasan *et al.* (1998) concluded that SWAT sediment accumulation predictions were satisfactory for the 279 km^2 Mill Creek Watershed, again located in north central Texas. Santhi *et al*. (2001) found that SWAT simulated sediment loads matched measured sediment loads well for two Bosque River (4,277 km^2) sub-watersheds, except in March. Arnold *et al.* (1999) compared estimated and SWAT simulated average annual sediment loads for five major Texas river basins (20,593 to 569,000 km^2) and concluded that in all the river basins, SWAT simulated sediment yields compared reasonably well with estimated sediment yields obtained from rating curves.

Behera and Panda (2006) concluded that SWAT simulated sediment yield satisfactorily throughout the entire rainy season based on comparisons with daily observed data for an agricultural watershed located in eastern India. Kaur *et al.* (2004) concluded that SWAT predicted annual sediment yields reasonably well for a test watershed in Damodar-Barakar, India, the second most seriously eroded area in the world. Tripathi *et al.* (2006) compared SWAT with observed daily sediment yield for the same watershed and found a close agreement with R^2 of 0.89 and NSE of 0.89. Hao *et al.* (2004) stated that SWAT was the first physically based watershed model validated in China's Yellow River Basin. They found that the predicted sediment loading accurately matched loads measured for the 4,623 km^2 Lushi subwatershed. Cheng *et al.* (2006) tested SWAT using sediment data collected from the Heihe River, another tributary of the Yellow River and reported that the resulting monthly NSE statistics were 0.74 and 0.76 for the calibration and validation periods, respectively.

Gikas *et al.* (2005) conducted an extensive evaluation of SWAT in Vistonis Lagoon, a mountainous agricultural watershed in northern Greece, and concluded that agreement between observed and SWAT sediment loads were acceptable. Bouraoui *et al.* (2005) evaluated SWAT for the Medjerda River Basin in northern Tunisia and reported that the predicted concentrations of suspended sediments are within an order of magnitude of corresponding measured values.

Bingner (1996) simulated runoff for 10 years for a watershed in northern Mississippi using the SWAT model and reported that it produced reasonable results in the simulation of runoff on a daily and annual basis from multiple sub-basins. Rosenthal and Hoffman (1999) successfully used SWAT and a spatial database to simulate flows, sediment, and nutrient loadings on a 9,000 km^2 watershed in central Texas. They reported that monthly stream flow rates were well predicted but the model overestimated stream flows in a few years during the spring/summer months.

Gassman *et al*. (2005) indicated that the use of SWAT model increased in USA, to support Total Maximum Daily Load analysis, studies of climate change, hydrologic processes, land use change, and water use and water quality applications. The model is also in use in many countries such as Canada, Australia, India and in the European catchments for various purposes (Fohrer and Arnold, 2005; Mapfumo *et al*., 2005; Watson *et al*., 2005; Gosian *et al*., 2005; Schmidt and Volk, 2005).

The suitability of SWAT in modeling sediment yield in the data scarce area was assessed using SWAT model by Ndomba *et al*. (2008) in Simiyu Ndagalu catchment in Tanzania. The results showed that SWAT model was adequately calibrated and verified against the field observed data. Pasricha (1999) applied SWAT model for simulating flow from Karso watershed, India, with an area of 27 km^2 and reported that the simulated and measured flows matched well.

The SWAT hydrologic subcomponents have been simulated and validated at a variety of scales. For example Arnold and Allen (1996) used measured data from three Illinois watersheds, ranging in size from 122 to 246 km^2 to successfully validate surface runoff, groundwater flow, ET, and PET. Santhi *et al*. (2001) performed extensive streamflow validations for two Texas watersheds that cover over 4,000 km^2. Arnold *et al*. (1999) evaluated streamflow and sediment yield data in the Texas Gulf basin with drainage area ranging from 2,253 to 304,260 km^2. In all these studies, the results showed that monthly streamflow rates were well predicted, but the model overestimated the flows in a few years during the spring/summer months. According to their suggestions, the overestimation may be accounted for by variable rainfall during those months.

Effects of Land Use Change on Runoff and Sediment Yields

Quantifying the effects of land use and land cover change on runoff dynamics of a river basin has been an area of interest for hydrologists in recent years. In water resources planning and management, a study of the land use changes and their effects on runoff and sediment yield patterns for a watershed is essential. Information on changing land-use within a watershed is vital for evaluating the hydrological impacts. Various studies in different countries showed that SWAT, a river basin scale model developed to quantify the impact of land management practices on water, sediment, and agricultural chemical yields, can adequately simulate the effects of land use on runoff volumes, sediment yield and stream flows.

In the earlier days, assessment of the impact of land use changes on runoff was mainly done through catchment experiments and different results had been obtained, with some even opposing the findings of the others. Langford (1976), for example, found out that there is no significant increase in runoff as a result of burning down of a stand of Eucalyptus. In contrast, after reviewing results from a number of catchment experiments, Hibbert (1967) concluded that there is clearly an increase in runoff volume due to reduction of forest cover, while he underlines on the unpredictability of the response. Bosch and Hewlett (1982) argued on Hibbert's later conclusion, giving specific figures on the changes of runoff volume due to changes in the amount of cover of different types of vegetations. On the other hand, some studies have indicated that urbanization leads to an increase in runoff. After synthesizing a number of studies, Hollis (1975) came to a conclusion that whilst small frequent floods are increased many times by urbanization, large rare floods are not significantly affected.

A study conducted by Nathaniel *et al*. (2009) in the selected Manipuai River sub watersheds with an aggregate area of 200 ha to simulate the effects of land use on runoff volumes, sediment yield, and stream flows showed that ArcSWAT adequately predicted peak flows and temporal variation of runoff volumes and sediment yields. They reported that both runoff volumes and sediment yields were increased and a decrease in stream flows was observed when 50% of the pasture area and grasslands are converted to agricultural lands. They stated that runoff was dramatically increased in volume when the whole sub-watershed is converted to agricultural land and it accounts for 39% to 45% of the annual rainfall to be lost as surface runoff.

A study conducted by Jayakrishnan *et al*. (2005) using SWAT to assess the environmental impacts of land use change on streamflow in Sondu River basin located in the western Kenya draining to Lake Victoria showed that the model successfully simulated flows and the simulated flows matched well with the measured flows. The SWAT modeling study by Zeray *et al*. (2007) aimed at quantifying the possible impacts of climate on water resources availability also reported a good result. Assessment of the spatial distribution of water resources and evaluation of the impacts of different land management practices on the hydrological response and soil erosion in the upper part of the Awash River basin in Ethiopia was conducted by Chekol *et al*. (2007). He developed nine land management scenarios to understand the effects of these changes on water quantity and sedimentation and stated that the results obtained were satisfactory.

Land use change impacts on water, sediment, solutes and nutrients can be evaluated (Slaymaker, 2003). Understanding how land use changes has influenced stream flow pattern may enable planners to formulate strategies to minimize the undesirable effects of future land-use changes. Alansi *et al*. (2009) studied the effects of land-use changes on rainfall-runoff and runoff-sediment relations and showed that land use change can be considered as one of the main reasons for increased runoff and sediment in tropical regions where the change in rainfall amount can be neglected.

The catchment experiment has since been used worldwide as a method for determining the effects of forest management practices on water yield. It has contributed considerably to our understanding of the hydrologic cycle and the effects of land use on it (Hewlett *et al*., 1979). Hibbert (1967) reviewed results from 39 catchment experiments throughout the world and made the following generalizations: 1) Reduction of forest cover increases the amount of runoff generated. 2) Establishment of forest cover on sparsely vegetated land decreases the volume of runoff. 3) Response to treatment is highly variable and, for the most part, unpredictable. From Hibbert's generalization it can be concluded that the amount of runoff that would be generated in any catchment increase with the reduction in the cover area and increasing the cover area of the catchment reduce the volume of runoff.

Soil and Water Assessment Tool (SWAT) 2005 (Neitsch *et al*., 2002; Arnold and Fohrer, 2005) was used to examine the impact of alternative management practices on water quantity and quality. The majority of conservation practices can be simulated in SWAT with straightforward parameter changes''. Many studies have used SWAT (Saleh *et al*., 2000; Vache *et al*., 2002; Shanti *et al*., 2003; Pandey *et al*., 2005; Tripathi *et al*., 2005; Arabi *et al*., 2006; Behera and Panda, 2006; Rode *et al*., 2008; Volk *et al*., 2009) to evaluate the effects of land use scenarios and management practices. Several studies have analyzed the long-term effects of structural best management practices on water quality (e.g. Kirsch *et al*., 2002; Chaplot *et al*., 2004; Bracmort *et al*., 2006).

It was reported by Dunne and Leopold (1978) that deforestations, urbanization, and other land-use activities can significantly alter the seasonal and annual distribution of stream flow within a watershed. It is likely that such changes can also affect the distribution and pattern of sedimentation (Kasai *et al*., 2005). Land use change is expected to have a greater impact on gully erosion than climate change (Walling and Fang, 2003; Valentin *et al*., 2005) which therefore represents an important sediment source in a range of environments and an effective links for transferring runoff and sediment (Poesen *et al*., 2003). It was reported that high infiltration rates under forest and an effective soil cover reduce surface runoff and erosion (Calder, 1992).

The changes from forest to agricultural land uses have had tremendous impacts. Soil erosion, which results from the combined influence of factors such as climate, topography, soil type, and land use (Molnar and Julien, 1998), is one of the most chronic environmental and economic problems of the present situation. Hillsides stripped of their protective covering of vegetation with no or less management are rapidly eroding, depositing huge amounts of silt into downstream reservoirs, streams and river valleys Bezuayehu (2006). It was also reported by Sileshi (2001) that floods are becoming more frequent and more sever leading to a number of problems such as decrease production per unit area of the land, leaching of plant nutrients, decrease water holding capacity of the soil, decrease soil depth, infiltration rate of the soil, increase sediment transport, siltation of dams, reservoirs, rivers, streams and oceans, deterioration of water quality (Lu and Higgitt, 1998; Le Bissonnais *et al*., 2001; Michael, 2004), loss of biological diversity, economic consequences/poverty and finally to social unrest and famine.

Agriculture has become so extensive in the area that it eventually led to the conversion of forest lands and grasslands into crop land. Gete (2000) reported that there has been an increase in the area of cultivated land and a decrease in the total forest cover in Denbecha, north Wello, Ethiopia, while Kebrom (2000) indicated that the shrub and forest cover had decreased as a result of settlement in Kalu, north-eastern Ethiopia. These changes have induced widespread soil erosion throughout the highlands of the country. Several studies reported the severity of soil erosion problem in the country. Hurni (1993) estimated that on average about 4.2 kg/m^2 of soil material is lost each year from the highlands of Ethiopia. Herweg and Ludi (1999) measured losses of 10.4 kg/m^2 per year on croplands at Angeni, north-western Ethiopia. Elwell (1994) also showed that the conversion of forest and bush lands to agricultural land significantly increased soil erosion and surface runoff.

Most of the knowledge on the effects of land use change on catchment runoff come from experimental catchment studies, statistical methods and hydrological modes. Yu *et al*. (2008) used fifteen experimental plots on the hills in Yingtan of Jiangxi Province, southern China to evaluate the efficiency of different land use scenarios in regulating rainwater and controlling flood. Lorup *et al*. (1998), Schreider *et al*. (2002) and Hundecha and Bardossy (2004) used hydrological models to study the effect of land use change in hydrology. They implemented trend analysis to the bias between the modeled and the observed runoff to investigate changes in the catchment runoff that might arise due to land use changes. In another approach, Wooldridge *et al*. (2001) assessed the influence of land use change on the hydrologic response of a catchment through a simple model for forest and non-forest land use classification and different climate regions. A few more attempts to implement hydrological models to investigate the impact of land use change have been reported in De Roo *et al*. (2001), Burns *et al*. (2005), Verstraeten and Prosser (2005), Siriwardena *et al*. (2006), Shi *et al*. (2007) and Podwojewski *et al*. (2008). On the other hand Lorup *et al*. (1998) used both hydrological models and statistical tests to assess long-term impacts of land use change on catchment runoff in semi-arid Zimbabwe.

Other studies have examined the effects of the land use change on rainfall-runoff and runoff sediment using statistical methods. Gallart and Llorens (2001) performed a preliminary analysis to investigate the relationships between land cover change and decrease in water flow in a sample of catchments in Spain. They concluded that, the relationships between change in forest cover and water flow decrease for these catchments were found similar to the relationships described elsewhere as experimental results. Lu *et al*. (2003) used the Spearman test to measure the association between the seasonal hydrological variables (monthly or extreme daily and sediment load) and its responses to land use changes and human activity in the year they occurred. The results showed that, most of these changes were caused by human activities such as deforestation, water use, and construction of reservoirs rather than by decadal climatic variations. The changes identified in water flow and sediment flux in both wet and dry seasons for some tributaries had significant implications with respect to flooding and water shortages. In another study by Zhao *et al*. (2004) double mass curve analysis was used to study the effect of land use change in semi-arid Zichang watershed of the Loess Plateau of China.

Many studies have been carried out to investigate effects of land use change on watershed hydrology and their impacts on rainfall-runoff and runoff-Sediment relationships under Arid and Semi-Arid condition (Wei *et al*., 2007), Mediterranean condition (Kosmas *et al*., 1997; Bellot *et al*., 2001; Taillefumier and Piegay, 2003; Wang *et al*., 2005) and continental condition (Karvonen *et al*., 1999 and Juckem *et al*., 2008), tropical and subtropical condition (Moraes *et al*., 1998; Rubiano, 2000; Giertz *et al*., 2005; Cotler and Ortega-Larrocea, 2006; Shi *et al*., 2007).

Lambin (2001) and El-Swaify (2002) showed that land use and land cover changes are the primary causes of soil degradation and by altering ecosystem affect the ability of biological systems to support human needs. It further affects the spatial distribution of water resources and overall hydrologic system of a watershed. A study conducted by Dixon *et al*. (1989) and Terry (1995) revealed that the environmental effects of land use changes comprise degradation of the upstream part of the watershed, sedimentation, and change in the downstream water quality and quantity. Land use change also has a negative effect on the forest coverage of the area which in turn resulted to loss of biodiversity.

Studies in various parts of Ethiopia have indicated that the underdevelopment of water resources caused many problems such as flooding (Sileshi, 2001) and submergence of settlement sites (Woube, 1999). It was also reported that reservoirs and water bodies are suffering from excessive sediment loads that have been caused by deforestation, soil erosion and absence of appropriate watershed management system. Dixon *et al*. (1989) reported that the increase in the volume of the Fincha Lake caused major land use changes in the area; and these changes had adverse social and environmental impacts on the communities living in the watershed.

Miller *et al.* (2002) simulated stream flow impacts with SWAT in response to historical land use changes in the 3,150 km^2 San Pedro Watershed in southern Arizona and the 1,200 km^2 Cannonsville Watershed in south central New York. Stream flows were predicted to increase in the San Pedro Watershed because of increased urban and agricultural land use, while a shift from agricultural to forest land use was predicted to result in a 4% stream flow decrease in the Cannonsville Watershed. Hernandez *et al.* (2000) further found that SWAT could accurately predict the relative impacts of hypothetical land use change in an 8.2 km^2 experimental sub-watershed within the San Pedro Watershed. Heuvelmans *et al.* (2005) also reported that SWAT produced reasonable stream flow and erosion estimates for hypothetical land use changes for the 29.2 km^2 Meerdaal and 12.1 km^2 Latem watersheds in the Flanders region of northern Belgium. Increased stream flow was predicted with SWAT for the 59.8 km^2 Aar Watershed in the German state of Hessen, in response to a grassland incentive scenario in which the grassland area increased from 20% to 41% while the extent forest coverage decreased by about 70% (Weber *et al.*, 2001).

Chen *et al*. (2004) applied a distributed hydrological model SWAT to simulate the rainfall-runoff relationship of the Suomo basin, China, under different land covers in order to evaluate the impact of land cover changes on runoff, evapotranspiration and peak flow. They found that if the land cover changed from a non-vegetation-cover to a full-forest-cover scenario, the runoff depth decreased and evaporation increased.

Pikounis *et al*. (2003) investigated the hydrological effects of land use changes in a catchment of the river Pinios in Thessaly using SWAT on a monthly time step. It was reported that of the three land use scenarios examined, the deforestation scenario resulted in the greatest modification of total monthly runoff. Tadele and Gerd (2007) investigated the effects of land use/cover dynamics and its consequent impacts on stream flow using SWAT in Hare watershed, Ethiopia and reported that the model satisfactorily predicted monthly and annual flows and concluded that it is useful to analyze the impacts of land use and land cover changes on stream flow even in basins with limited data.

Fohrer *et al*. (2001) applied the physically based hydrological model SWAT to a meso-scale catchment for the prediction of the impact of land use changes on the annual water balance and temporal runoff dynamics. It was shown that the decrease in the area of forest and grassland cover accelerated the peak flow rate thus increasing the risk of flooding. The study concluded that surface runoff was most susceptible to land use changes. SWAT is also applied to a meso-scale watershed to assess the impact of land use changes on the annual hydrological process (Santhi *et al*., 2001, Van Liew, and Garbrecht, 2003) and was reported that land use change significantly affect surface runoff.

Binh *et al*., (2010) applied SWAT model to examine changes of water and sediment yields and assess soil erosion over a 38, 739 km^2 area of the Black (Da) river basin, North of Vietnam as the result of extreme weather conditions as well as due to the impact of land use. The model was calibrated and validated in accordance with the observed daily stream flows at selected gauging stations. They reported that the predicted and observed sediment yields matched well and concluded that the result of this study are important for future further SWAT modeling studies in other regions of Vietnam.

Cao *et al*. (2008) applied the soil and water assessment tool (SWAT) model for evaluating the impacts of land use/cover change on annual water yields, groundwater flow, and quick flow in a large, heterogeneous river catchment of the Motueka River catchment in New Zealand. They developed two land use/cover scenarios and reported that the annual total water yields, quick flow and base flow decreased moderately in the two scenarios when compared with the current actual land use. The annual water balance for the pine potential land cover scenario did not differ substantially from the prehistoric scenario for the catchment as a whole.

MATERIALS AND METHODS

Description of the study area

Location

Ethiopia is located in East Africa between $3^{o}30'$ to $14^{o}50'$ N latitudes and $32^{o}42'$ to $48^{o}12'$ E longitudes (Figure 1). It has a surface area of about 1.127 million km^{2}. Based on topography and geographic location, the country is categorized into three major climatic zones: the cool zone (elevation > 2,400 masl), temperate zone (elevation between 1,500 to 2,400 masl), and hot zone (elevation < 1,500 masl).

The temperature of Ethiopia ranges from nearly freezing in the cool zone region to over 30°C in the hot zone. Annual rainfall varies from less than 100 mm in the low lands along the border with Somalia and Djibouti to 2,400 mm in the southwest high-lands. The topography of Ethiopia ranges from one of the lowest elevation in Africa (the Danakil depression, 125 meters below sea level) to very high Semien Mountains (Ras Dashen) which reaches as high as 4,620 meters above sea level (masl) and Tulu Dimtu in the Bale Mountains (4,377 masl). The main rainy season is from June to September.

The Fincha watershed is a medium sized left bank tributary of the Blue Nile Basin originating in the high plateau block of Ethiopia. It is located in Horro Guduru Wollegga Zone, Oromiya Regional State, Ethiopia, between 9° 10′ 05″ and 10° 00′ 59″ N latitude, and 37° 00′ 16″ and 37° 33′ 20″ E longitude. The drainage area of the Fincha watershed is about 3,251 km^2. The watershed is bordered on the north by the Blue Nile River (also called Abbay River in Ethiopia), on the east by the Guder River Basin, on the south by Awash River Basin, and on the west by Diddessa River Basin. The location of the Fincha watershed is shown on Figure 1.

The southern boundary of the watershed is a line of high hills separating the watershed from the Awash River Basin and extending to an elevation of 3,000 meters. The eastern boundary adjoining the Guder River Basin is low, dropping off in places into deep valley tributary to the Guder River. The boundary on the west is composed of low hills separating the watershed from that of the Angar River, which is tributary to the Didessa River. The boundary on the north is composed of low divides separating the watershed from Abbay River.

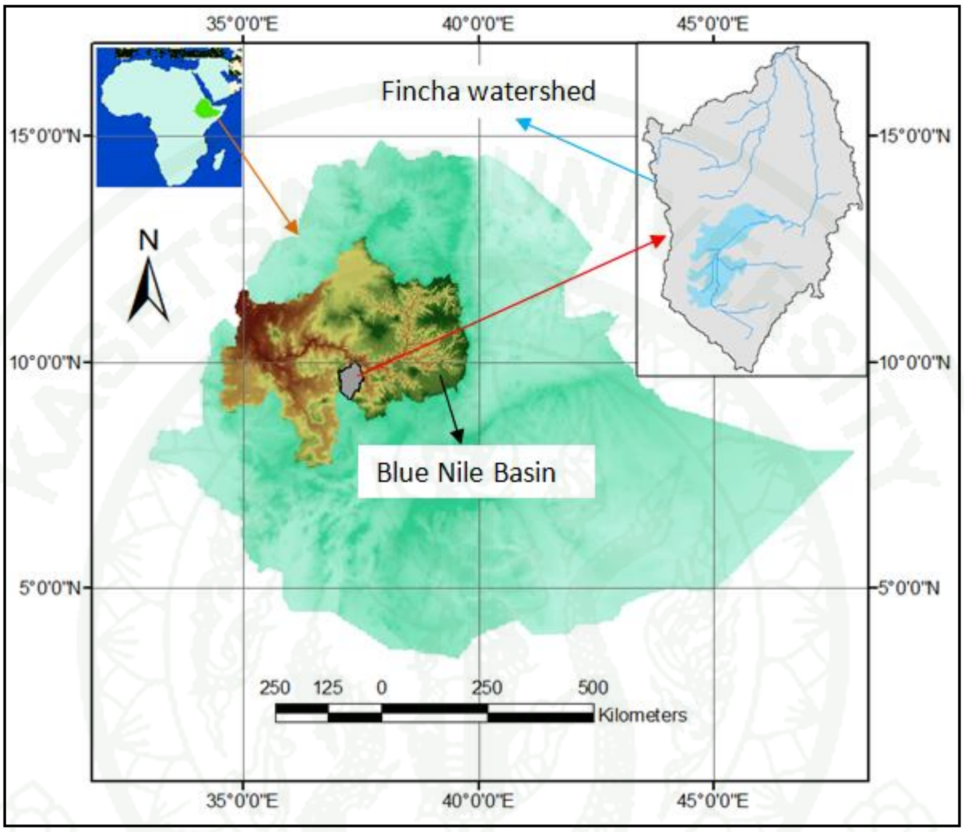

Figure 1 Location of Fincha watershed in Blue Nile Basin, Ethiopia.

Topography

The topography of the Fincha watershed signifies two distinct features: the highlands, ragged mountainous area in the upper and western part of the watershed and the lowland valley area with flat topography in the lower part of the watershed. The altitude in the watershed ranges from 1,043 meter above sea level (masl) in the lowlands up to 3,200 masl in the highlands. The major portion of the watershed area is situated between altitude ranges of 2,100 to 2,360 masl (Figure 2).

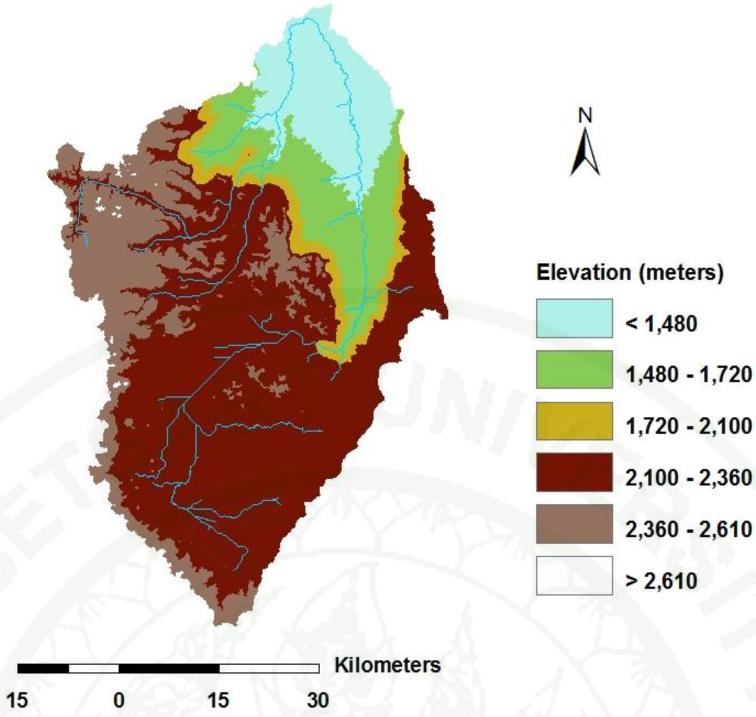

Figure 2 Topography of the study area.

The divide between the upper and lower parts of the watershed is a high escarpment over which the Fincha River plunges in a series of waterfalls in to Fincha valley. The upper part comprises the largest portion of the watershed and is on the high plateau including the Fincha Reservoir. The major land form of the upper part of the watershed includes flat, gently sloping to undulating plains, hills, mountains, highly rugged and rolled topography with steep slopes. The lower part of the watershed is an area immediately downstream of the Fincha Reservoir and is characterized by valley floor with flat to gentle slopes.

Table 1 presents the slope classes of the Fincha watershed. About 25% of the watershed area is flat (0-3% slope). Gently sloping (3-8% slope) to sloping (8-15% slope) areas cover about 50% of the watershed area, and the remaining 25% of the watershed is steep (15-30% slope) to very steep (>30% slope). The slope class range of the study watershed is shown on Figure 3.

Table 1 Slope classes of Fincha watershed.

Description	Slope range	Area (ha)	% Area
Flat	0 – 3%	81744	25.15
Gently slopping	3 – 8%	95336	29.33
Slopping	8 – 15%	67534	20.77
Steep	15 – 30%	60126	18.50
Very steep	> 30%	20336	6.26
	Total	325076	100.00

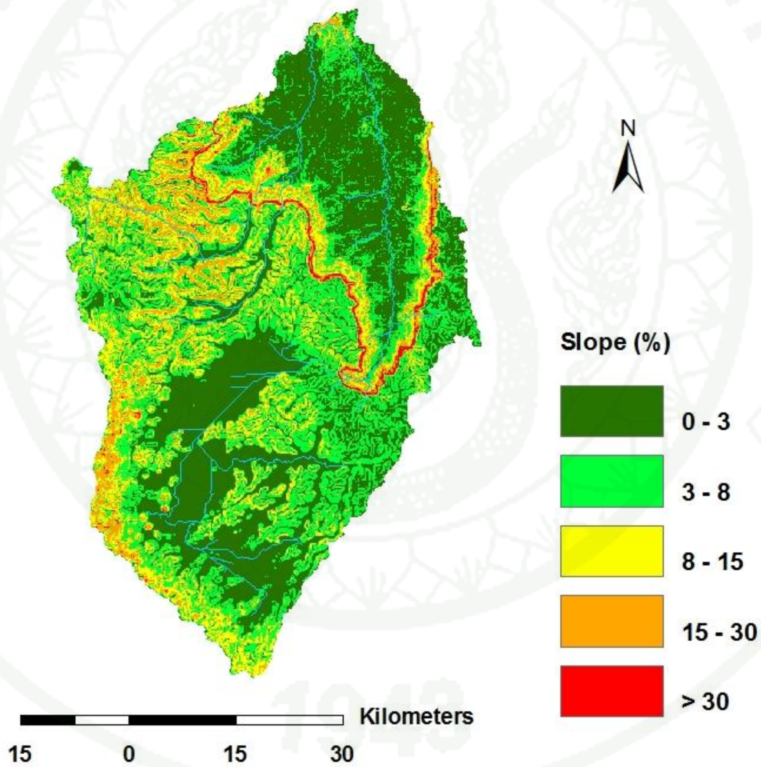

Figure 3 Slope class ranges in Fincha watershed.

Climate

The climate of the southern and western part of the Fincha watershed is typical of the highland areas, and that of the northern part is typical of the lowland areas. The mean monthly temperature of the Fincha watershed varies from 15.50°C to 18.62°C.

Temperature is higher in the northern lowlands with a maximum of 29^{0}C - 31.5^{0}C and minimum of 14^{0}C - 16^{0}C. Temperature variations from month to month are small between the warmest and the coolest average monthly temperatures.

The watershed has an average annual rainfall ranging between 960 mm and 1,835 mm. Lower annual rainfall less than 1,100 mm in the northern lowlands of the watershed and higher rainfall greater than 1,300 mm in the western and southern highlands were observed. Most of the rain falls during the months of June to September with peaks occurring during July to August and virtually dry from November through April. The average monthly rainfall and temperature of the study area are shown on Figure 4.

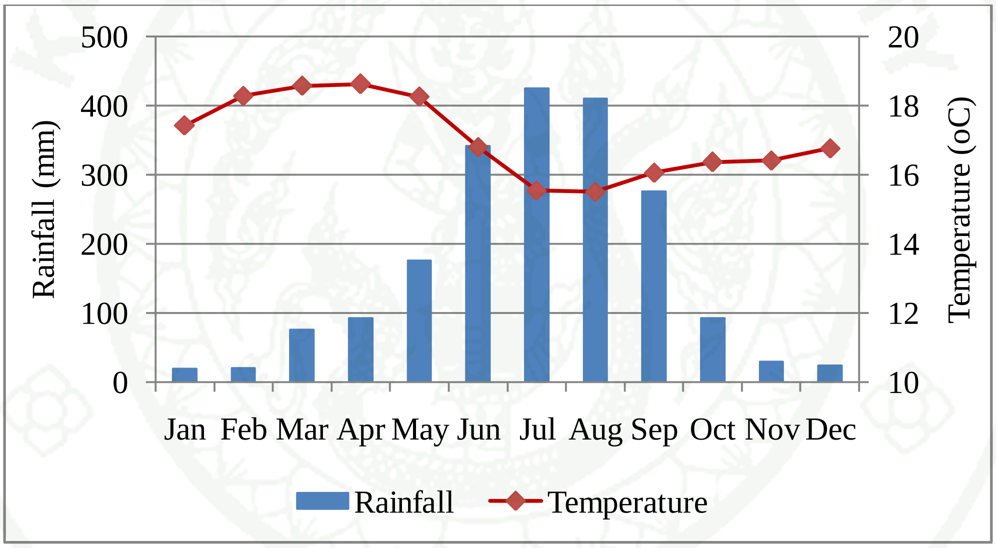

Figure 4 Average monthly rainfall and temperature of Fincha watershed.

Potential Evapotranspiration (PET) in the watershed is generally between 1,365 mm and 1,970 mm per year. PET is higher (> 1,800 mm/yr), in the lowlands of the watershed where high temperature is observed. The highlands in the southern and western parts of the watershed show lower PET (< 1,600 mm/yr).

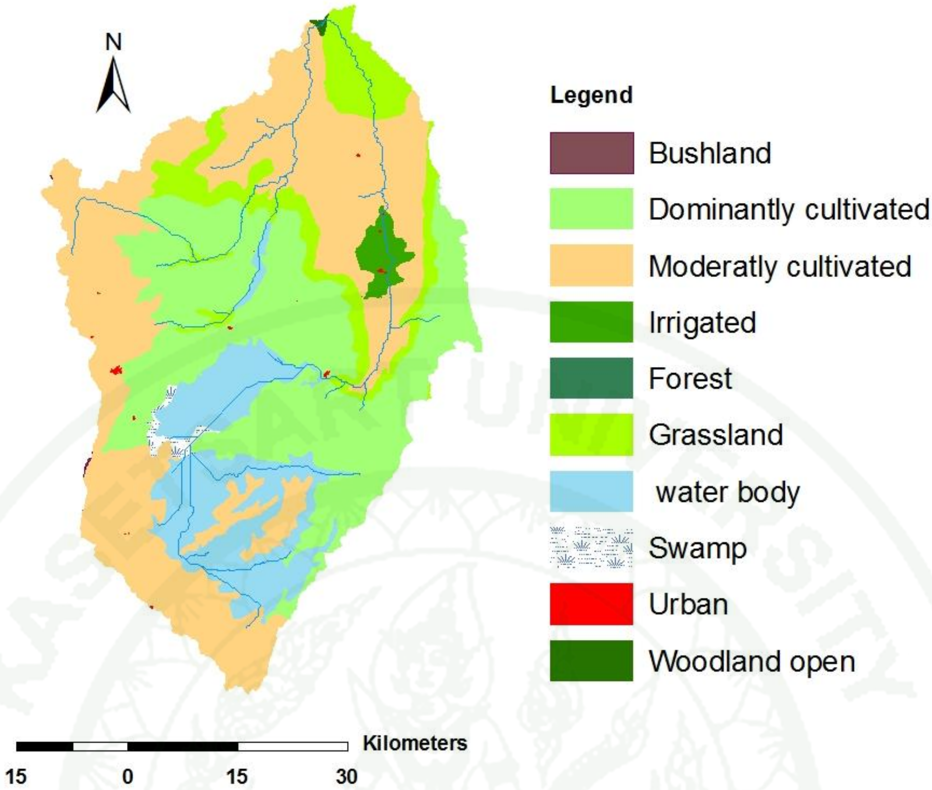

Figure 5 Major land use/cover in Fincha watershed.

Land use

The land use in Fincha watershed is dominated by cultivated and irrigated agriculture. Pastoral land is also practiced in the northern parts of the watershed. The major land use/cover types of the Fincha watershed is shown on Figure 5. Based on the Global Land Cover Facility (GLCF) land cover classification, the land use in Fincha watershed is dominated by cultivated areas and croplands particularly in the upstream highlands of the watershed. The Fincha valley (downstream of the Fincha reservoir) up to the out let of the watershed where it joins the Blue Nile River (Abbay River) is dominated by irrigated agriculture. This lowland area is typically characterized by plain area. Other land use/cover types in the study area include open forest, shrub lands, grass lands, and herbaceous cover.

Soil

The watershed has a wide range of soil types mainly dominated by Alisols, Cambisols, and Nitosols, with the occurrence of Arenosols and Luvisols. The largest portion of the watershed is characterized by clay soil commonly associated with swamps and temporary wetlands on the plain grounds with good to moderate fertility. The major soil types of the Fincha watershed are shown in Figure 6.

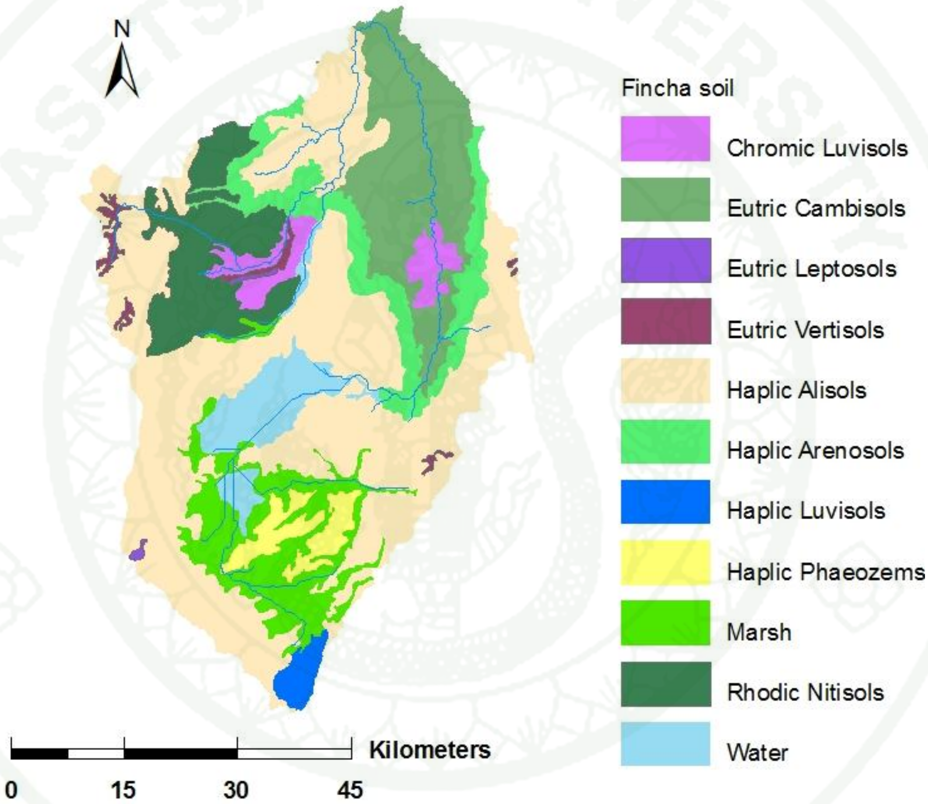

Figure 6 Major soil types in Fincha watershed.

Fincha Reservoir

In Fincha watershed there was no significant water body except stream flow before the construction of the Fincha hydro reservoir dam in 1973. Originally, it was swamp area used as grazing land and was fed by numerous streams and intermittent rivers arising from a chain of mountainous plateaus. This was evidenced from the 1957 aerial photos interpretation by Bezuayehu (2006) that showed only traces of river courses. The reservoir was created by backing water into Fincha and Chomen swamps after the construction of the Dam and the area under the water body has been increasing year after year. The interpretation of the 1980 aerial photo indicated that about 151.1 km^2 was under water body. Moreover, the volume of the reservoir also increased following the diversion of Amarti River into Fincha reservoir in 1987, which provide an annual runoff of about 138.8 Mm^3 to the reservoir (EELPA, 1994). Currently the water body covers an area of about 405 km^2.

Socio economic situation

The administrative structure of the country is hierarchical, from Regional States, to Zones, Weredas (Districts) and Peasant Associations (PA) or Kebeles. Accordingly, the watershed covers partly six districts of Horro Guduru Wollega Zone namely: Jimma Geneti, Horro, Abbay Chomen, Ababo Guduru, Guduru, and Jimmaa Rare. The total population of the Fincha watershed is about 329,265 people (CSA, 2008). Population density is about 101 people per km^2 with an average family size of eight people per household.

Since agriculture is the dominant economic sector in the country, mixed farming (integrated crop–livestock production) is the main agricultural system in the watershed. The major portion of the watershed is under intensive cultivation of annual crops and *teff*, maize, barley, wheat, bean, and Niger seed are the major crops grown in the watershed. Livestock keeping is also the major pre-occupation of the people living in the area.

Description of Models

Analytical background of Markov modeling

Markov chains have been used to model changes in land use and land cover at a variety of spatial scales. It is a convenient tool for modeling land use change when changes and processes in the landscape are difficult to describe. A Markovian process is one in which the future state of a system can be modeled purely on the basis of the immediately preceding state. Markov analysis looks at a sequence of event and analyzes the tendency of one event to be followed by another. Using this analysis we can generate a new sequence of random but related events, which appear similar to the original. Land use studies using Markov chain models involve both urban and non-urban areas (Bell and Hinojosa, 1977; Robinson, 1978; Jahan, 1986; Muller and Middleton, 1994). All of these studies use the first-order Markov chain models and stationarity has usually been assumed (Bourne, 1971; Bell, 1974).

Markov chain models have several assumptions (Stewart, 1994). One basic assumption is to regard land use and land cover change as a stochastic process, and different categories are the states of a chain. A chain is defined as a stochastic process having the property that the value of the process at time *t*, X_t, depends only on its value at time *t*-1, X_{t-1}, and not on the sequence of values X_{t-2}, X_{t-3}, . . ., X_0 that the process passed through in arriving at X_{t-1}. In this article, index *t* represents time. The process is considered discrete in time and t = {0, 5, 10 …} years approximately, which is a reasonable time unit for studying land use and land cover change phenomenon. Stochastic processes generate sequences of random variables by probabilistic laws. If the stochastic process is a Markov process then the sequence of random variables will be generated by the Markov property (Weng, 2002) as:

$$P\left\{X_t = a_j \mid X_0 = a_0, X_1 = a_1, \ldots, X_{t-1} = a_i\right\}$$
$$= P\left\{X_t = a_j \mid X_{t-1} = a_i\right\} \quad (1)$$

The $P\left\{X_t = a_j \mid X_{t-1} = a_i\right\}$, known as the one-step transitional probability, gives the probability that the process makes the transition from state a_i to state a_j in one time period. When ℓ steps are needed to implement this transition, the $P\left\{X_t = a_j \mid X_{t-1} = a_i\right\}$ is then called the ℓ-step transition probability, $P_{ij}^{(l)}$. If the $P_{ij}^{(l)}$ is independent of times and dependent only upon states a_i, a_j, and ℓ, then the Markov chain is said to be homogeneous. In this study, the treatment of Markov chains will be limited to first-order homogeneous process. A first-order process is a process where the transition from one class to any other does not require intermediate transitions to other states. In this event:

$$P\left\{X_t = a_j \mid X_{t-1} = a_i\right\} = P_{ij} \quad (2)$$

where P_{ij} can be estimated from observed data by tabulating the number of times the observed data went from state i to j, n_{ij}, and by summing the number of times that state a_i occurred, n_i. Then

$$P_{ij} = n_{ij} / n_i \tag{3}$$

Markov model also assumes that the future is independent of the past given the present. That means, as the Markov chain advances in time, the probability of being in state j after a sufficiently large number of steps becomes independent of the initial state of the chain. When this situation occurs, the chain is said to have reached a steady state. Then the limit probability, P_j, is used to determine the value of $P_{ij}^{(l)}$:

$$\lim_{n} P_{ij}^{(n)} = P_j \tag{4}$$

Where:

$P_j = P_i P_{ij}^{(n)}$ j= 1; 2, . . . m (state)

P_i =1 P_j > 0

As land use change reflects the dynamics and interplay of economic, social, and biophysical factors over time, it would be implausible to expect stationarity in land use data. However, it might be practical to regard land use change to be reasonably stationary through time. A stationary system is one in which the probabilities that govern the transitions from state to state remain constant with time. In other words, the probability of transition from some state i to another state j is the same regardless of the point in time that the transition occurs.

Soil and water assessment tool (SWAT) model

Several simulation modeling techniques are available for predicting the effects of land use/cover change and management practices on the hydrological processes of a watershed. They range from simple to complex models. However, for this study the Soil and Water Assessment Tool (SWAT) model is selected due to:

1. Its ability to characterize complex watershed representations to explicitly account for spatial variability of rainfall distribution, soils and vegetation heterogeneity;

2. Its ability to show effects of different land management practices on surface runoff and sediment yield;

3. Its ability to characterize mechanisms/processes responsible for producing surface runoff and sediment yield; and

4. It is free.

Moreover the model:

a) *Is physically based*. Rather than incorporating regression equations to describe the relationship between input and output variables, SWAT requires specific information about weather, topography, soil properties, vegetation, and land management practices occurring in the watershed. The physical processes associated with water movement, sediment movement, crop growth, nutrient cycling, etc. are directly modeled by SWAT using this input data.

b) *Uses readily available inputs*. While SWAT can be used to study more specialized processes such as bacteria transport, the minimum data required to make a run are commonly available from government agencies.

c) *Is computationally efficient*. Simulation of very large basins or a variety of management strategies can be performed without excessive investment of time or money.

d) *Enables users to study long-term impacts*. Many of the problems currently addressed by users involve the gradual buildup of pollutants and the impact on downstream water bodies. To study these types of problems, results are needed from runs with output spanning over several decades.

Description of SWAT model

SWAT, an acronym for Soil and Water Assessment Tool, is developed by the United States Department of Agriculture (USDA) Agricultural Research Service (ARS) (Arnold *et al*., 1995). It is a physically-based, conceptual, and continuous-time river basin simulation model originated from agricultural models with spatially distributed parameters operating on a daily time step. The model is used to quantify the impact of land management practices on water, sediment, and agricultural chemical yields (nutrient loss) in large complex watersheds with varying soils, land use, and management conditions over long period of time (Arnold and Fohrer, 2005; Behera and Panda, 2006; Gassman *et al.*, 2007). The computational components of SWAT can be placed into eight major divisions: hydrology, weather, sedimentation, soil, temperature, crop growth, nutrients, pesticides, and land management (Arnold *et al.*, 1998).

Within SWAT conceptual framework, simulation of the hydrology of a watershed is separated into two phases: the land phase of the hydrologic cycle which controls the amount of water, sediment, nutrient and pesticide loadings to the main channel in each subbasin; and the water or routing phase of the hydrologic cycle which simulates the movement of water, sediments, etc. through the channel network of the watershed to the outlet.

For modeling the land phase, the watershed is first divided into subbasins based on threshold area. In the second stage, each subbasin is further divided into one or several homogeneous hydrological response units (HRUs). HRU are the smallest unit representing relatively unique combinations of land use, soil, and topographic conditions in a watershed, where the vertical flows of water and nutrients are calculated individually for each subbasin, and then aggregated at the subbasin level and routed to the associated reach and to the catchment outlet through the channel network. The subdivision of the watershed into subbasins enables the model to reflect differences in evapotranspiration for various crops and soils. Runoff is predicted separately for each HRU and routed to obtain the total runoff for the watershed. This increases accuracy and gives a much better physical description of the water balance. The water balance of each HRU in the watershed is represented by several storage volumes. SWAT allows a number of different physical processes to be simulated in a watershed.

The hydrologic cycle simulated by SWAT is based on the water balance equation:

$$SW_t = SW_0 + \sum_{i=1}^{t}(R_{day} - Q_{surf} - E_a - W_{seep} - Q_{gw}) \tag{5}$$

where SW_t is the final soil water content (mm), SW_o is the initial soil water content on day i (mm), t is the time (days), R_{day} is the amount of precipitation on day i (mm), Q_{surf} is the amount of surface runoff on day i (mm), E_a is the amount of evapotranspiration on day i (mm), W_{seep} is the amount of water entering the vadose zone from the soil profile on day i (mm), and Q_{gw} is the amount of return flow on day i (mm).

SWAT incorporates the effects of weather, surface runoff, evapotranspiration, irrigation, sediment transport, groundwater flow, crop growth, nutrient loading, pesticide loading, and water routing, as well as the long term effects of varying agricultural management practices (Neitsch *et al*., 2002, 2005).

Nitrogen movement and transformation are simulated as a function of the nitrogen cycle (Neitsch *et al*., 2002; Jha *et al*., 2004). The SWAT model monitors five different pools of nitrogen in the soils: two inorganic (ammonium (NH_4^+) and nitrate (NO_3^-)) and three organic (fresh organic nitrogen (associated with crop residue and microbial biomass) and active and stable organic nitrogen (associated with the soil humus)). Plants uptake of nitrogen and phosphorus is estimated using a supply and demand approach. The demand is determined daily based on the optimal N and P crop concentration for each growth stage. For the present study, default values provided by SWAT crop database (Arnold *et al*., 1998) were used. Nitrogen is added to the soil by fertilizer, manure or residue application, fixation by bacteria, and rain (Neitsch *et al*., 2002). Nitrogen losses occur by plant uptake, surface runoff in the solution and the eroded sediment. Nitrogen and phosphorus can be lost in both particulate and dissolved forms. Additional details are given by Arnold *et al*. (1998).

Background for the crop growth and the management practices is the EPIC crop growth model, which is a comprehensive field scale model. EPIC was originally developed to simulate the impact of erosion on crop productivity and has now evolved into a comprehensive agricultural management, field scale, nonpoint source loading model (Benson *et al*., 1988; King *et al*., 1996; Neitsch *et al*., 2002). The management practices are defined by specific management operations (e.g. the beginning and end of growing season, timing of tillage operations as well as timing and amount of fertilizer, pesticide, and irrigation application). These management operations take place in every

HRU. The operations in turn are defined by specific management parameters (e.g. tillage depth, biological soil mixing efficiency, etc).

Surface runoff

Surface runoff, also called overland flow, is the flow that occurs along a slopping surface. It occurs when the soil is no longer capable of absorbing rainwater, or removing it via the processes of transpiration, infiltration, and sub-surface runoff. When water is initially applied to a dry soil, the infiltration rate is usually very high. However, it will decrease as the soil becomes wetter. When the application rate is higher than the infiltration rate, surface depressions begin to fill. If the application rate continues to be higher than the infiltration rate once all surface depressions have filled, surface runoff will commence.

SWAT provides two methods for estimating surface runoff: the SCS curve number procedure (USDA Soil Conservation Service 1972) or the Green & Ampt infiltration method (Green and Ampt, 1911). Using daily or sub-daily rainfall amounts, SWAT simulates surface runoff volumes and peak runoff rates for each HRU. In this study, surface runoff is estimated from daily rainfall using modified SCS-CN method which is defined as follows:

$$Q_{surf} = \frac{(R_{day} - I_a)^2}{(R_{day} - I_a + S)} \tag{6}$$

where Q_{surf} is the accumulated runoff or rainfall excess (mm), R_{day} is the rainfall depth for the day (mm), I_a is the initial abstractions which includes surface storage, interceptions and infiltration prior to runoff (mm), S is the retention parameter (mm). The retention parameter varies spatially due to change in soils, land use, management and slope and temporally due to changes in soil water content. The retention parameter is defined as follows:

$$S = 25.4\left(\frac{1000}{CN} - 10\right) \tag{7}$$

where CN is curve number. The initial abstractions, I_a, is commonly approximated as 0.2S. Therefore, the SCS curve number equation (6) becomes:

$$Q_{surf} = \frac{(R_{day} - 0.2S)^2}{(R_{day} + 0.8S)} \tag{8}$$

Runoff occurs only when $R_{day} > I_a$.

SCS curve number

The SCS curve number is a function of the soil's permeability, land use and antecedent soil moisture conditions. SCS defines three antecedent moisture conditions: I - dry (wilting point), II - average moisture, and III - wet (field capacity). The moisture condition I curve number is the lowest value the daily curve number can assume in dry conditions. The curve numbers for moisture conditions I and III are calculated with the equations:

$$CN_1 = CN_2 - \frac{20(100 - CN_2)}{\left(100 - CN_2 + \exp\left[2.533 - 0.0636(100 - CN_2)\right]\right)} \tag{9}$$

$$CN_3 = CN_2 \times \exp\left[0.00673(100 - CN_2)\right] \tag{10}$$

where CN_1 is the moisture condition I curve number, CN_2 is the moisture condition II curve number, and CN_3 is the moisture condition III curve number.

The typical moisture condition II curve numbers for various land covers and soil types provided in various tables (Neitsch *et al*., 2005) are assumed to be appropriate for slopes of 5%. Therefore, in order to adjust the curve number for higher slopes an equation developed by Williams (1995) was used which is defined as follows:

$$CN_{2s} = \frac{(CN_3 - CN_2)}{3}\left[1 - 2\exp(-13.86 slp)\right] + CN_2 \tag{11}$$

where CN_{2s} is the moisture condition II curve number adjusted for slope, CN_3 is the moisture condition III curve number for the default 5% slope, CN_2 is the moisture condition II curve number for the default 5% slope, and *slp* is the average fraction slope of the subbasin.

SWAT2005 version includes two methods for calculating the retention parameter: the first method is that the retention parameter varies with soil profile water content and the second method is that the retention parameter varies with accumulated plant evapotranspiration. Calculation of the daily *CN* value as a function of plant evapotranspiration was added because the soil moisture method was predicting too much runoff in shallow soils. By calculating daily *CN* as a function of plant evapotranspiration, the value is less dependent on soil storage and more dependent on antecedent climate.

When the retention parameter varies with soil profile water content, the following equation is used:

$$S = S_{\max}\left(1 - \frac{SW}{\left[SW + \exp\left(w_1 - w_2 \times SW\right)\right]}\right) \tag{12}$$

where S is the retention parameter for a given day (mm), S_{max} is the maximum value the retention parameter can achieve on any given day (mm), SW is the soil water content of the entire profile excluding the amount of water held in the profile at wilting point (mm), and w_1 and w_2 are shape coefficients. The maximum retention parameter value, S_{max}, is calculated by solving equation (7) using CN_1.

$$S_{\max} = 25.4\left(\frac{1000}{CN_1} - 10\right) \tag{13}$$

When the retention parameter varies with plant evapotranspiration, the following equation is used to update the retention parameter at the end of every day:

$$S = S_{prev} + E_o * \exp\left(\frac{-cncoef - S_{prev}}{S_{\max}}\right) - R_{day} - Q_{surf} \tag{14}$$

where S is the retention parameter for a given day (mm), S_{prev} is the retention parameter for the previous day (mm), E_o is the potential evapotranspiration for the day (mm/day), *cncoef* is the weighting coefficient used to calculate the retention coefficient for daily curve number calculations dependent on plant evapotranspiration, S_{max} is the maximum value the retention parameter can achieve on any given day (mm), R_{day} is the rainfall depth for the day (mm), and Q_{surf} is the surface runoff (mm). The initial value of the retention parameter is defined as $S = 0.9 \times S_{max}$.

Peak runoff rate

The peak runoff rate is the maximum runoff flow rate that occurs with a given rainfall event. The peak runoff rate is an indicator of the erosive power of a storm and is used to predict sediment loss. SWAT calculates the peak runoff rate with a modified rational method.

The rational method is widely used in the design of ditches, channels and storm water control systems. The rational method is based on the assumption that if a rainfall of intensity i begins at time t = 0 and continuous indefinitely, the rate of runoff will increase until the time of concentration, $t = t_{conc}$, when the entire of the subbasin is contributing to flow at the outlet simultaneously.

$$q_{peak} = \frac{C \times i \times Area}{3.6} \tag{15}$$

where q_{peak} is the peak runoff rate (m^3/s), C is the runoff coefficient, i is the rainfall intensity (mm/hr), *Area* is the subbasin area (km^2) and 3.6 is a unit conversion factor.

Time of concentration

The time of concentration is the amount of time from the beginning of a rainfall event until the entire subbasin area is contributing to flow at the outlet. In other words, the time of concentration is the time for a drop of water to flow from the remotest point in the subbasin to the subbasin outlet. It is calculated by summing the overland flow time (the time it takes for flow from the remotest point in the subbasin to reach the channel) and the channel flow time (the time it takes for flow in the upstream channels to reach the outlet):

$$t_{conc} = t_{ov} + t_{ch} \tag{16}$$

where t_{conc} is the time of concentration for the subbasin (hr), t_{ov} is the time of concentration for overland flow (hr), and t_{ch} is the time of concentration for channel flow (hr).

The overland flow time of concentration, t_{ov}, can be computed using the equation:

$$t_{ov} = \frac{L_{slp}}{3600 v_{ov}} \tag{17}$$

where L_{slp} is the subbasin slope length (m), v_{ov} is the overland flow velocity (m/s) and 3600 is a unit conversion factor.

The overland flow velocity can be estimated from Manning's equation by considering a strip of 1 meter wide down the sloping surface:

$$v_{ov} = \frac{q_{ov}^{0.4} \times slp^{0.3}}{n^{0.6}} \tag{18}$$

where q_{ov} is the average overland flow rate (m^3/s), slp is the average slope in the subbasin (m/m), and n is Manning's roughness coefficient for the subbasin. Assuming an average flow rate of 6.35 mm/hr and converting units would gives:

$$v_{ov} = \frac{0.005 L_{slp}^{0.4} \times slp^{0.3}}{n^{0.6}} \tag{19}$$

Substituting equation (19) into equation (16) gives

$$t_{ov} = \frac{L_{slp}^{0.6} \times n^{0.6}}{18 slp^{0.3}} \tag{20}$$

The channel flow time of concentration, t_{ch}, can be computed using the equation:

$$t_{ch} = \frac{L_c}{3.6 v_c} \tag{21}$$

where L_c is the average flow channel length for the subbasin (km), v_c is the average channel velocity (m/s), and 3.6 is a unit conversion factor.

The average channel flow length can be estimated using the equation:

$$L_c = \sqrt{L \times L_{cen}} \tag{22}$$

where L is the channel length from the most distant point to the subbasin outlet (km), and L_{cen} is the distance along the channel to the subbasin centroid (km). Assuming L_{cen} = 0.5L, the average channel flow length is

$$L_c = 0.71L \tag{23}$$

The average velocity can be estimated from Manning's equation assuming a trapezoidal channel with 2:1 side slopes and a 10:1 bottom width-depth ratio.

$$v_c = \frac{0.489 q_{ch}^{0.25} \times slp_{ch}^{0.375}}{n^{0.75}} \tag{24}$$

where v_c is the average channel velocity (m/s), q_{ch} is the average channel flow rate (m^3/s), slp_{ch} is the channel slope (m/m), and n is Manning's roughness coefficient for the channel. To express the average channel flow rate in units of mm/hr, the following expression is used:

$$q_{ch} = \frac{q_{ch}^{*} \times Area}{3.6} \tag{25}$$

where q_{ch}^{*} is the average channel flow rate (mm/hr), *Area* is the subbasin area (km^2), and 3.6 is a unit conversion factor. The average channel flow rate is related to the unit source area flow rate (unit source area = 1ha)

$$q_{ch}^{*} = q_0^{*} \left(100 Area\right)^{-0.5} \tag{26}$$

where q_0^{*} is the unit source area flow rate (mm/hr), *Area* is the subbasin area (km^2), and 100 is a unit conversion factor. Assuming the unit source area flow rate is 6.35 mm/hr and substituting equations (25) and (26) into equation (24) gives:

$$v_c = \frac{0.317 Area^{0.125} \times slp_{ch}^{0.375}}{n^{0.75}} \tag{27}$$

Substituting equations (23) and (27) into equation (21) gives:

$$t_{ch} = \frac{0.62 L n^{0.75}}{Area^{0.125} \times slp_{ch}^{0.375}} \tag{28}$$

where t_{ch} is the time of concentration for channel flow (hr), L is the channel length from the most distant point to the subbasin outlet (km), n is Manning's roughness coefficient for the channel, *Area* is the subbasin area (km^2), and slp_{ch} is the channel slope (m/m).

Runoff coefficient

The runoff coefficient is the ratio of the inflow rate, $i \cdot Area$, to the peak discharge rate, q_{peak}. The coefficient will vary from storm to storm and is calculated with the equation:

$$C = \frac{Q_{surf}}{R_{day}} \tag{29}$$

where Q_{surf} is the surface runoff (mm) and R_{day} is the amount of rain falling during the day (mm).

Rainfall intensity

The rainfall intensity is the average rainfall rate during the time of concentration. Based on this definition, it can be calculated with the equation:

$$i = \frac{R_{tc}}{t_{conc}} \tag{30}$$

where i is the rainfall intensity (mm/hr), R_{tc} is the amount of rain falling during the time of concentration (mm), and t_{conc} is the time of concentration for the subbasin (hr).

An analysis of rainfall data collected by Hershfield (1961) for different durations and frequencies showed that the amount of rain falling during the time of concentration was proportional to the amount of rain falling during the 24-hr period.

$$R_{tc} = \alpha_{tc} \times R_{day} \tag{31}$$

where α_{tc} is the fraction of daily rainfall that occurs during the time of concentration.

For short duration storms, all or most of the rain will fall during the time of concentration, causing α_{tc} to approach its upper limit of 1. The minimum value of α_{tc} would be seen in storms of uniform intensity (i_{24} = i). This minimum value can be defined by substituting the products of time and rainfall intensity into equation (31)

$$\alpha_{tc,\min} = \frac{R_{tc}}{R_{day}} = \frac{i \times t_{conc}}{24 i_{24}} = \frac{t_{conc}}{24} \tag{32}$$

Thus, α_{tc} falls in the range $t_{conc}/24 \leq \alpha_{tc} \leq 1$.

SWAT estimates the fraction of rain falling in the time of concentration as a function of the fraction of daily rain falling in the half-hour of highest intensity rainfall.

$$\alpha_{tc} = 1 - \exp\left[2 t_{conc} \times \ln\left(1 - \alpha_{0.5}\right)\right] \tag{33}$$

where $\alpha_{0.5}$ is the fraction of daily rain falling in the half-hour highest intensity rainfall.

Modified rational formula

The modified rational formula used to estimate the peak flow rate is given by:

$$q_{peak} = \frac{\alpha_{tc} \times Q_{surf} \times Area}{3.6 \times t_{conc}} \tag{34}$$

where q_{peak} is the peak runoff rate (m^3/s), α_{tc} is the fraction of daily rainfall that occurs during the time of concentration, Q_{surf} is the surface runoff (mm), *Area* is the subbasin area (km^2), t_{conc} is the time of concentration for the subbasin (hr) and 3.6 is a unit conversion factor.

Erosion

Erosion is the wearing down of a landscape over time. It includes the detachment, transport, and deposition of soil particles by the erosive forces of raindrops and surface flow of water. Raindrop impact can detach soil particles on unprotected land surfaces between rills and initiate transport of these particles to the rills. From the small rills, the particles move to larger rills, then into ephemeral channels and then into continuously flowing rivers. Entrainment and deposition of particles can occur at any point along the path. When erosion occurs without human influence, it is called geologic erosion. Accelerated erosion occurs when human activity increases the rate of erosion.

Erosion caused by rainfall and runoff is computed with the Modified Universal Soil Loss Equation (MUSLE) (Williams, 1975). MUSLE is a modified version of the Universal Soil Loss Equation (USLE) developed by Wischmeier and Smith (1965, 1978).

USLE predicts average annual gross erosion as a function of rainfall energy. In MUSLE, the rainfall energy factor is replaced with a runoff factor. This improves the sediment yield prediction, eliminates the need for delivery ratios, and allows the equation to be applied to individual storm events. Sediment yield prediction is improved because runoff is a function of antecedent moisture condition as well as rainfall energy. Delivery ratios are required by the USLE because the rainfall factor represents energy used in detachment only. Delivery ratios are not needed with MUSLE because the runoff factor represents energy used in detaching and transporting sediment.

The Modified Universal Soil Loss Equation (Williams, 1975) is given by:

$$Sed = 11.8(Q_{surf} \times q_{peak} \times area_{hru})^{0.56} K_{USLE} \times C_{USLE} \times P_{USLE} \times LS_{USLE} \times CFRG \qquad (35)$$

where Sed is sediment yield on a given day (metric tons), Q_{surf} is surface runoff (mm/ha), q_{peak} is peak runoff rate (m^3/s), $area_{hru}$ is area of HRU (ha), K_{USLE} is USLE soil erodibility factor, C_{USLE} is USLE cover and management factor, P_{USLE} is USLE support practice factor, LS_{USLE} is USLE topographic factor, and $CFRG$ is coarse fragment factor.

Soil erodibility factor

Some soils erode more easily than others even when all other factors are the same. This difference is termed soil erodibility and is caused by the properties of the soil itself. Wischmeier and Smith (1978) define the soil erodibility factor as the soil loss rate per erosion index unit for a specified soil as measured on a unit plot. Wischmeier and Smith

(1978) noted that a soil type usually becomes less erodible with decrease in silt fraction, regardless of whether the corresponding increase is in the sand fraction or clay fraction.

Direct measurement of the erodibility factor is time consuming and costly. Wischmeier *et al*. (1971) developed a general equation to calculate the soil erodibility factor when the silt and very fine sand content makes up less than 70% of the soil particle size distribution.

$$K_{USLE} = \frac{0.00021M^{1.14}\left(12 - OM\right) + 3.25\left(C_{soilstr} - 2\right) + 2.5\left(C_{perm} - 3\right)}{100} \qquad (36)$$

where K_{USLE} is the soil erodibility factor, M is the particle-size parameter, OM is the percent organic matter (%), $C_{soilstr}$ is the soil structure code used in soil classification, and C_{perm} is the profile permeability class.

The particle-size parameter, M, is calculated by:

$$M = \left(m_{silt} + m_{vfs}\right)\left(100 - m_c\right) \qquad (37)$$

where m_{silt} is the percent silt content (0.002-0.05 mm diameter particles), m_{vfs} is the percent very fine sand content (0.05-0.10 mm diameter particles), and m_c is the percent clay content (< 0.002 mm diameter particles).

The percent organic matter content, OM, of a layer can be calculated by:

$$OM = 1.72 org\ C \qquad (38)$$

where $orgC$ is the percent organic carbon content of the layer (%).

Williams (1995) proposed an alternative equation:

$$K_{USLE} = f_{csand} \times f_{cl-si} \times f_{orgc} \times f_{hisand} \qquad (39)$$

where f_{csand} is a factor that gives low soil erodibility factors for soils with high coarse-sand contents and high values for soils with little sand, f_{cl-si} is a factor that gives low soil erodibility factors for soils with high clay to silt ratios, f_{orgc} is a factor that reduces soil erodibility for soils with high organic carbon content, and f_{hisand} is a factor that reduces soil erodibility for soils with extremely high sand contents. The factors are calculated from:

$$f_{csand} = \left(0.2 + 0.3 \exp\left[-0.256 m_s \left(1 - \frac{m_{silt}}{100} \right) \right] \right) \quad (40)$$

$$f_{cl-si} = \left(\frac{m_{silt}}{m_c + 100} \right)^{0.3} \quad (41)$$

$$f_{orgc} = \left(1 - \frac{0.25 orgC}{orgC + \exp\left[3.72 - 2.95 orgC \right]} \right) \quad (42)$$

$$f_{hisand} = \left(1 - \frac{0.7 \left(1 - \frac{m_s}{100} \right)}{\left(1 - \frac{m_s}{100} \right) + \exp\left[-5.51 + 22.9 \left(1 - \frac{m_s}{100} \right) \right]} \right) \quad (43)$$

where m_s is the percent sand content (0.05-2.00 mm diameter particles), m_{silt} is the percent silt content (0.002-0.05 mm diameter particles), m_c is the percent clay content (< 0.002 mm diameter), and $orgC$ is the percent organic carbon content of the layer (%).

Cover and management factor

The USLE cover and management factor, C_{USLE}, is defined as the ratio of soil loss from land cropped under specified conditions to the corresponding loss from clean-tilled, continuous fallow (Wischmeier and Smith, 1978).

Because plant cover varies during the growth cycle of the plant, SWAT updates C_{USLE} daily using the equation:

$$C_{USLE} = \exp\left(\left[\ln(0.8) - \ln(C_{USLE,mn}) \right] \cdot \exp\left[-0.00115 \cdot rsd_{surf} \right] + \ln\left[C_{USLE,mn} \right] \right) \quad (44)$$

where $C_{USLE,mn}$ is the minimum value for the cover and management factor for the land cover, and rsd_{surf} is the amount of residue on the soil surface (kg/ha).

The minimum cover and management factor, C can be estimated from a known average annual C factor using the following equation (Arnold and Williams, 1995):

$$C_{USLE,mn} = 1.463 \ln\left[C_{USLE,aa}\right] + 0.1034 \tag{45}$$

where $C_{USLE,mn}$ is the minimum cover and management factor, C for the land cover and $C_{USLE,aa}$ is the average annual cover and management factor, C for the land cover.

Support practice factor

The support practice factor, P_{USLE}, is defined as the ratio of soil loss with a specific support practice to the corresponding loss with up-and-down slope culture. Support practices include contour tillage, strip cropping on the contour, and terrace systems. Stabilized waterways for the disposal of excess rainfall are a necessary part of each of these practices.

Topographic factor

The topographic factor, LS_{USLE}, is the expected ratio of soil loss per unit area from a field slope to that from a 22.1-m length of uniform 9 percent slope under otherwise identical conditions. The topographic factor is calculated:

$$LS_{USLE} = \left(\frac{L_{hill}}{22.1}\right)^m \left(65.41 \sin^2(\alpha_{hill}) + 4.56 \sin \alpha_{hill} + 0.065\right) \tag{46}$$

where L_{hill} is the slope length (m), m is the exponential term, and *hill* is the angle of the slope. The exponential term, m, is calculated:

$$m = 0.6\ (1\text{- } \exp\ [-35.835 slp]) \tag{47}$$

where slp is the slope of the HRU expressed as rise over run (m/m). The relationship between α_{hill} and slp is:

$$slp = tan\alpha_{hill} \tag{48}$$

Coarse fragment factor

The coarse fragment factor is calculated:

$$CFRG = \exp(-0.053\ rock) \tag{49}$$

where *rock* is the percent rock in the first soil layer (%).

Routing phase of the hydrologic cycle

In the SWAT model a command structure is used for routing runoff and chemicals through a watershed similar to the structure for routing flows through streams and reservoirs, adding flows, and inputting measured data on point sources. Using the routing command language, the model can simulate a basin subdivided into cells or sub-watersheds. Additional commands have been developed to allow measured and point source data to be input to the model and routed with simulated flows. Routing in the main channel is divided into four components: water, sediment, nutrients and organic chemicals.

Water routing

As water flows downstream, a portion may be lost due to evaporation and transmission through the bed of the channel. Another potential loss is removal of water from the channel for agricultural or human use. Flow may be supplemented by the fall of rain directly on the channel and/or addition of water from point source discharges. Water is routed through the channel network using the variable storage routing method developed by Williams (1969) or the Muskingum River routing method. Both the variable storage and Muskingum routing methods are variations of the kinematic wave model. A detailed discussion of the kinematic wave flood routing model can be found in Chow *et al.*, 1988.

SWAT uses Manning's equation to define the rate and velocity of flow and assumes the main channels, or reaches, to have a trapezoidal shape. Manning's equation for uniform flow in a channel is used to calculate the rate and velocity of flow in a reach segment for a given time step:

$$q_{ch} = \frac{A_{ch} \times R_{ch}^{2/3} \times slp_{ch}^{1/2}}{n} \tag{50}$$

$$v_c = \frac{R_{ch}^{2/3} \times slp_{ch}^{1/2}}{n} \tag{51}$$

where q_{ch} is the rate of flow in the channel (m^3/s), A_{ch} is the cross-sectional area of flow in the channel (m^2), R_{ch} is the hydraulic radius for a given depth of flow (m), slp_{ch} is the slope along the channel length (m/m), n is Manning's "n" coefficient for the channel, and v_c is the flow velocity (m/s).

SWAT routes water as a volume. The daily value for cross-sectional area of flow, A_{ch}, is calculated by:

$$A_{ch} = \frac{V_{ch}}{1000 L_{ch}} \tag{52}$$

where V_{ch} is the volume of water stored in the channel (m^3), and L_{ch} is the channel length (km).

The variable storage routing method was developed by Williams (1969) and used in the HYMO (Williams and Hann, 1973) and ROTO (Arnold *et al*., 1995) models. For a given reach segment, storage routing is based on the continuity equation:

$$V_{in} - V_{out} = \Delta V_{stored} \tag{53}$$

where V_{in} is the volume of inflow during the time step (m^3), V_{out} is the volume of outflow during the time step (m^3), and S_{stored} is the change in volume of storage during the time step (m^3).

The Muskingum routing method models the storage volume in a channel length as a combination of wedge and prism storages. When a flood wave advances into a reach segment, inflow exceeds outflow and a wedge of storage is produced. As the flood wave recedes, outflow exceeds inflow in the reach segment and a negative wedge is produced.

In addition to the wedge storage, the reach segment contains a prism of storage formed by a volume of constant cross-section along the reach length. A detailed discussion of both the variable storage and Muskingum routing methods can be found in SWAT2005 (Neitsch *et al.*, 2005).

Sediment routing

Sediment transport in the channel network is a function of two processes: deposition and degradation, operating simultaneously in the reach. SWAT will compute deposition and degradation using the same channel dimensions for the entire simulation. Alternatively, SWAT will simulate down-cutting and widening of the stream channel and update channel dimensions throughout the simulation.

The maximum amount of sediment that can be transported from a reach segment is a function of the peak channel velocity. The peak channel velocity, $v_{ch,pk}$, is calculated by:

$$v_{ch,pk} = \frac{q_{ch,pk}}{A_{ch}} \tag{54}$$

where $q_{ch,pk}$ is the peak flow rate (m^3/s) and A_{ch} is the cross-sectional area of flow in the channel (m^2). The peak flow rate is defined as:

$$q_{ch,pk} = prf \times q_{ch} \tag{55}$$

where prf is the peak rate adjustment factor, and q_{ch} is the average rate of flow (m^3/s). The maximum amount of sediment that can be transported from a reach segment is calculated:

$$conc_{sed,ch,mx} = c_{sp} \times v_{ch,pk}^{\ \ spexp} \tag{56}$$

where $conc_{sed,ch,mx}$ is the maximum concentration of sediment that can be transported by the water (ton/m^3 or kg/L), c_{sp} is a coefficient defined by the user, $v_{ch,pk}$ is the peak channel velocity (m/s), and $spexp$ is an exponent defined by the user. The exponent, $spexp$, normally varies between 1.0 and 2.0 and was set at 1.5 in the original Bagnold stream power equation (Arnold *et al.*, 1995).

The maximum concentration of sediment calculated with equation (56) is compared to the concentration of sediment in the reach at the beginning of the time step, $conc_{sed,ch,i}$. If $conc_{sed,ch,i} > conc_{sed,ch,mx}$, deposition is the dominant process in the reach segment and the net amount of sediment deposited is calculated by:

$$sed_{dep} = \left(conc_{sed,ch,i} - conc_{sed,ch,mx}\right) \times V_{ch} \tag{57}$$

where sed_{dep} is the amount of sediment deposited in the reach segment (metric tons), $conc_{sed,ch,i}$ is the initial sediment concentration in the reach (kg/L or ton/m^3), and V_{ch} is the volume of water in the reach segment (m^3).

If $conc_{sed,ch,i} < conc_{sed,ch,mx}$, degradation is the dominant process in the reach segment and the net amount of sediment re-entrained is calculated by:

$$sed_{\deg} = \left(conc_{sed,ch,mx} - conc_{sed,ch,i}\right) \times V_{ch} \times K_{CH} \times C_{CH} \tag{58}$$

where sed_{deg} is the amount of sediment reentrained in the reach segment (metric tons), K_{CH} is the channel erodibility factor (cm/hr/Pa), and C_{CH} is the channel cover factor.

Once the amount of deposition and degradation has been calculated, the final amount of sediment in the reach is determined by:

$$sed_{ch} = sed_{ch,i} - sed_{dep} + sed_{\deg} \tag{59}$$

where sed_{ch} is the amount of suspended sediment in the reach (metric tons), $sed_{ch,i}$ is the amount of suspended sediment in the reach at the beginning of the time period (metric tons). The amount of sediment transported out of the reach is calculated by:

$$sed_{out} = sed_{ch} \times \frac{V_{out}}{V_{ch}} \tag{60}$$

where sed_{out} is the amount of sediment transported out of the reach (metric tons), V_{out} is the volume of outflow during the time step (m^3), and V_{ch} is the volume of water in the reach segment (m^3).

Nutrient routing

Nutrient transformations in the stream are controlled by the in stream water quality component of the model. The in-stream kinetics used in SWAT for nutrient routing are adapted from QUAL2E (Brown and Barnwell, 1987). The model tracks nutrients dissolved in the stream and nutrients adsorbed to the sediment. Dissolved nutrients are transported with the water while those sorbed to sediments are allowed to be deposited with the sediment on the bed of the channel.

Channel pesticide routing

While an unlimited number of pesticides may be applied to the HRUs, only one pesticide may be routed through the channel network of the watershed due to the complexity of the processes simulated. As with the nutrients, the total pesticide load in the channel is partitioned into dissolved and sediment-attached components. While the dissolved pesticide is transported with water, the pesticide attached to sediment is affected by sediment transport and deposition processes. Pesticide transformations in the dissolved and sorbed phases are governed by first-order decay relationships. The major in-stream processes simulated by the model are settling, burial, re-suspension, volatilization, diffusion and transformation.

Materials

Input Data

Acquisition of satellite imagery data

Landsat TM (Thematic Mapper) image acquired on 22 November, 1985 and Landsat ETM+ (Enhanced Thematic Mapper plus) images acquired on 25 November, 1995 and 24 November, 2005 were used as the base data layer from which the land use and land cover maps of the study area were derived. The images were downloaded from Global Land Cover Facility (GLCF) an Earth Science Data Interface. The images have a ground resolution of a 28.5-m and were used to map the land use/cover patterns of the study area. The dates of the images were chosen as closely as possible to be in the same vegetation season.

Input data for SWAT model

The basic spatially distributed data (GIS input) needed for the ArcSWAT interface include the digital elevation model (DEM), land use/cover data and soil data. Data on weather and river discharge were also used for calibration purposes.

Digital elevation model

Digital elevation model (DEM) is one of the main inputs for the SWAT model. A 30-m grid digital elevation model was downloaded from ASTER (Advanced Spaceborne Thermal Emission and Reflection Radiometer) GDEM (Global Digital Elevation Model). The DEM was used to define the topography that describes the elevation of any point in a given area at a specific spatial resolution. Moreover, it is used to generate variations in sub-watershed configurations such as sub-watershed delineation and stream network delineation. Terrain parameters such as slope gradient, slope length and the stream network characteristics such as channel slope, length, and width were also derived from the DEM. The DEM of Fincha watershed is shown in Figure 7.

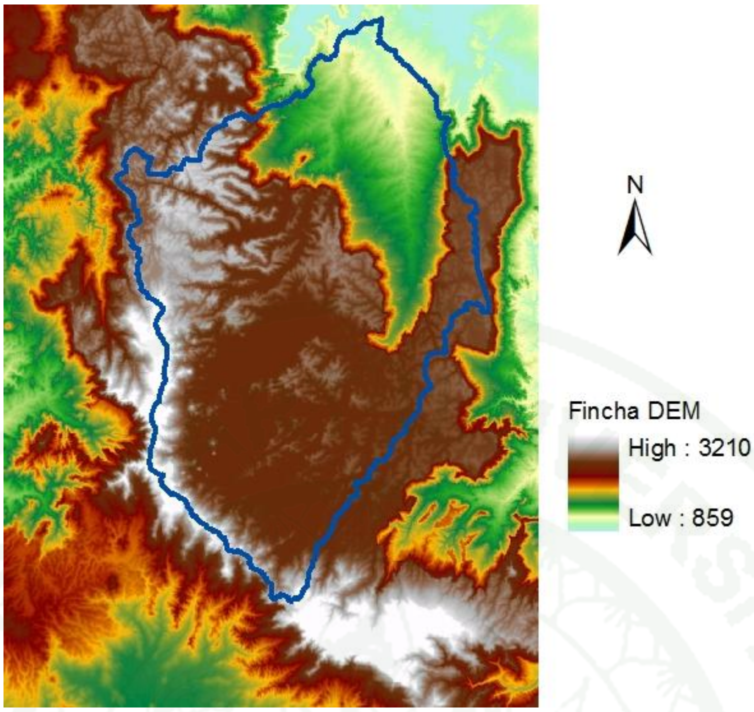

Figure 7 Digital elevation model of Fincha watershed.

Land use/cover data

Land use map is a critical input for the SWAT model. It is one of the most important factors that affect surface erosion, runoff, and evapotranspiration in a watershed. The land use map of the study area was obtained from the Ministry of Water Resources (MoWR) of Ethiopia. We have reclassified the land use map of the area based on the available topographic map (1:50,000), aerial photographs and satellite images. The reclassification of the land use map was done to represent the land use according to the specific land use/cover types required by the model.

A look up table that identifies the four-letter SWAT code for the various land use/cover categories were prepared so as to relate the grid values to SWAT land use/cover classes. The major land use/cover types in the study watershed with their corresponding four-letter SWAT codes are presented in Table 2.

Table 2 Land cover types with their corresponding 4-letters SWAT code.

Land use/cover	SWAT definition	SWAT code
Agricultural land	Agricultural land generic	AGRL
Forest land	Forest mixed	FRST
Grazing land	Grazing land	GRZL
Water bodies	Water	WATR
Swamp areas	Swamp area	SWAP
Shrub land	Shrub lands	SHRL

Soil data

Soil plays an important role in the modeling of various hydrological processes of a watershed. The soil textural and physicochemical properties required by the SWAT model includes soil texture, available water content, hydraulic conductivity, bulk density and organic carbon content for each soil types. These data were obtained from different sources including Ministry of Water Resources (MoWR) of Ethiopia, Soil and Terrain Database for northeastern Africa (FAO, 1998), Major Soils of the world (FAO, 2002), and Digital Soil Map of the World (FAO, 2005). Some of the physical and hydrological properties of the major soil types of the Fincha watershed used during the set up of the SWAT model are presented in Table 3.

Meteorological data

The weather variables required by the SWAT model for driving the hydrological processes of a watershed are daily rainfall and daily minimum and maximum temperatures. The data were obtained from the National Meteorological Service Agency (NMSA) of Ethiopia. They were collected from five stations (Fincha, Shambu, Hareto, Gabate, and Kombolcha) that are located within the watershed and cover a period of twenty two years (January 1985 to December 2006). Table 4 presents the geographical locations of the climate stations in the study watershed with their elevation. The locations of climate stations are also shown on Figure 8.

Table 3 Properties of major soils in Fincha Watershed.

Soil type	Hydro group	Bulk density (g/cm^3)	AWC (mm H_2O /mm soil)	Hydraulic conductivity (mm/h)	Textural composition (% by weight)			Organic carbon (% by weight)
					Clay	Silt	Sand	
Eutric Cambisols	C	1·31	0·096	60	35	36	29	2·00
Rhodic Nitosols	C	1·28	0·128	250	51	34	15	2·12
Eutric Leptosols	C	1·37	0·097	500	26	34	40	1·58
Chromic Luvisols	C	1·10	0·109	50	65	26	9	1·78
Eutric Vertisols	C	1·20	0·151	1000	36	54	10	0·63
Haplic Luvisols	D	1.13	0.119	55	60	28	12	1.75
Haplic Alisols	C	1·15	0·151	150	50	30	20	1.64
Haplic Arenosols	D	1.61	0.142	100	45	40	15	1.72
Haplic Phaezems	D	1.43	0.121	65	60	25	15	1.74

Table 4 Geographical location of climate stations.

Station name	XPR	YPR	Latitudes	Longitudes	Elevation
Fincha	320516	1057411	9.56	37.36	1910
Shambu	291684	1057670	9.56	37.10	2350
Hareto	293287	1035712	9.36	37.12	1895
Gabate	326410	1039398	9.40	37.42	1960
Kombocha	325756	1080967	9.77	37.41	1750

XPR: X coordinate in the defined projection
YPR: Y coordinate in the defined projection

Hydrological data

The observed runoff and sediment yield data at the outlet of the watershed (at confluence point with Abbay) were obtained from the Hydrology Department of the Ministry of Water Resources (MoWR) of Ethiopia. These data are required for the calibration and validation of the SWAT model.

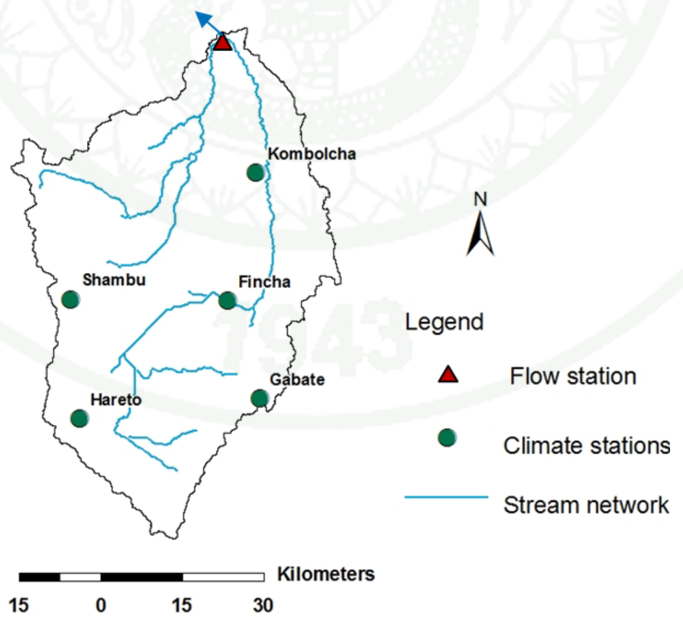

Figure 8 Location of climate stations in Fincha watershed.

Methods

Analysis of Land Use/Cover Changes

The overall methods or steps of this research work are shown on the flowchart of Figure 9. The first step is to classify the land use/cover types of the study watershed over time based on the available satellite imagery data. The second step is to predict the land use/cover changes of the study area about twenty years in to the future from 2005 onwards using the Markov model. The final step of this research work is to simulate the effects of land use change and management practices on the hydrological processes of the study area particularly on runoff volumes and sediment yields.

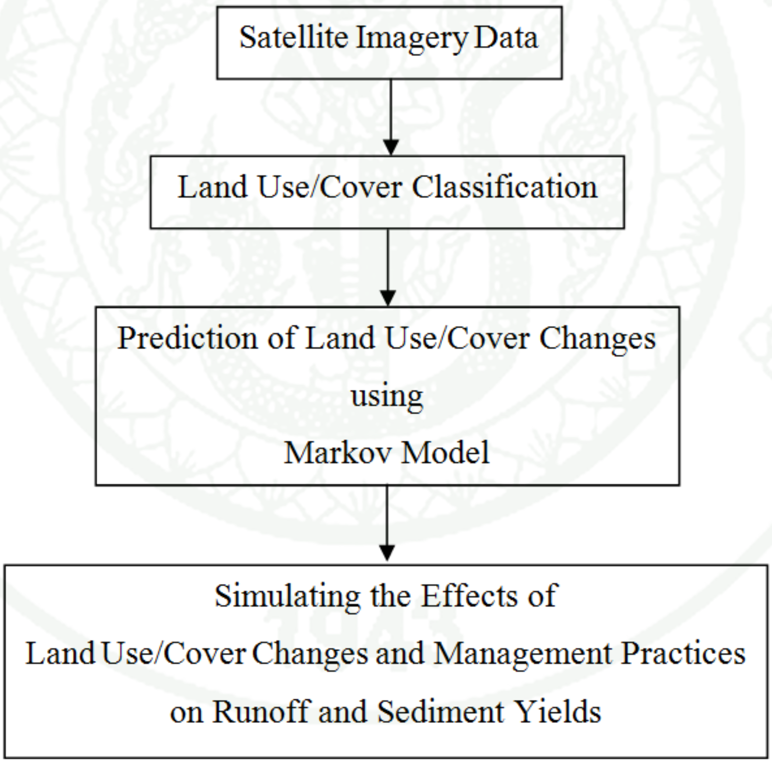

Figure 9 Flowchart showing the overall procedures of the study.

Land use/cover classification

In order to analyze the land use/cover changes of the Fincha watershed over the last 20 years, measure the rate of these changes, and relate the overall changes to the hydrological processes and physical features of the watershed, three land use/cover map of the study area were produced through supervised classification based on minimum distance algorithms. The remotely sensed satellite images were interpreted from Landsat TM (Thematic Mapper) and Landsat ETM+ (Enhanced Thematic Mapper Plus) with a resolution of 28.5-m. Reclassification of land use/cover was based on the available topographic map, aerial photographs and satellite images.

Image preprocessing

Preprocessing of satellite images prior to image classification and change detection is essential (Teillet, 1986). It improves the image data that suppresses undesired distortions or enhances some image features relevant for further processing and analysis task. Preprocessing commonly comprises a series of sequential operations, including radiometric normalization, image registration, geometric correction, and masking (e.g., for clouds, water, irrelevant features) (Coppin and Bauer, 1996). The normalization of satellite imagery takes into account the combined, measurable reflectance of the atmosphere, aerosol scattering and absorption, and the earth's surface (Kim and Elman, 1990). It is the volatility of the atmosphere which can introduce variation between the reflectance values or digital numbers of satellite images acquired at different times. Geometric rectification of the imagery resamples or changes the pixel grid to fit that of a map projection or another reference image.

To conform the pixel grids and remove any geometric distortions in the imagery, the first Landsat TM 1985 image was registered and geo-referenced to the UTM, WGS84 (zone 37) coordinate system based on 1:50,000 scale topographic maps. Each of the Landsat ETM+ 1995 and ETM+ 2005 images were then registered to the 1985 image (image to image registration). To keep the original brightness values of pixels unchanged, the data were re-sampled using the nearest neighborhood algorithm. This method uses the value of the closest pixel to assign to the output pixel value and thus transfers original data values without averaging them, therefore, the extremes and subtleties of the data values are not lost (ERDAS, 1999).

Image classification

Image classification refers to the extraction or grouping of a digital image from raw remotely sensed digital satellite data into different classes within a particular dataset, based on attribute values. It is done to replace visual analysis of the image data with quantitative techniques. Image classification can be either supervised or unsupervised classification. In this study, since the identity and location of some of the land use and land cover types such as, agricultural land, forest land, shrub land, water body, etc were known based on the *priori* knowledge of the study area, author's personal experience, ground truth data, and information from previous studies in the area, a supervised signature extraction with a minimum distance algorithm was used in ERDAS Imagine 9.1 (ERDAS Inc., 2801 Buford Highway, NE, Atlanta, Georgia 30329-2137 USA) to classify the images. Multi-temporal signatures were generated from the Landsat TM and Landsat ETM+ images. All visible and infrared bands of 1, 2, 3, 4, 5, and 7 except band 6 (the thermal infrared) were included in the analysis. The flowchart in Figure 10 shows the procedures how the land use/cover map of the Fincha watershed is produced.

Supervised classification process involves the initial selection of training sites on the image which represent specific land classes to be mapped. Training sites are sets of pixels that represent what is recognized as a discernable pattern, or potential land cover class (ERDAS, 1999). Training sites for signature generation were developed from ground truth data. In this study, a total of 200 training sites were chosen for each image to ensure that all spectral classes constituting each land use and land cover category were adequately represented in the training statistics.

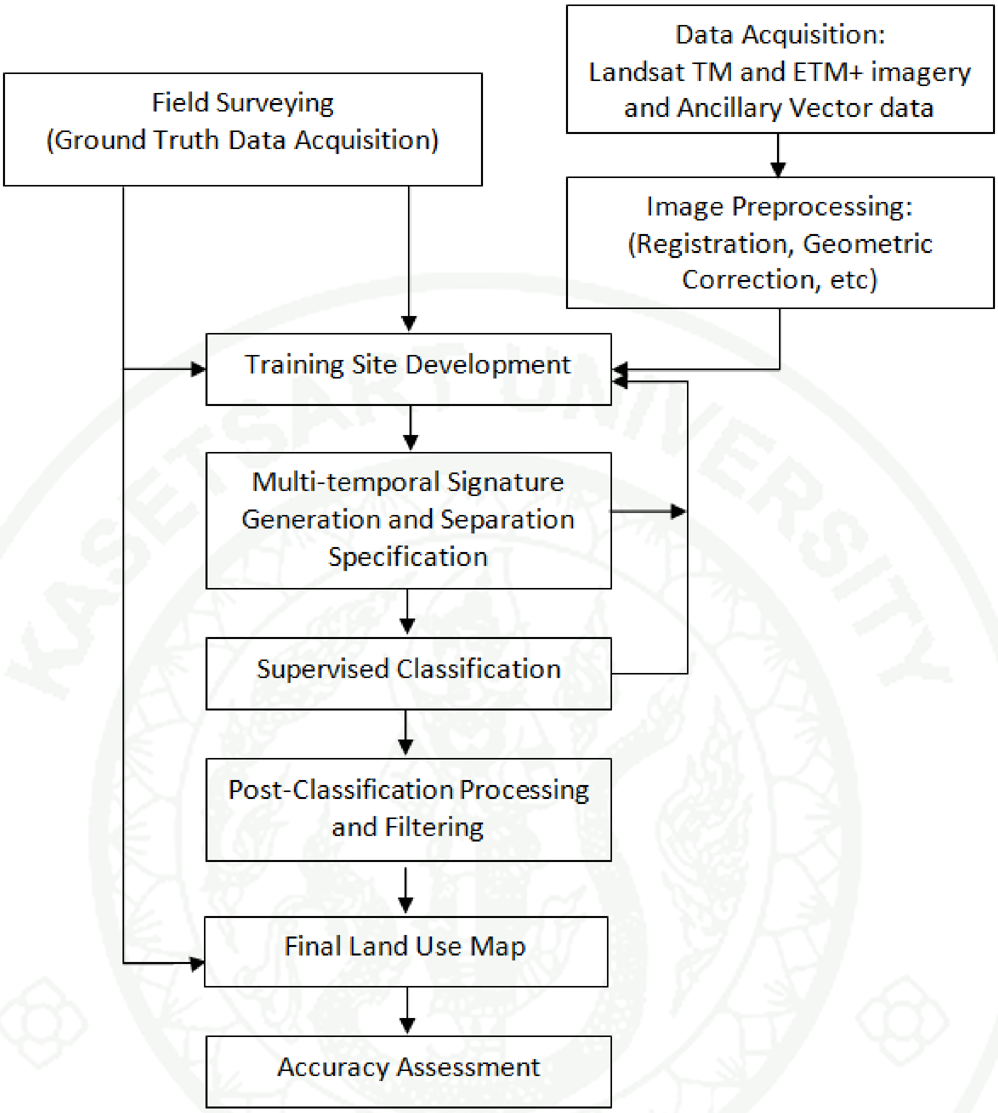

Figure 10 Flowchart showing land use/cover mapping procedures.

Based on a modified version of the Anderson scheme of land use and land cover classification method (Anderson *et al*., 1976), six land use/cover classes were established for the study area namely; (1) agricultural land, (2) forest land, (3) grazing land, (4) water bodies, (5) shrub lands, and (6) swamp areas. The descriptions of the land use/cover classes of the study watershed are presented in Table 5.

Table 5 Description of land use classes in Fincha watershed.

Land use/cover	Description
Agricultural land	Areas used for cultivation, including fallow lands and homestead farms, urban, and settlement areas
Forest land	Areas covered with natural dense forests, mixed forests with higher density of trees forming closed canopy, plantations
Grazing land	Areas covered with grasses and trees used for grazing
Water bodies	Areas completely inundated by water, rivers, streams, etc.
Swamp areas	Areas flat and swampy during both wet and dry seasons
Brush land	Areas consisting of tropical lands with short vegetations, grasses

Accuracy assessment

Land use/cover maps derived from remote sensing always contain some sort of errors due to several factors which range from classification technique to method of satellite data capture. In order to wisely use the land cover maps which are derived from remote sensing and the accompanying land resource statistics, the errors must be quantitatively explained in terms of classification accuracy. Therefore, after the completion of classification it is necessary to assess the accuracy of the results obtained. This procedure allows a degree of confidence to be attached to those results and will serve to indicate whether the analysis objectives have been achieved. Accuracy is determined empirically, by selecting a sample of pixels from the map and checking their labels against classes determined from reference data (desirably gathered during site visit). Often reference data is referred to as ground truth.

The most common and typical method used by many researchers to assess classification accuracy is the use of an error matrix (Congalton and Green, 1999). It is the most common and very effective way to represent the accuracy of the classification results as the accuracy of each category is clearly described (Fan *et al.*, 2007). It is also sometimes referred as confusion matrix or contingency table. An error matrix is a square array of numbers defined in rows and columns that represent the number of sample units (i.e., pixels, clusters of pixels, or polygons) assigned to a particular category relative to the actual category as verified on the ground. The rows in the matrix represent the remote sensing derived land use map, while the columns represent the reference data that were collected during fieldwork. These tables produce many statistical measures of accuracy including overall classification accuracy, percentage of omission and commission error and the kappa coefficient, an index that estimates the influence of chance (Congalton and Green, 1999).

The ground truth data (reference data) used was collected from field survey and existing land use/cover maps that have been field-checked using stratified random sampling method, by which a sample of 100 pixels were randomly selected for each land use and land cover category. Overall accuracy, user's and producer's accuracies, the Kappa statistics, as well as, the commission and omission errors were derived from the error matrices.

Overall classification accuracy is computed by dividing the total correct (sum of the major diagonal) by the total number of pixels in the error matrix. The user's accuracy, calculated by dividing the number of correctly classified pixels in a class by the total number of pixels assigned to that class, is the probability that the mapped class (e.g., Agricultural land) correctly represents its ground distribution. The producer's accuracy, calculated by dividing the total number of correctly classified pixels in a class by the total number of reference measurements of that class, is the probability that a class identified from the reference data is correctly classified on the map. Commission errors are those that misclassify a pixel to another class, while omission errors occur when pixels are erroneously excluded from a class (Congalton and Green, 1999). Errors of commission reduce user's accuracy while errors of omission reduce producer's accuracy (Stehman, 1997).

KAPPA analysis is a discrete multivariate technique of use in accuracy assessment (Congalton and Mead, 1983). KAPPA analysis yields a K_{hat} statistic (an estimate of Kappa) that is a measure of agreement or accuracy (Rosenfield and Fitzpatrick-Lins, 1986; Congalton, 1991). The K_{hat} statistic is computed as

$$K_{hat} = \frac{N\sum_{i=1}^{r} x_{ii} - \sum_{i=1}^{r}(x_{i+} \times x_{+i})}{N^2 - \sum_{i=1}^{r}(x_{i+} \times x_{+i})} \tag{61}$$

Where r is the number of rows in the matrix, x_{ii} is the number of observations in row i and column i, and x_{i+} and x_{+i} are the marginal totals for row i and column i, respectively, and N is the total number of observations.

Markovian analysis of land use/cover change process

Markovian modeling is used to examine the stochastic nature of the dynamics of land use/cover data and to project the stability of future land development in the study area. Based on the land use/cover change data derived from satellite images, this study also establishes the validity of the Markov process for describing and projecting land use and land cover changes in the study area, by examining statistical independence, Markovian compatibility, and stationarity of the data.

The testing of statistical independence hypothesis involves a procedure for comparing the expected numbers under the Markovian hypothesis with the actual data. If the number of land use and land cover categories is n, then the statistic to be computed is chi-square distribution (χ^2) with $(n\text{-}1)^2$ degrees of freedom. Letting N_{ik} stands for the number of cells having category i in 1985 and k in 2005, and E_{ik} for the expected number under the Markov hypothesis, the statistic is then

$$\chi^2 = \sum_{i} \sum_{j} \left(N_{ik} - E_{ik}\right)^2 / E_{ik} \tag{62}$$

The 0.05 critical region for n = 6 is thus any value of χ^2 greater than 37.65. Any computed value of less than this critical number will lead to a conclusion that the data are compatible with the hypothesis of independence.

The land use/cover transition probabilities for the time step were derived from the row tally matrix developed between the two years of the study period. In this study, the row tally matrix between 1985 and 1995, 1995 and 2005, and between 1985 and 2005 are presented in Appendix Tables 1, 2, and 3, respectively. The land use/cover transition probability matrix (P) over the first (1985 - 1995) and the second (1995 – 2005) ten years of the study period and over twenty years of the whole study period (1985 – 2005) are presented in Appendix Tables 4, 5, and 6, respectively. The computation of expected number E_{ik} requires a direct application of the Chapman–Kolmogorov equation (Stewart, 1994), which states that transition probabilities from years 1985 to 2005 can be calculated by multiplying the transition probabilities matrix from years 1985 to 1995 by the transition probabilities matrix from years 1995 to 2005. These transition probabilities are used in the following formula to calculate the expected numbers:

$$E_{ik} = \sum_{j} (N_{ij})(N_{jk}) / N_{j} \tag{63}$$

Where:

N_{ij} is the number of transitions from category i to j during the period 1985 to 1995;

N_{jk} is the number of transitions from category j to k during the period 1995 to 2005; and

N_{j} is the number of hectares cells in category j in 1995.

To test for first-order Markovian dependence, a chi-square goodness-of-fit test is used. This statistical test judges whether or not a particular distribution adequately describes a set of observations by making a comparison between the actual number of observations and the expected number of observations. The statistic is calculated from the relationship:

$$\chi_c^2 = \sum_{i} \sum_{j} \left(O_{ik} - E_{ik} \right)^2 / E_{ik} \tag{64}$$

where O_{ik} and E_{ik} are the observed and expected number of transition probability from 1985 to 2005 respectively.

The distribution of E_{ik} is a chi-square distribution (χ_c^2) with $(n\text{-}p\text{-}1)^2$ degrees of freedom where n is the dimension of the matrices, and p is the number of parameters estimated from the data. The hypothesis that the data are from the Markovian distribution is rejected if

$$\chi^2 > \chi_c^2 \tag{65}$$

Finally, the hypothesis of stationarity is tested. The significance of stationarity of a Markovian process is that one can project future land development based on the current transition probabilities. According to the stationarity assumption, the changes recorded over the first 10-year period (1985 to 1995) and the second 10-year period (1995 to 2005) should result from the same transition mechanism. If this holds true, the TPs during both periods can be used to project the pattern of distribution indefinitely into the future. The resulting equilibrium, or steady state distributions, may provide an indication of the ultimate trend of the land development process.

Simulation of Hydrological Processes Using SWAT Model

The ArcSWAT interface was used for the setup and parameterization of the model. The methodologies followed include watershed delineation, analysis of hydrologic response unit (HRU), importing of weather generator data, calibration and validation processes. The required spatial datasets were projected in ArcGIS 9.3 to the same projection called Adindan UTM Zone 37N which is the transverse mercator projection parameters for Ethiopia.

Watershed delineation

Watershed delineation is used for segmenting watersheds into several hydrologically connected sub-watersheds for use in watershed modeling with SWAT. The watershed delineation process includes five major steps: DEM setup, stream definition, outlet and inlet definition, watershed outlets selection and definition and calculation of subbasin parameters. The digital elevation model (DEM) of the study watershed in ESRI grid format was first imported into the SWAT model. A masking polygon (in grid format) was also loaded into the model in order to extract area of interest, delineate the boundary of the watershed, and digitize stream networks of the study area.

For the stream definition the threshold based stream definition option was used to define the minimum size of the subbasin. The ArcSWAT interface allows the user to fix the number of subbasins by deciding the initial threshold area. The threshold area defines the minimum drainage area required to form the origin of a stream. In this study, the minimum threshold area used to discretize the watershed into subbasins was selected as 5,000ha.

Analysis of hydrologic response units (HRU)

Hydrologic models like SWAT require land use and soil data to determine the area and the hydrologic parameters of each land-soil category simulated within each sub-watershed. It is often not practical to simulate individual fields with a specific land use, management and soil type. Therefore, it is necessary to subdivide the area into hydrologic response units (HRUs) and determine the land use/soil/slope class combinations and distributions for the delineated watershed and each respective sub-watershed. Subdividing the areas into hydrologic response units enables the model to reflect the evapotranspiration and other hydrologic conditions for different land cover/crops and soils. Moreover, HRU definition minimizes the computational costs of simulations by lumping all similar soil and land use areas into a single unit (Neitsch *et al*., 2002). Hence, the land use/cover and soil map of the study area (in grid format) were imported into the model and made to overlay to obtain a unique combination of land use/soil/slope class within the watershed to be modeled. A user look up table was created to identify the SWAT code for the different categories of land cover/land use on the map as per the required format. The soil map was linked with the soil database which is designed to hold data for soils not included in the U.S. soil database.

Runoff is predicted separately for each HRU and routed to obtain the total runoff for the watershed. This process increases the accuracy of load predictions and provides a much better physical description of the water balance. In this study, in order to define the distributions of HRUs, multiple HRU definition with 10 percent land use, 20 percent soil, and 10 percent slope thresholds was used. This threshold level is set to eliminate minor land uses, soils and slope classes in each subbasin so that a maximum of 10 HRUs with unique land use/soil/slope combinations would be created in each subbasin as recommended in the SWAT2009 user manual. Land uses, soils or slope that cover a percentage of the subbasin area less than the threshold level were eliminated. After the elimination processes the area of the land use, soil or slope is reallocated so that 100 percent of the land area, soil or slope in the subbasin is included in the simulation.

Importing weather data

The weather input data consists of precipitation, maximum and minimum temperature, wind speed, relative humidity and the weather generator file. The monthly statistical precipitation and temperature data for the whole study period is prepared and entered into the SWAT data base. These statistical data for the Fincha, Shambu, Hareto, Gabate, and Kombolcha climate stations are presented in Appendix Table 7, 8, 9, 10, and 11, respectively. Time series data of twenty two years (1985 to 2006) of daily rainfall and daily minimum and maximum temperatures were also prepared in appropriate format (.dbf) and imported into the model. After importing the weather data, additional inputs such as management data, soil parameters, manning's roughness coefficient for overland flow and in-stream water quality parameters were set up and edited as per the requirement and objective of the study. In the data file, runoff curve numbers for Ethiopian conditions as well as those prescribed in SWAT user manual were adopted for different land use classes based on the land use type and hydrologic soil group (HSG).

Model calibration

The SWAT model was built with state-of-the-art components with an attempt to simulate the processes physically and realistically. Most of the model inputs are physically based (that is, based on readily available information). It is important to understand that SWAT is not a "parametric model" with a formal optimization procedure (as part of the calibration process) to fit any data. Instead, a few important variables that are not well defined physically such as runoff curve number and Universal Soil Loss Equation's cover and management factor, or C factor may be adjusted to provide a better fit.

SWAT model includes a large number of parameters that describe the different hydrological conditions and characteristics across the watershed. During the calibration process, model parameters are subject to adjustments, in order to obtain model results that correspond better to measured data sets. After setting up, the model was run for simulation using the default parameter values. The default simulation outputs were compared with the observed data. In this study, the model was calibrated on monthly basis using time series data from January 1985 to December 1996. The first two years of the modeling period were used for 'model warm-up'. The warm-up period allows the model to get the hydrologic cycle fully operational.

First, the hydrological component of the model was calibrated by adjusting the curve number (CN) to optimize runoff volume predictions. The erosion component was then calibrated by adjusting the management factor (parameter used in the MUSLE equation) for the various land covers until predicted and measured suspended sediment concentrations were in close agreement.

Calibration procedures

Model outputs were calibrated to fall within a percentage of average measured values and then monthly regression statistics (R^2 and E_{NS}) were evaluated. If measured and simulated means met the calibration criteria and monthly R^2 and E_{NS} did not, then additional checking was performed to ensure that rainfall variability and plant growing seasons were properly simulated over time. Model calibration was performed using both manual and auto-calibration techniques and model outputs were compared with observed data. The procedure for calibrating the model for flow and sediment yield is shown in Figure 11.

Flow was the first output calibrated by adjusting the parameter CN2 (Initial SCS runoff curve number for moisture condition II) because results of many studies indicated curve number as the most sensitive parameter (Arabi *et al*., 2008; Das *et al*., 2007; Parajuli *et al*., 2007; Wang *et al*., 2008). The curve numbers were adjusted within 10 percent from the tabulated curve numbers to reflect conservation tillage practices and soil residue conditions of the watershed. CN is a soil moisture balance parameter that allows the model to modify moisture condition of the soil to estimate surface runoff. As the value of CN is reduced, the model allows less water to runoff from the surface. Other flow related model parameters such as re-evaporation coefficient for ground water

(REVAPC), soil evaporation compensation factor (ESCO), and plant evaporation compensation factor (EPCO) were kept with the default values. Flow was calibrated until the difference between average measured and simulated surface runoff was within 15% and monthly $R^2 \geq 0.6$ and $E_{NS} \geq 0.5$.

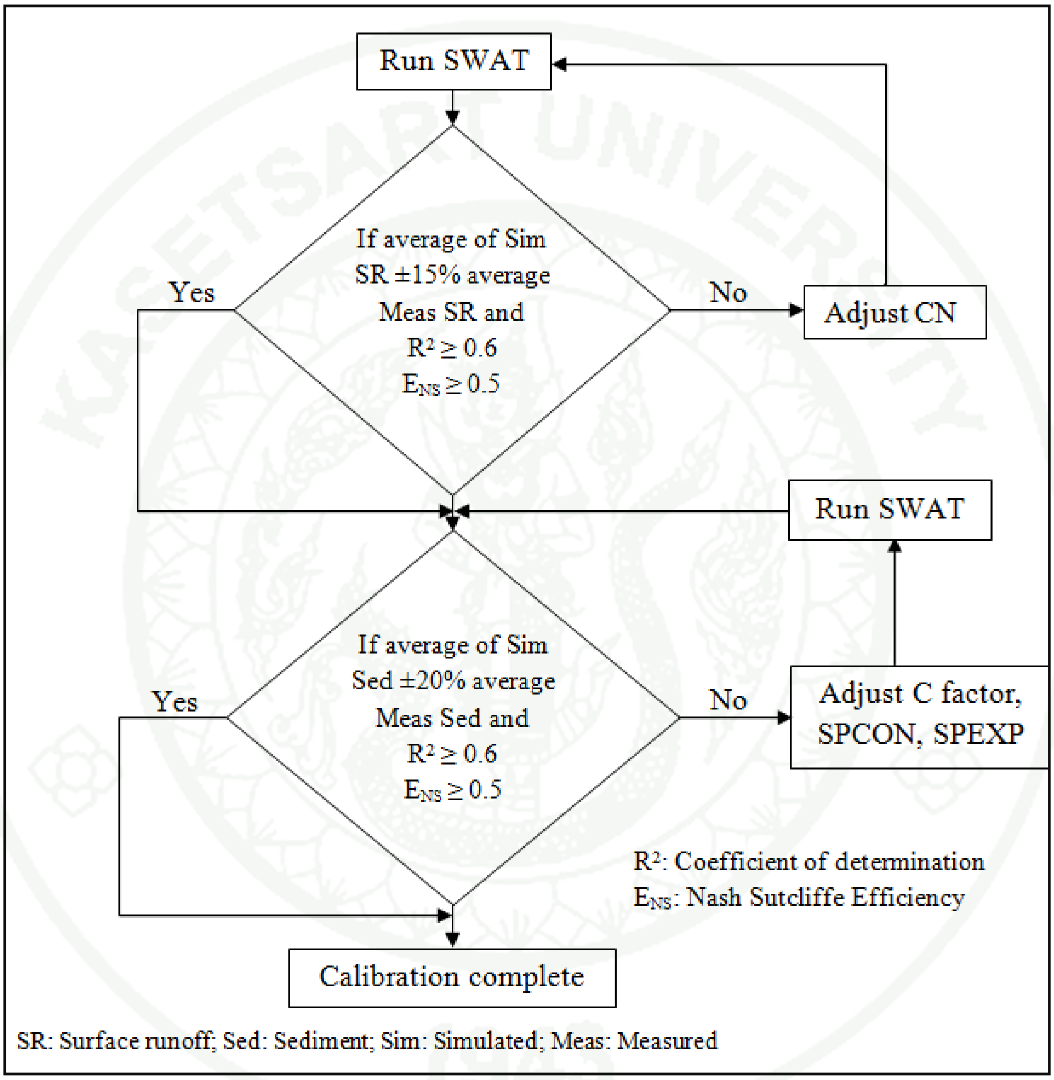

Figure 11 Calibration procedure for flow and sediment yields in the SWAT model.

Sediment was calibrated by adjusting the Universal Soil Loss Equation crop cover management factor (USLE C) (Williams, 1975) until the average measured and simulated values were in close agreement. The C-factor was adjusted to represent the surface cover better in grazing and agricultural lands. The USLE C factor is defined as the ratio of soil loss from cropped land under specific conditions to the corresponding loss from clean-tilled, continuous fallow land (Wischmeier and Smith, 1978). It is one of the most widely used sediment calibration factors (Parajuli *et al.*, 2007). Channel sediment routing variables such as the linear factor for calculating the maximum amount of sediment during channel sediment routing (SPCON) and the exponential factor for calculating the sediment in the channel sediment routing (SPEXP) were also adjusted during the calibration. Sediment was calibrated after flow until the difference between the averages of the simulated and measured sediment yield values fall within 20% and monthly $R^2 \geq 0.6$ and $E_{NS} \geq 0.5$.

Model validation

In the validation process, the model is operated with input parameters set during the calibration process without any change and the results were compared against an independent set of observed data. In this study, the model was validated on monthly basis using time series data from January 1997 to December 2006.

Evaluation of model performance

Performance of the model was evaluated in order to assess how the model simulated values fitted with the observed values. Several statistical measures are available for evaluating the performance of a hydrological model. In this study, during calibration and validation periods, the goodness-of-fit between the simulated and measured values were evaluated using the coefficient of determination (R^2) and Nash-Sutcliffe coefficient of efficiency (E_{NS}) (Nash and Sutcliffe, 1970).

The coefficient of determination (R^2) describes the proportion of the total variance in the measured data that can be explained by the model. It is an indicator of strength of relationship between the observed and simulated values. It measures how well the simulated versus observed regression line approaches an ideal match and ranges from 0 to 1, with a value of 0 indicating no correlation and a value of 1 representing that the predicted values area exactly equal to the measured values (Krause *et al.*, 2005). It is defined as:

$$R^2 = \left[\frac{\sum_{i=1}^{N} \left[(O_i - O_{avg})(S_i - S_{avg}) \right]}{\left[\sum_{i=1}^{N} \left(O_i - O_{avg} \right)^2 \right]^{0.5} \left[\sum_{i=1}^{N} \left(S_i - S_{avg} \right)^2 \right]^{0.5}} \right]^2 \quad (66)$$

where, O_i is the i^{th} observed parameter, O_{avg} is the mean of the observed parameters, S_i is the i^{th} simulated parameter, S_{avg} is the mean of model simulated parameters and N is the total number of events.

The Nash-Sutcliffe coefficient of efficiency (E_{NS}) has been reported in scientific literatures for model simulations of flow, and water quality constituents such as sediment, nitrogen, and phosphorus yields (Moriasis *et al*., 2007). It is used to assess the predictive power of hydrological models and indicates how well the plot of the observed versus simulated values fit the 1:1 line. The closer the model efficiency is to 1, the more accurate the model is. It is defined as:

$$E_{NS} = 1 - \frac{\sum_{i=1}^{n} (O_i - S_i)^2}{\sum_{i=1}^{n} (O_i - O_{av})^2} \quad (67)$$

where E_{NS} is the Nash-Sutcliffe efficiency of the model; O_i and S_i are the observed and simulated values, respectively, and O_{av} is the average observed values.

SWAT developers in Santhi *et al*. (2001) assumed an acceptable calibration result of $R^2 > 0.6$ and $E_{NS} > 0.5$. Moriasi *et al*. (2007) also proposed that E_{NS} values should exceed 0.5 in order for model results to be judged as satisfactory for hydrologic and pollutant loss evaluations performed on a monthly time step and these values are also considered in this study as adequate statistical values for accepting calibration results.

Effects of Land Use/Cover Changes and Management Practices on the Hydrological Processes

Evaluation of land use change scenarios

To evaluate the effects of land use changes on the hydrological responses of the study watershed mainly on surface runoff and sediment yields, five land use scenarios were formulated and the model was run to simulate runoff and sediment yields under these scenarios. The land use scenarios formulated were based on the patterns of historical land use change, actual growth rate of population, and the land use transition probabilities of the study area from 1985 to 2005 as predicted by Markov model. Moreover, the change under the areas of water bodies and swamp area will be insignificant, and hence considered to remain unchanged during the formulation of land use scenarios.

For developing the various land use scenarios, a neighborhood operation of the spatial analyst tool in GIS is used. It involves a center cell and a set of surrounding cells. In this study, a 3-by-3 rectangular area is used. The center cell was converted to the majority (land use category that occupies the largest percentage of the cell's area). Besides, even though it was tedious and time consuming, pixel-by-pixel editing was used using the editor tool in GIS. For example, when converting forest land or shrub land to agricultural land using this method, the cell under forest land or shrub land next to agricultural land has the highest probability to be converted to agricultural land. Because, farmers usually expand their agricultural land by clearing forest land or shrub land which is found adjacent to their farm lands.

Evaluation of management practice scenarios

In order to understand the effects of land management practices on runoff volumes and sediment yield it is necessary to develop various land management practices or soil conservation interventions scenarios which in turn will help in the planning and management of the land and water resources of the area.

Therefore, to evaluate the variability of hydrologic responses (runoff and sediment yields) due to management practices, the calibrated model was run under the aforementioned land use change scenarios (with and without soil conservation interventions). In order to achieve this purpose, the MUSLE crop cover and management factor (P) was modified in the appropriate SWAT input files. The MUSLE P factor of 0.6 and 1.0, respectively were used during calibration to reflect the condition of the watershed with and without soil conservation intervention.

The possible management practices or soil conservation interventions could be crop residuals, contour tillage, strip cropping on the contour, and terrace systems. Crop residues, for example, intercepts falling raindrops so near the surface that drops regain no fall velocity. They also obstruct runoff flow, reducing its velocity and transport capacity. Contour tillage, strip cropping on the contour, and planting will provide almost complete protection against erosion from storms. Terrace systems, on the other hand, are known for tackling of soil erosion, thus reducing sediment transportation problems.

RESULTS AND DISCUSSION

Analysis of Land Use/Cover Changes

Land use/cover classification

The land use/cover changes of Fincha watershed was analyzed from 1985 to 2005 using remote sensing, GIS, and Markov modeling. The land use/cover maps were produced from Landsat images through supervised classification techniques based on minimum distance algorithms. Analysis was performed using change detection comparison method. Classification was based on a modified version of Anderson scheme of land use/cover classification. Accordingly, the land use/cover of the study watershed for the year 1985, 1995, and 2005 were produced and depicted on Figure 12, 13, and 14, respectively. Six land use/cover classes were established for the study area namely: agricultural land, forest land, grazing land, water bodies, shrub lands, and swamp areas. The land use/cover classes of the study area in hectare and their proportion in each cover type is presented in Table 6.

Table 6 Major land use/cover classes and their proportion in each cover type.

Land use/cover class	1985		1995		2005	
	Area (ha)	%	Area (ha)	%	Area (ha)	%
Agricultural land	113,086	34.79	142,900	43.96	173,692	53.43
Forest land	71,755	22.07	54,824	16.86	35,531	10.93
Grazing land	55,644	17.12	47,001	14.46	38,267	11.77
Water body	20,606	6.34	31,082	9.56	39,790	12.24
Swamp area	38,834	11.95	26,336	8.10	18,885	5.81
Shrub land	25,151	7.74	22,933	7.05	18,911	5.82
Total	325,076	100	32,5076	100	325,076	100

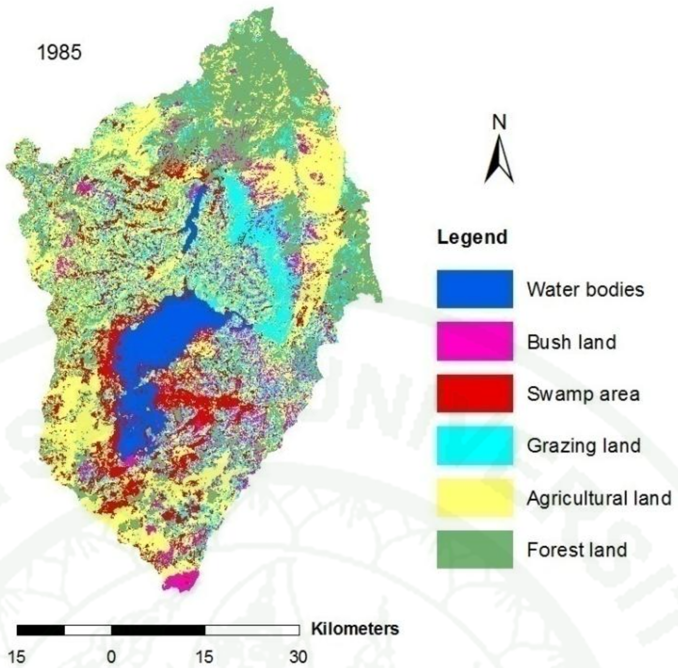

Figure 12 Land use/cover map of Fincha watershed, 1985.

Table 7 Error matrix for the land use/cover of 2005.

	Land use class	Reference data						
		Agricultural land	Forest land	Grazing land	Water body	Swamp area	Shrub land	Row total
Sample data	Agricultural land	45	2	2	2	1	2	54
	Forest land	1	47	2	0	2	3	55
	Grazing land	3	2	47	1	1	2	56
	Water body	0	0	1	50	4	0	55
	Swamp	1	0	3	4	46	2	56
	Shrub land	2	3	2	1	1	40	58
	Column total	52	54	57	58	55	58	334

The overall classification accuracies of the land use/cover maps for the year 1985, 1995, and 2005 were found to be 86.18%, 86.76%, and 87.5%, respectively and the respective KAPPA indices are 0.83, 0.84, and 0.85. This indicates that these data can meet the minimum standard of 85 percent stipulated by the USGS classification scheme (Anderson *et al*., 1976). Overall, the user's and producer's accuracies were high. The confusion or error matrix for the land use/cover of the year 2005 is presented in Table 7.

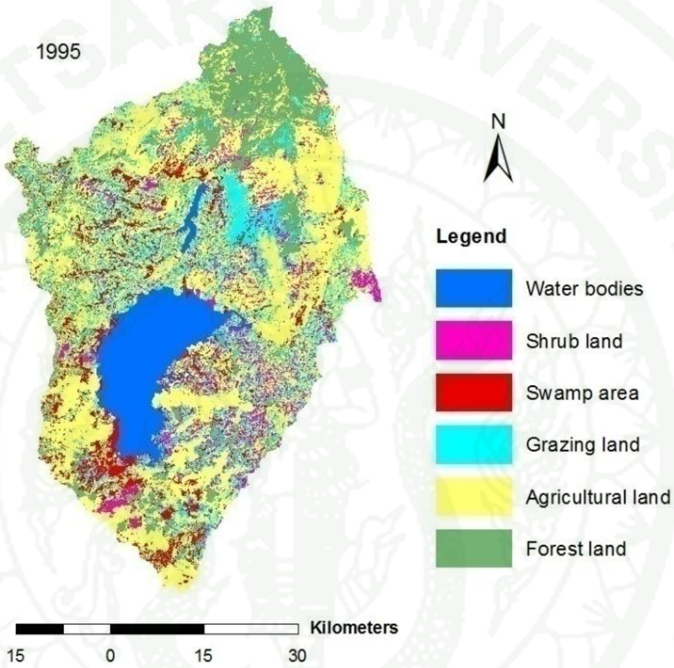

Figure 13 Land use/cover map of Fincha watershed, 1995.

Land use/cover change detection

Change detection is the process of identifying differences in the state of an object or phenomenon by observing it at some interval or at different times (Singh, 1989). Change detection is an important process in monitoring, managing, and evaluation of natural resources because it provides quantitative analysis of the spatial distribution of the population of interest. Remote sensing and GIS based change detection studies have predominantly focused on providing the knowledge of how much, where, what type of land use and land cover change has occurred.

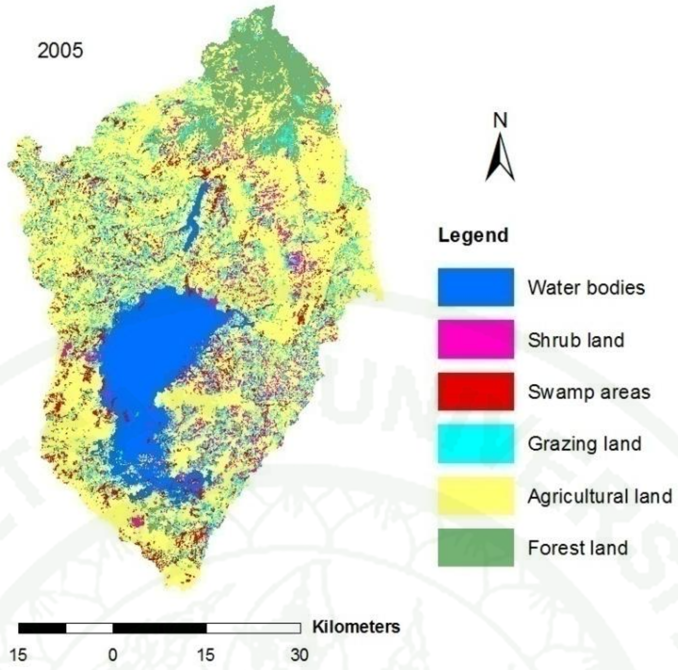

Figure 14 Land use/cover map of Fincha watershed, 2005.

In performing the land use/cover change detection, a post-classification comparison change detection method, the most commonly used quantitative method of change detection (Jensen *et al*., 1993) was used. The maps were compared on a pixel-by-pixel basis using a cross-tabulation detection method (change detection matrix). Pixel-based comparison was used to produce information on pixel basis and, thus interpret the changes more efficiently taking the advantage of "from - to" information. That means change matrix gives the knowledge of the main direction of changes (from-to information) in the study area. Classified image pairs of consecutive years were compared using cross-tabulation in order to determine qualitative and quantitative aspects of the change.

Accordingly cross tabulation or change detection matrix was produced between two consecutive study periods and quantitative areal data of the overall land use/cover changes as well as gains and losses in each category for the study periods were compiled. It is a means to determine amounts of conversion from a particular land use/cover to the other land use/cover categories at later date. In cross tabulation, difference between row and column totals of a particular land use/cover type yields the amount of gains (positive) or losses (negative) between two dates.

Table 8 Land use/cover change matrix between 1985 and 1995.

1985	1995 Agricultural land	Forest land	Grazing land	Water body	Swamp	Shrub land	1985 total
Agricultural land	68,841	31,270	6,414	81	346	6,134	113,086
Forest land	37,094	17,152	10,302	449	935	5,823	71,755
Grazing land	28,517	1,388	15,018	8,540	449	1,731	55,644
Water body	147	0	2,095	15,893	2,157	313	20,606
Swamp	520	493	10,475	2,336	20,247	4,762	38,834
Shrub land	7,781	4,521	2,698	3,783	2,200	4,169	25,151
1995 total	142,900	54,824	47,001	31,082	26,336	22,932	325,076

Land use change between 1985 and 1995

Cross-tabulation of the 1985 and 1995 classification clearly shows large amounts of conversions mainly from forest, grazing, shrub lands and swamp areas. The cross-tabulation or the land use/cover change detection matrix (in hectare) between 1985 and 1995 is presented in Tables 8. The amount or quantity of changes (gains or losses) during this period is presented in Table 9. During this period, agricultural land and water bodies have increased in area by as much as 29,814 ha (26.36%) and 10,476 ha (50.84%), respectively. In contrast, forest land, grazing land, swamp areas, and shrub lands have decreased in area by16,931 ha (23.60%), 8,642 ha (15.53%), 12,498 ha (32.18%), and 2,218 ha (8.82%), respectively.

Table 9 Quantity of changes (gains or losses) between 1985 and 1995.

Land use/cover class	1985 Area (ha)	1995 Area (ha)	Change (ha)	Change (%)
Agricultural land	113,086	142,900	29,814	26.36
Forest land	71,755	54,824	16,931	-23.60
Grazing land	55,644	47,001	8,643	-15.53
Water body	20,606	31,082	10,476	50.84
Swamp area	38,834	26,336	12,498	-32.18
Shrub land	25,151	22,933	2,218	-8.82

Land use change between 1995 and 2005

The land use/cover change detection matrix (in hectare) between 1995 and 2005 is presented in Tables 10. The quantity of changes during this period is also presented in Table 11. During this period, agricultural land and water bodies have increased in area by 30,792 ha (21.55%) and 8,708 ha (28.02%), respectively. But, forest land, grazing land, swamp areas, and shrub lands have decreased in area by 19,293 ha (35.19%), 8,734 ha (18.58%), 7,450 ha (28.29%), and 4,022 ha (17.54%), respectively.

Table 10 Land use/cover change matrix between 1995 and 2005.

1995	2005 Agricultural land	Forest land	Grazing land	Water body	Swamp	Shrub land	1995 total
Agricultural land	107,778	22,392	6,063	81	426	6,161	142,900
Forest land	29,424	9,016	9,327	449	936	5,671	54,824
Grazing land	28,525	1,550	7,691	7,728	482	1,025	47,001
Water body	204	0	1,851	26,477	2,133	417	31,082
Swamp	520	4,93	10,475	1,280	12,125	1,442	26,336
Shrub land	7,240	2,080	2,860	3,775	2,784	4,194	22,932
2005 total	173,692	35,531	38,267	39,790	18,885	18,911	325,076

Table 11 Quantity of changes (gains or losses) between 1995 and 2005.

Land use/cover class	1995 Area (ha)	2005 Area (ha)	Change (ha)	Change %)
Agricultural land	142,900	173,692	30,792	21.55
Forest land	54,824	35,531	19,293	-35.19
Grazing land	47,001	38,267	8,734	-18.58
Water body	31,082	39,790	8,708	28.02
Swamp area	26,336	18,885	7,451	-28.29
Shrub land	22,933	18,911	4,022	-17.54

Land use change between 1985 and 2005

The land use/cover change detection matrix (in hectare) between 1985 and 2005 is presented in Tables 12. The quantity of changes during this period is presented in Table 13. During the whole study period (1985-2005), there has been an appreciable increase in the area of agricultural land and water bodies with associated shrinkage in the area of forest land, grazing land, swamp areas, and shrub lands. In these 20 years of the study period, agricultural land increased from 113,086 ha in 1985 to 173,692 ha in 2005. That means the area under agricultural land increased by 60,606 ha (53.59%) within 20 years. Similarly, the area of water bodies has increased from 20,606 ha in 1985 to 39,790 ha in 2005. This indicated that the area of water body have increased by 19,184 ha (93.10%).

On the other hand, the area under forest land, grazing land, swamp areas, and shrub lands have dramatically decreased. Within 20 years of the study period (from 1985 to 2005), forest lands, grazing lands, swamp areas, and shrub lands have decreased in area by as much as 36,225 ha (50.48%), 17,376 ha (31.23%), 19,948 ha (51.37%), and 6,240 ha (24.81%), respectively.

Table 12 Land use/cover change matrix between 1985 and 2005.

	2005						
1985	Agricultural land	Forest land	Grazing land	Water body	Swamp	Shrub land	1985 total
Agricultural land	100,996	1,444	5,583	974	426	3,663	113,086
Forest land	33,859	28,502	2,179	449	944	5,823	71,755
Grazing land	30,142	1,388	15,814	7,728	457	115	55,644
Water body	367	0	2,176	17,217	533	313	20,606
Swamp	548	489	9,817	8,827	14,326	4,827	38,834
Shrub land	7,781	3,709	2,698	4,595	2,200	4,169	25,151
2005 total	173,692	35,531	38,267	39,790	18,885	18,911	325,076

Table 13 Quantity of changes (gains or losses) between 1985 and 2005.

Land use/cover class	1985 Area (ha)	2005 Area (ha)	Change (ha)	Change %)
Agricultural land	113,086	173,692	60,606	53.59
Forest land	71,755	35,531	36,224	-50.48
Grazing land	55,644	38,267	17,377	-31.23
Water body	20,606	39,790	19,184	93.10
Swamp area	38,834	18,885	19,949	-51.37
Shrub land	25,151	18,911	6,240	-24.81

Land use/cover change analysis

Analysis results between 1985 and 2005 (Table 8) clearly revealed that for the increase in the area of agricultural land, about one-third and one-forth increase are from forest and grazing lands, respectively. The contribution from shrub lands is less than 7%. This is an indicator of agricultural expansion in the watershed. The analysis further indicated that grazing land, swamp areas, and shrub lands have contributed about 41%, 11%, and 18%, respectively to the increase in the area of the water bodies.

During the second ten years of the study period from 1995 to 2005 (Table 10), it is evident from the result that, about 40% increase in the area of agricultural land comes from forest and grazing lands. Shrub land has contributed only about 5%. During the same period, about 24.86% and 12.15% increase to the area of water bodies are from grazing land and swamp areas, respectively. The contribution from shrub land is less than 5%.

Analysis of the remote sensing data also clearly indicated that, during the whole twenty years of the study period (Table 12), for the increase in the area of agricultural land about 30% and 26% increase comes from forest lands and grazing lands, respectively. The contribution from shrub lands is estimated to only less than 7%. The results further indicated that grazing lands, swamp areas, and shrub lands contributed about 37%, 42%, and 22%, respectively to the increase in the area of water bodies.

The increase in the area of water body was resulted following the diversion of Amarti River to Fincha reservoir through a tunnel of 1.5 km in 1987 which supplies about 138.8 Mm^3 of runoff annually to the reservoir (EELPA, 1994). The increase in the total volume of water in the reservoir resulted to the increase in the area of backing water that inundated large areas of swamp, grazing land, shrub land, and agricultural lands. Some forest lands were also inundated by the backing water. Moreover, runoff that comes from inappropriate farming practices surrounding the reservoir deposits huge amounts of sediments into the reservoir, thereby decreasing the depth of the reservoir and increasing the backing water.

During the study period land use/cover change from one category to another was observed throughout the watershed. However, compared to other areas much changes were observed adjacent to and downstream of the Fincha reservoir. The land use/cover change observed surrounding the Fincha reservoir is due to two reasons. The first reason is as the result of the increase in the volume of the Reservoir the backing water inundated large areas of swamp, grazing lands, agricultural lands, and shrub lands and evicted many people from their original places. The second reason is that the displaced farmers moved to the upstream areas and open up new farm lands on the expenses of forest lands, grazing lands, shrub lands, and other marginal areas that resulted in much greater change.

On the other hand, the vast conversion of forest lands, grazing lands, and shrub lands to agricultural lands downstream of the Fincha reservoir has to do with the expansion of sugar cane production for the newly established sugar factory. This is clearly evidenced by the fact that the area under sugar cane production has been increasing from year to year.

Stability of land use/cover change process

Markovian chain analysis describes land use change from one period to another and uses this as the basis to project future changes. This is achieved by developing a transition probability (TP) matrix of land use change from time one to time two, which shows the nature of change while still serving as the basis for projecting to a later time period. Though the transition probabilities may be accurate on a per category basis, there is no knowledge of the spatial distribution of occurrences within each land use category.

The transition probabilities governing the periods 1985 - 1995, 1995 - 2005, and 1985 - 2005 are presented in Tables 14, 15, and 16, respectively. For instance, during the whole study period of twenty years (1985 – 2005), the TP from forest land, grazing land, and shrub lands to agricultural land was 0.0236, 0.271, and 0.0155, respectively; and so forth. The computation is based on the actual number of observations in land use/cover change during the same study period.

Table 14 Land use/cover transition probabilities (%), 1985–1995.

	1995					
1985	Agricultural land	Forest land	Grazing land	Water body	Swamp	Shrub land
Agricultural land	96.09	2.77	0.57	0.01	0.03	0.54
Forest land	5.17	92.39	1.44	0.06	0.13	0.81
Grazing land	5.12	0.25	92.70	1.53	0.08	0.31
Water body	0.07	0.00	1.02	97.71	1.05	0.15
Swamp	0.13	0.13	2.70	0.60	95.21	1.23
Shrub land	3.09	1.80	1.07	1.50	0.87	91.66

The expected transition probabilities from 1985 to 2005 under the Markov hypothesis are presented in Table 17. They were obtained by multiplying the periods 1985-1995 and 1995-2005 matrices using Chapman–Kolmogorov. From the table, it can be noted that if the land use and land cover change process was Markovian, the TP to agricultural lands from forest lands, grazing lands, and shrub lands would have been 0.101, 0.1065, and 0.608, respectively and so forth.

Table 15 Land use/cover transition probabilities (%), 1995–2005.

	2005					
1995	Agricultural land	Forest land	Grazing land	Water body	Swamp	Shrub land
Agricultural land	97.54	1.57	0.42	0.01	0.03	0.43
Forest land	5.37	91.64	1.70	0.08	0.17	1.03
Grazing land	6.07	0.33	91.64	1.64	0.10	0.22
Water body	0.07	0.00	0.60	98.52	0.69	0.13
Swamp	0.20	0.19	3.98	0.49	94.60	0.55
Shrub land	3.16	0.91	1.25	1.65	1.21	91.83

Table 16 Land use/cover transition probabilities (%), 1985–2005.

	2005					
1985	Agricultural land	Forest land	Grazing land	Water body	Swamp	Shrub land
Agricultural land	99.47	0.06	0.25	0.04	0.02	0.16
Forest land	2.36	96.99	0.15	0.03	0.07	0.41
Grazing land	2.71	0.12	96.42	0.69	0.04	0.01
Water body	0.09	0.00	0.53	99.18	0.13	0.08
Swamp	0.07	0.06	1.26	1.14	96.84	0.62
Shrub land	1.55	0.74	0.54	0.91	0.44	95.83

The computed value of the statistic χ^2 is $1.31*10^5$, much greater than 37.65 (value of χ^2 from table at $\alpha = 0.05$ with degree of freedom of 25). The hypothesis of statistical independence is therefore rejected. The land use/cover change data are statistically dependent, but the question is whether this dependence can be characterized by first-order Markov dependence, or by higher order dependence. The hypothesis that land use and land cover change are dependent is thus accepted. In other words, it can be hypothesized that the data are generated by a Markov process at a risk of 5%.

Table 17 Expected values of land use TPs under Markov hypothesis, 1985–2005.

	2005					
1985	Agricultural land	Forest land	Grazing land	Water body	Swamp	Shrub land
Agricultural land	93.93	4.05	0.98	0.03	0.07	0.94
Forest land	10.11	84.76	2.93	0.18	0.29	1.73
Grazing land	10.65	0.62	84.99	3.04	0.19	0.52
Water body	0.20	0.01	1.56	96.29	1.66	0.28
Swamp	0.53	0.32	6.28	1.12	90.10	1.66
Shrub land	6.08	2.53	2.21	3.01	1.96	84.21

Table 18 Comparison of steady state probabilities.

Study period	Agricultural land	Forest land	Grazing land	Water bodies	Swamp	Shrub land
1985 - 1995	0.4478	0.1819	0.1180	0.1395	0.0515	0.0613
1995 - 2005	0.5325	0.1098	0.0893	0.1765	0.0418	0.0501
1985 - 2005	0.6696	0.0264	0.0835	0.1688	0.0173	0.0344

Whether the land use/cover change process in the area has been stabilized is a more critical issue relating to land development policies. To answer this question, steady state probabilities of the three different periods were computed and compared and presented in Table 18. These values show the probabilities that a cell (parcel of land) will be in the different categories at a sufficiently distant point in time. A short inspection of this table indicates that the three distributions are distinctly different, implying the differences in transition mechanism. As a result, the idea that the process is stationary may be rejected although this assumption has not been thoroughly tested as a hypothesis. However, if the three transition mechanisms are to continue in a stationary manner, the distribution of land use/cover categories can be projected for a remote future: 66.96% of the watershed will be agriculture land, 2.64% will be forest lands, 8.35% will be grazing lands, 16.88% will be water bodies, 1.73% will be swamp area, and, 3.44% will be shrub lands.

It was also attempted to predict the future land use/cover patterns of the study area about 20 years in to the future from 2005 onwards based on the land use/cover transition probabilities from 1985 to 1995, 1995 to 2005, and 1985 to 2005. In order to achieve this purpose input data for Markov model was prepared using these transition probabilities. The respective input data are presented in Appendix Table 12, 13, and 14, respectively and Markov model make use of these data in order to predict the land use/cover patterns of the study watershed for the year 2025. The projected land use/cover of the study area and their proportion in each cover type are presented in Tables 19, 20, and 21. However, since the three study periods have different transition mechanisms, the land use/cover pattern of the study area projected for the year 2005 by Markov model based on the three transition probabilities are different.

In order to evaluate the effects of land use change on the hydrological responses of the watershed (particularly on runoff volumes and sediment yields) about twenty years in to the future, the possible land use pattern of the study area was formulated based on the land use transition probabilities of the study area from 1985 to 2005 as predicted by Markov model (Table 21).

Table 19 Matrix projection by Markov model based on the land use transition probability from 1985-1995.

Year	% in each cover type					
	Agricultural land	Forest land	Grazing land	Water body	Swamp	Shrub land
2005	43.70	18.30	13.50	10.60	7.20	6.70
2006	43.90	18.30	13.40	10.70	7.00	6.70
2007	44.00	18.30	13.30	10.80	6.90	6.70
2008	44.10	18.30	13.20	10.90	6.80	6.60
2009	44.20	18.20	13.10	11.00	6.70	6.60
2010	44.40	18.20	13.00	11.20	6.60	6.60
2011	44.50	18.20	13.00	11.20	6.50	6.60
2012	44.50	18.20	12.90	11.30	6.40	6.60
2013	44.60	18.20	12.80	11.40	6.30	6.50
2014	44.70	18.20	12.80	11.50	6.30	6.50
2015	44.80	18.20	12.70	11.60	6.20	6.50
2016	44.80	18.30	12.60	11.70	6.10	6.50
2017	44.90	18.30	12.60	11.80	6.10	6.50
2018	44.90	18.30	12.50	11.80	6.00	6.40
2019	45.00	18.30	12.50	11.90	5.90	6.40
2020	45.00	18.30	12.40	12.00	5.90	6.40
2021	45.00	18.30	12.40	12.00	5.80	6.40
2022	45.10	18.30	12.40	12.10	5.80	6.40
2023	45.10	18.30	12.30	12.20	5.70	6.40
2024	45.10	18.30	12.30	12.20	5.70	6.40
2025	45.20	18.30	12.30	12.30	5.60	6.40

Table 20 Matrix projection by Markov model based on the land use transition probability from 1995-2005.

Year	% in each cover type Agricultural land	Forest land	Grazing land	Water body	Swamp	Shrub land
2005	50.60	13.10	12.10	11.80	6.30	6.10
2006	51.10	12.90	12.00	11.90	6.10	6.00
2007	51.40	12.70	11.80	12.10	6.00	6.00
2008	51.80	12.60	11.60	12.20	5.90	5.90
2009	52.10	12.40	11.50	12.40	5.80	5.80
2010	52.40	12.30	11.30	12.50	5.70	5.80
2011	52.60	12.20	11.20	12.70	5.60	5.70
2012	52.90	12.10	11.00	12.80	5.50	5.70
2013	53.10	12.00	10.90	12.90	5.40	5.70
2014	53.30	11.90	10.80	13.10	5.30	5.60
2015	53.50	11.90	10.70	13.20	5.20	5.60
2016	53.60	11.80	10.60	13.30	5.10	5.60
2017	53.80	11.80	10.50	13.40	5.10	5.50
2018	53.90	11.70	10.40	13.50	5.00	5.50
2019	54.10	11.70	10.30	13.60	4.90	5.50
2020	54.20	11.60	10.20	13.70	4.90	5.40
2021	54.30	11.60	10.10	13.80	4.80	5.40
2022	54.40	11.60	10.00	13.90	4.80	5.40
2023	54.40	11.60	10.00	13.90	4.70	5.40
2024	54.50	11.50	9.90	14.00	4.70	5.40
2025	54.60	11.50	9.80	14.10	4.60	5.30

Table 21 Matrix projection by Markov model based on the land use transition probability from 1985-2005.

Year	% in each cover type					
	Agricultural land	Forest land	Grazing land	Water body	Swamp	Shrub land
2005	49.10	13.50	13.10	10.90	7.30	6.10
2006	49.60	13.20	12.90	11.00	7.10	6.00
2007	50.10	12.90	12.80	11.20	7.00	6.00
2008	50.60	12.60	12.70	11.40	6.80	5.90
2009	51.10	12.30	12.50	11.50	6.70	5.90
2010	51.60	12.10	12.40	11.70	6.50	5.80
2011	52.00	11.80	12.30	11.80	6.40	5.70
2012	52.50	11.50	12.20	11.90	6.20	5.70
2013	52.90	11.30	12.00	12.10	6.10	5.60
2014	53.30	11.00	11.90	12.20	6.00	5.60
2015	53.70	10.80	11.80	12.30	5.80	5.50
2016	54.10	10.60	11.70	12.50	5.70	5.50
2017	54.50	10.30	11.60	12.60	5.60	5.40
2018	54.80	10.10	11.50	12.70	5.50	5.40
2019	55.20	9.90	11.40	12.80	5.40	5.30
2020	55.50	9.70	11.30	12.90	5.30	5.30
2021	55.90	9.50	11.20	13.00	5.20	5.20
2022	56.20	9.30	11.10	13.10	5.10	5.20
2023	56.50	9.10	11.10	13.20	5.00	5.10
2024	56.80	8.90	11.00	13.30	4.90	5.10
2025	57.10	8.70	10.90	13.40	4.80	5.00

Simulation of the Hydrological Processes Using SWAT Model

The Soil and Water Assessment Tool (SWAT) model has been calibrated and validated on monthly bases to predict the hydrological processes from the Fincha watershed using time series data of 22 years from 1985- 2006. The first two years of the modeling period were used for 'model warm-up'. Data pertaining to year 1987- 1996 were used for the calibration period and the remaining data sets from 1997-2006 were reserved for the validation period. During the delineation process, using a threshold value of 5,000 ha, the watershed is subdivided into 19 subbasins which accounts for the main drainage lines within the watershed. This resulted in a better representation of the hydrological processes and good estimation of simulated values which had a better model efficiency while comparing with the observed values. Figure 15 shows the subbasins of the Fincha watershed automatically delineated during watershed delineation.

Analysis of hydrologic response units (HRUs) showed that the overlay of land use, soil, and slope maps resulted into the definitions of 72 HRUs. This resulted in detailed land use, slope, and soil database, containing many HRUs which in turn represent the heterogeneity of the study area. The distribution of land use, soil, and slope characteristics within each HRU have great impact on the predicted values. The calibrated values of various model parameters for optimum model outputs are presented in Table 22.

Table 22 Calibrated values of model parameters.

Parameter	Description	Model range	Fitted value
CN2	Initial SCS runoff curve number for moisture condition II	±10%	+5%
C-factor	Cover or management factor	0.003 - 0.45	0.2
SPCON	Linear factor for channel sediment routing	0.0001- 0.01	0.0008
SPEXP	Exponential factor for channel sediment routing	1.0 - 1.5	1.0

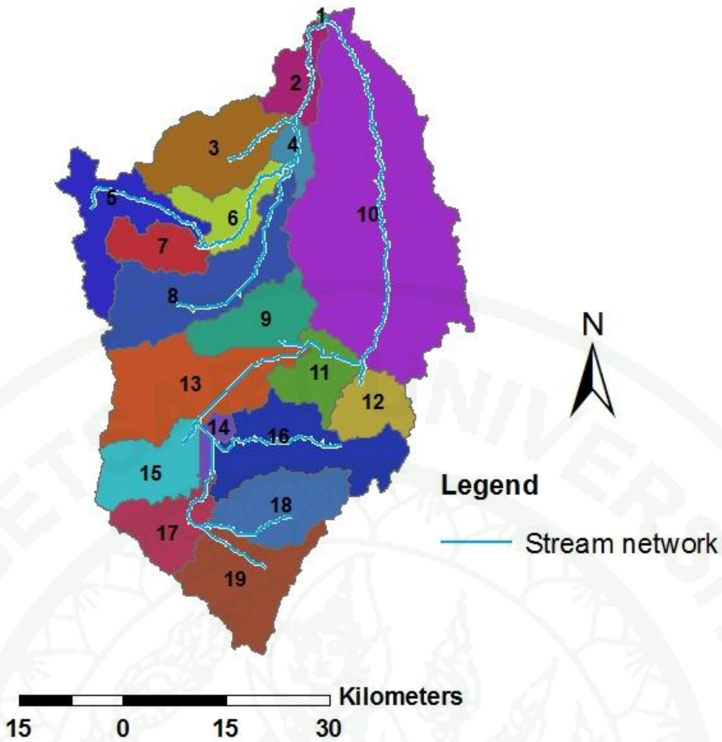

Figure 15 Subbasins of Fincha watershed.

Model calibration

During the calibration period from 1987- 1996, the simulated average monthly flow matched well with the average monthly measured flow (with R^2 = 0.82 and E_{NS} = 0.72). Figure 20 shows the comparison of the simulated versus observed average monthly flow. It may be observed from the figure that the simulated average monthly flow (shown as solid line) is consistently lower than the observed average monthly flow. This shows that the trend of seasonal variability and monthly average discharges are generally well captured. The adequacy of the model is further indicated by its clear response to extreme rainfall events resulting in high runoff volume (Example in August 1994). However, the model underestimated the peak monthly flow during the first five (1987-1991) and the last two years (1995 and 1996) of the simulation periods and overestimated the peak monthly flow from 1992-1994 (Figure 16). Nevertheless, as it can be clearly seen on the scatter plot of the simulated versus observed average monthly flow (Figure 17), the predicted values were generally underestimated by the model.

Table 23 Monthly calibration and validation statistical results.

Description	R^2	E_{NS}	Mean		Standard Deviation	
			Observed	Simulated	Observed	Simulated
Flow (cms)						
Calibration	0.82	0.72	140.35	129.73	145.84	139.58
Validation	0.81	0.77	121.26	114.95	124.73	122.29
Sediment yield (t/ha)						
Calibration	0.82	0.80	30.18	26.94	39.85	44.93
Validation	0.80	0.78	25.38	22.84	35.79	36.77

The monthly calibrated and validated statistical results are presented in Table 23. The results clearly showed that means and standard deviations of the average monthly simulated and observed flows are within a difference of 7.57% and 4.29%, respectively during calibration period and 5.20% and 1.96%, respectively during validation period.

The simulated monthly runoff volume (in mm) for the entire simulation period is presented in Table 24. The simulated average monthly runoff volumes are in close agreement with the average monthly observed runoff volumes. They are within a difference of 3 - 9% of the monthly observed runoff volumes. This close agreement shows that the SWAT model is able to simulate flows in Fincha watershed.

The model also showed adequacy in predicting the average monthly sediment yields in the study area with R^2 and E_{NS} values of 0.81 and 0.78, respectively during calibration (Table 23). From the table it is clearly indicated that means and standard deviations of the average monthly simulated and observed sediment yields are within a difference of 10.73% and 12.75%, respectively during calibration and 10.0% and 2.74%, respectively during validation.

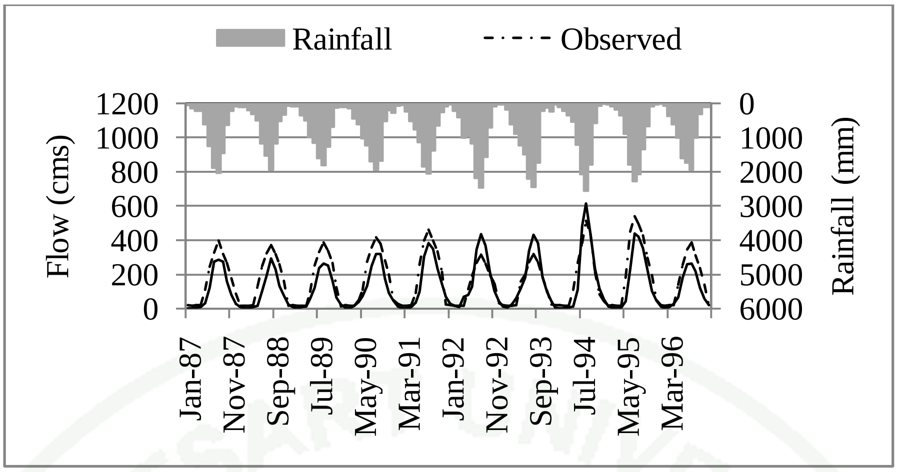

Figure 16 Simulated and observed average monthly flows during calibration.

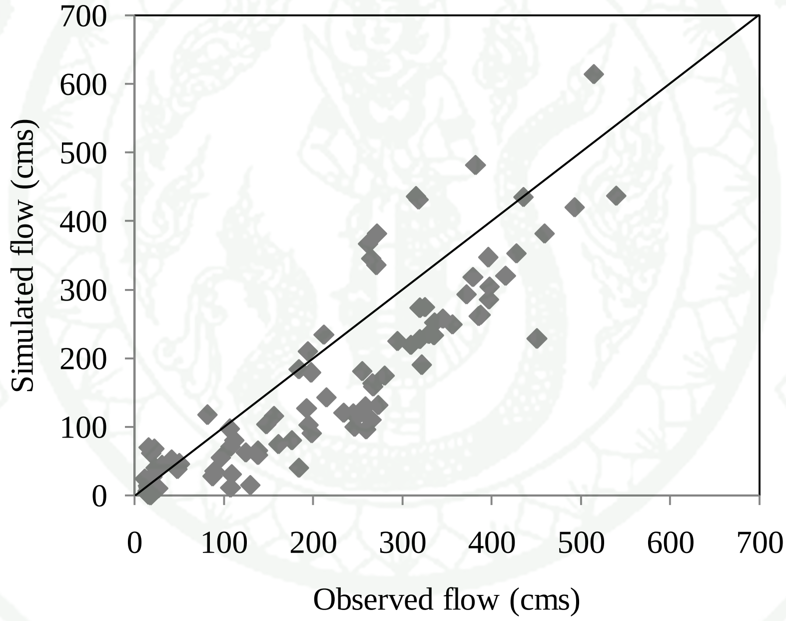

Figure 17 Scatter plot of the simulated vs. observed average monthly flow during calibration.

During this period, the simulated average monthly sediment yields matched well with the measured average monthly sediment yields (Figure 18 and 19). However, the scatter plot of the simulated versus observed average monthly sediment yields shown on Figure 19 clearly indicated that the model over-predicted the sediment yield values during wet season from 1991-1995. On the other hand, during the first four years of wet season periods (1987-1990) and the last wet season period (1996), the average monthly sediment yield values were under predicted by the model which could be the result of siltation of more sediments into the reservoir. Moreover, such behavior of the simulated sediment yields indicated the high deposition of sediments as they travel along the channel.

The simulated monthly sediment yields (in t/ha) for the entire simulation period is presented in Table 25. The simulated values are in close agreement with the observed values. They are within a difference of 2 - 11% of the average monthly observed sediment yields. This close agreement proved that the SWAT model can realistically simulate sediment yield in the study watershed.

The average annual basin values for the entire watershed during the whole simulation period (1985-2006) are presented in Table 26. The overall average annual water yield as simulated by the SWAT model for the entire watershed is about 1049.02 mm. The average annual values of various water balance components for the study watershed are: precipitation 1890.57 mm, percolation 474.13 mm, actual ET 732.63 mm, potential ET 1719.74 mm, base flow 440.25 mm, lateral soil flow 472.84 mm, and surface flow 139.33 mm. Moreover, the average annual sediment yield is 42.41 t/ha. The result showed that base flow, lateral flow, and surface flow accounts for about 42%, 45%, and 13% of the total water yield, respectively. This shows that on average about 13% of the total water yield is annually lost as surface runoff from the watershed.

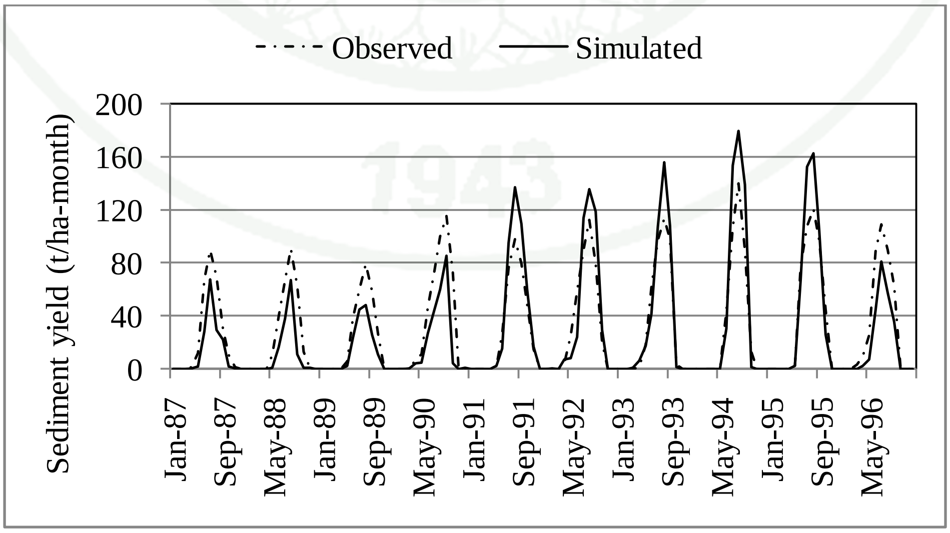

Figure 18 Simulated and observed average monthly sediment yields during calibration.

Table 24 Simulated monthly runoff volumes.

Year	Jan	Feb	Mar	Apr	May	Jun	Jul	Aug	Sep	Oct	Nov	Dec	Total
1985	0	0	0.1	8.26	2.82	20.36	89.75	101.74	24.73	0.6	0	0	248.36
1986	0	0	0.05	2.43	4.43	11.34	35.32	19.24	8.9	0.86	0	0	82.57
1987	0	0	0	0.37	0.49	15.37	53.78	37.47	19.63	6.18	0.68	0	133.97
1988	0	0	0	0.01	0.08	13.62	25.25	30.27	13.42	4.33	1.02	0	88.01
1989	0	0	0.03	1.3	3.85	12.05	33.36	17.84	12.93	4.43	0	0	85.79
1990	0	0	0.15	1	3.06	14.49	32.59	29.56	16.86	0.08	0	0	97.79
1991	0	0	0	0.01	1.41	12.18	49.7	51.34	29.13	6.8	0.82	0	151.39
1992	0	0.11	0.09	6.03	2.42	12.75	60.59	65.7	23.46	2.24	0	0	173.39
1993	0	0	0.49	3.39	5.58	17.87	59.39	53.7	24.12	0.09	0	0	164.63
1994	0	0	0.01	0.21	0.51	19.53	109.41	118.47	24.12	1.07	0.01	0	273.34
1995	0	0	0.04	0.27	2.66	35.76	80.19	45.1	20.94	2.92	0	0	187.88
1996	0	0	1.22	2.07	3.97	31.84	41.07	24.02	6.8	0	0	0	110.99

Table 24 (Continued).

Year	Jan	Feb	Mar	Apr	May	Jun	Jul	Aug	Sep	Oct	Nov	Dec	Total
1997	0	0	0	0.86	1.65	12	23.35	4.98	3.49	0	0	0	46.33
1998	0	0	0	0.07	0.02	27.51	25.28	10.44	4.69	0	0	0	68.01
1999	0	0	0.05	0.47	1.2	9.33	18.17	17.33	3.7	0	0.32	0	50.57
2000	0	0	0.03	0	1.58	18.78	42.46	34.98	25.54	8.9	0.65	0	132.92
2001	0	0	0.12	1.91	2.34	14.81	39.84	38.8	19.31	0.75	0	0.06	117.94
2002	0	0.67	0.13	9.44	4.62	22.26	87.12	73.9	20.16	0.3	0	0	218.6
2003	0	0.05	0.01	2.43	2.75	15.67	62.48	32.75	8.35	0	0	0	124.49
2004	0	0	0.52	4.54	12.72	42.6	33.67	25.08	6.52	0.01	0	0	125.66
2005	0	0	0	0	0.04	20.92	77.7	82.73	16.69	0.03	0	0	198.11
2006	0	0	0.04	1.26	14.9	47.25	68.06	38.46	12.35	2.28	0	0	184.6
Average	0	0.04	0.14	2.1	3.32	20.38	52.21	43.36	15/72	1.9	0.16	0	139.33

Table 25 Simulated monthly sediment yields.

Year	Jan	Feb	Mar	Apr	May	Jun	Jul	Aug	Sep	Oct	Nov	Dec	Total
1985	0	0	0	2	0.4	5.03	16.9	21.3	4.51	0.2	0	0	50.38
1986	0	0	0	0.2	0.8	2.55	5.63	1.84	0.67	0.3	0	0	12.05
1987	0	0	0	0	0	3.79	9.04	6.17	5.19	3.2	0.3	0	27.78
1988	0	0	0	0	0	2.35	7.9	10.6	6.31	2.6	0.6	0	30.38
1989	0	0	0	0.2	0.6	2.36	11.3	6.23	4.78	2.3	0	0	27.83
1990	0	0	0	0.2	0.6	3.41	7.74	11.1	6.33	0	0	0	29.37
1991	0	0	0	0	0.4	2.9	18.7	30.9	18.8	8.7	0.9	0	81.36
1992	0	0	0	2.3	0.4	2.77	20.4	24.6	10.4	1.8	0	0	62.63
1993	0	0	0.2	0.6	1.2	4.75	17.7	18.3	7.26	0	0	0	50.01
1994	0	0	0	0	0	8.07	35.4	55	10.6	0.2	0	0	109.3
1995	0	0	0	0.1	0.6	12.8	23.7	15.4	8.63	1.9	0	0	63.02
1996	0	0	0.2	0.2	0.5	6.93	9.81	5.79	1.78	0	0	0	25.27

Table 25 (Continued).

Year	Jan	Feb	Mar	Apr	May	Jun	Jul	Aug	Sep	Oct	Nov	Dec	Total
1997	0	0	0	0.2	0.7	3.13	4.7	0.6	1.41	0	0	0	10.68
1998	0	0	0	0	0	8.39	5.81	1.91	1.6	0	0	0	17.71
1999	0	0	0	0.1	0.2	2.63	5.4	5.42	0.93	0	0.1	0	14.81
2000	0	0	0	0	0.4	8.61	13.3	8.74	9.31	7.7	0.1	0	48.23
2001	0	0	0	0.6	0.9	4.58	15.7	18.8	7.52	0.5	0	0	48.52
2002	0	0.2	0	2.2	1	8.87	25.7	19.8	7.24	0.1	0	0	65.06
2003	0	0.1	0	0.6	0.3	4.47	14.2	6.25	1.64	0	0	0	27.53
2004	0	0	0.4	1.4	3.7	16.5	8.87	5.06	1.18	0	0	0	37.11
2005	0	0	0	0	0	5.4	17.9	19.7	3.42	0	0	0	46.49
2006	0	0	0	0.3	8.7	16.2	13.1	6.34	2.32	0.5	0	0	47.46
Average	0	0.01	0.04	0.51	0.97	6.21	14.04	13.64	5.54	1.36	0.09	0	42.41

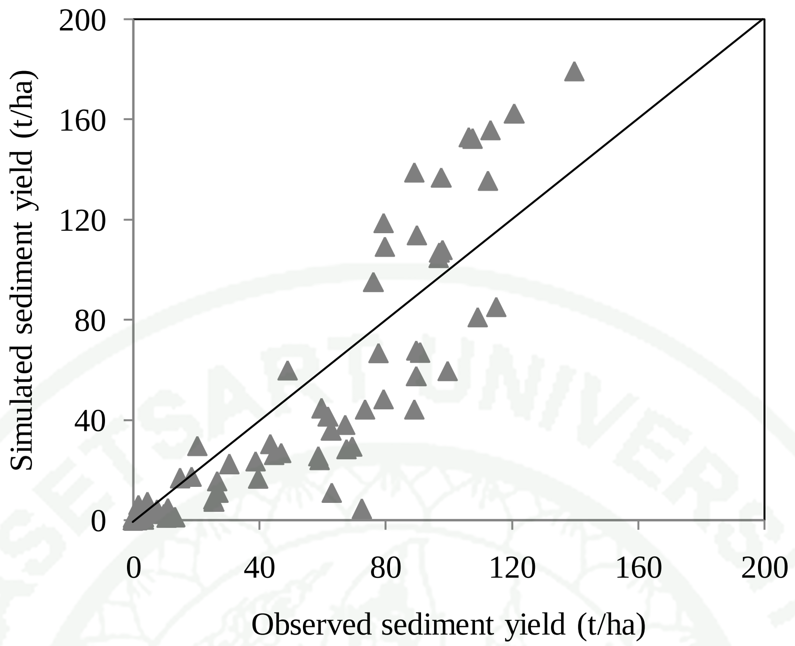

Figure 19 Scatter plot of the simulated vs observed average monthly sediment yields during calibration.

Model validation

SWAT model also successfully validated for flow from 1997 to 2006 (Table 23). Monthly flow rates were well predicted and measured and simulated monthly flows matched well (with R^2 = 0.81 and E_{NS} = 0.77) (Figure 20 and 21). The model under predicted the flow during the years from 1997-2000 and from 2003-2004; and over predicted from 2001-2002, and from 2005-2006. However, the trend of seasonal variability and monthly average discharges were generally well captured.

Model validation results also showed that the monthly predicted and observed sediment yields matched well with R^2 and E_{NS} values of 0.80 and 0.78, respectively (Table 23) except for the month of July 2002 when the flow was also overestimated by the model. Figure 22 shows the simulated and observed sediment yields during validation period. The scatter plot of the observed versus simulated sediment yields is shown on Figure 23.

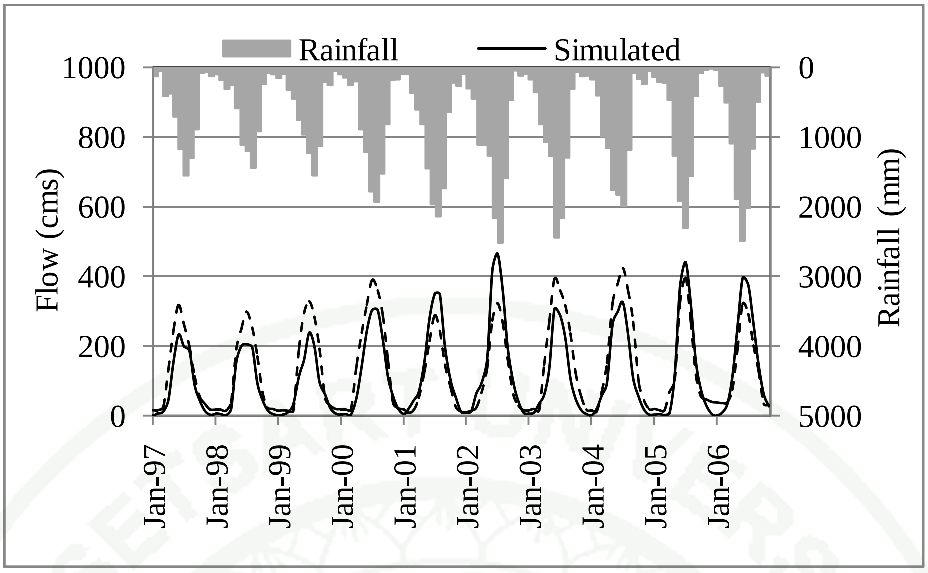

Figure 20 Simulated and observed average monthly flows during validation.

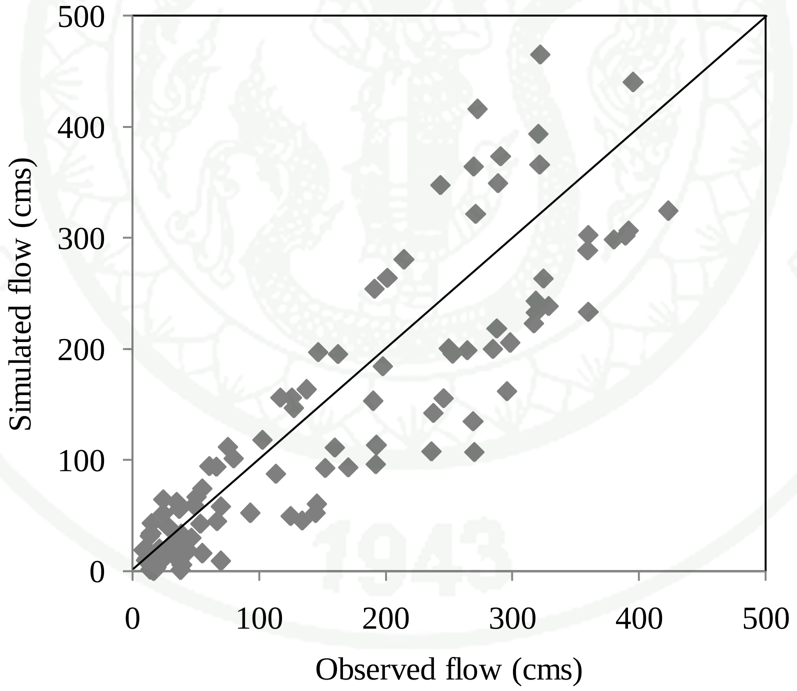

Figure 21 Scatter plot of the simulated vs. observed average monthly flows during validation.

Table 26 Simulated average annual basin values.

Year	Rainfall (mm)	Surface flow (mm)	Lateral flow (mm)	Base flow (mm)	Perco. (mm)	Soil water (mm)	Actual ET (mm)	Potential ET (mm)	Water yield (mm)	Sediment yield (mm)
1985	2048	248	524	569	622	92.8	630	1672	1338	50.4
1986	1534	82.6	363	356	376	98.5	689	1527	798.7	12.1
1987	1677	134	404	342	373	83.8	712	1792	876.2	27.8
1988	1568	88	378	306	333	91.2	720	1952	769.5	30.4
1989	1738	85.8	430	315	340	89.7	784	1671	827.1	27.8
1990	2040	97.8	507	399	437	91.4	869	1666	1000	29.4
1991	2070	151	534	500	559	83.6	760	2035	1181	81.4
1992	2277	173	606	565	590	95.7	789	1899	1340	62.6
1993	2325	165	602	587	626	101	805	1457	1349	50
1994	2302	273	615	597	642	89.2	641	1720	1480	109
1995	2178	188	594	587	627	87.5	672	1830	1365	63
1996	1680	111	400	414	439	88.6	710	1884	922	25.3

Table 26 (Continued).

Year	Rainfall (mm)	Surface flow (mm)	Lateral flow (mm)	Base flow (mm)	Perco. (mm)	Soil water (mm)	Actual ET (mm)	Potential ET (mm)	Water yield (mm)	Sediment yield (mm)
1997	1416	46.3	333	307	332	80.9	708	1815	683.9	10.7
1998	1418	68	321	300	325	85.6	699	1732	685.8	17.7
1999	1461	50.6	332	283	313	91.4	758	1711	663.3	14.8
2000	1885	133	452	480	526	97.7	740	1638	1061	48.2
2001	2129	118	525	532	564	98.5	845	1555	1170	48.5
2002	2358	219	602	595	636	109	777	1480	1411	65.1
2003	1750	125	392	359	383	90.3	791	1750	872.9	27.5
2004	1860	126	487	418	449	101	684	1495	1027	37.1
2005	1864	198	472	397	429	88.5	649	1610	1064	46.5
2006	1998	185	529	482	518	88.3	670	1853	1191	47.5
Average	1890.57	139.33	472.84	440.25	474.13	92.13	732.63	1719.74	1049.02	42.41

During both calibration and validation periods, the difference between the simulated and observed values might be attributed to inadequate representation of rainfall inputs, due to either uneven distribution of rain gauge stations in the catchment, the spatial variability of rainfall, error during the record of data, or due to local rainfall storms that were not well represented by the rainfall data used in the hydrologic simulations. The other possible reason might be attributed to lack of data on the management and various water use abstractions from the reservoir such as water for domestic use and irrigation projects. Clearly there is abstraction of water from the reservoir for irrigation and other domestic purposes. However, since there is no available information on the amount of water used for these purpose, these water use were not included in the simulation.

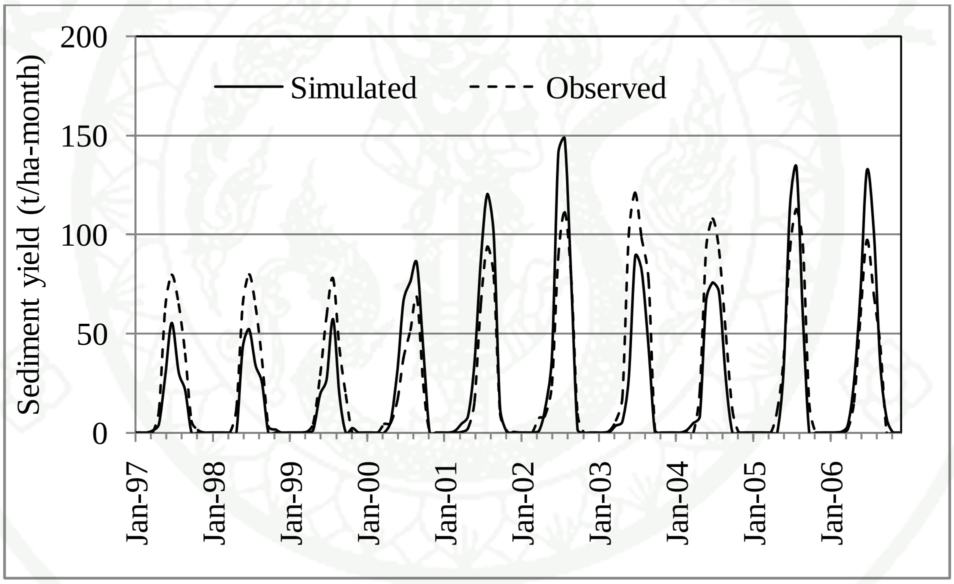

Figure 22 Simulated and observed average monthly sediment yields during validation.

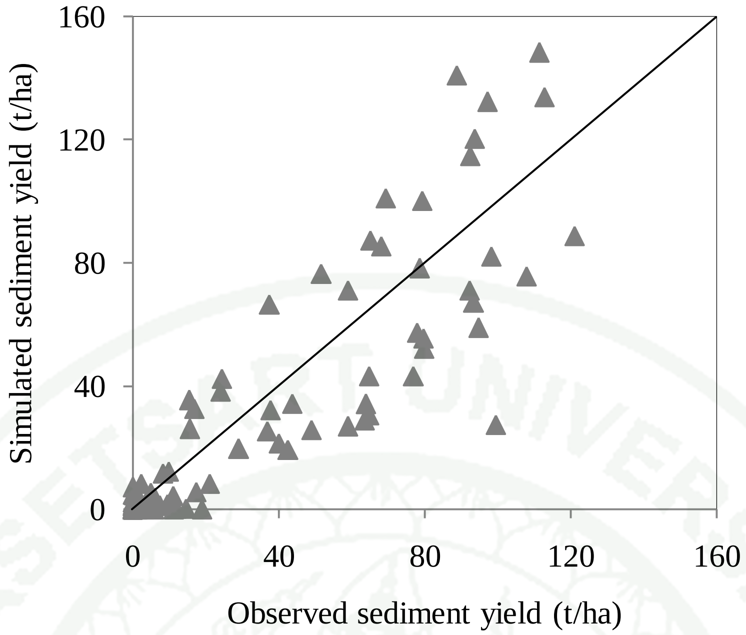

Figure 23 Scatter plot of the simulated vs. observed average monthly sediment yields during validation.

The results of this study agreed with that conducted by Tadele and Forch (2007) using SWAT for simulating stream flows from the Hare watershed in Ethiopia, where the flows were predicted with R^2 and E_{NS} values of 0.74 and 0.69, respectively. Chekol *et al.* (2007) applied SWAT for the assessment of the spatial distribution of water resources and the evaluation of the impacts of different land management practices on the hydrological response and soil erosion in the upper part of the Awash River Basin in Ethiopia; their model performed well with both R^2 and E_{NS} values greater than 0.79 during both the calibration and validation periods. They concluded that the SWAT model accurately tracked the measured flows and simulated the monthly sediment yield well.

Effects of Land Use Change and Management Practices on the Hydrological Processes of a Watershed

Land use changes have altered the hydrology because different land uses have different effects on the way water moves through the soil. Even a very small change in land use can greatly affect the volume of runoff that occurs. With the removal of vegetation from an area, not only has the rate of runoff increased from that area, but the amount of sediment load that enters nearby water bodies may also increase. Compared to other land use types, for example, forests have less runoff because the leaves and trees slow the rainfall that hits the ground, plant roots absorb water, and water is able to infiltrate into the soil. On the other hand, pavement has greater runoff because nothing slows the rainfall, and water is not able to soak into the ground.

Changes in land cover result in commensurate changes in watershed condition and hydrologic response. Land use change and types of management practices have significantly affecting the amounts of runoff, soil loss, and sediment loads generated (Thomas *et al*., 1992). Rainfall-runoff relationships within a watershed are the result of the interplay of many factors, but are driven primarily by the interaction of climate, land cover, and soils. Therefore, watershed response can be used as indicators of condition and as predictors for the ramifications associated with land cover change.

The SWAT model has been calibrated and validated to evaluate the impact of land use/cover change and management practices on the hydrological process of the Fincha watershed specifically on runoff and sediment yields under various land use scenarios. The formulated land use scenarios are:

Scenario A: Base scenario (land use of 2005).

Scenario B: Conversion of 7106.2 ha (20%) of forest land to agricultural land.

Scenario C: Conversion of 7653.4 ha (20%) of grazing to agricultural land.

Scenario D: Conversion of 3782.2 ha (20%) of brush land to agricultural land.

Scenario E: Conversion of 20% of each of forest, grazing and shrub lands simultaneously to agricultural land.

The first Scenario A (Figure 24), is the land use map of the study area for the year 2005; that is 173,692 ha (53.43%) was agricultural land, 35,531 ha (10.93%) was forest land, 38,267 ha (11.77%) was grazing land, 18,911 ha (5.82%) was shrub land, and the remaining 18.05% was under swamp and water body. In Scenario B (Figure 25), 20% of forest land was converted to agricultural land and other land uses did not change; therefore, agricultural land climbed to 180,798.2 ha (55.62%) and forest land dropped to 28,424.8 ha (8.74%). In Scenario C (Figure 26), 20% of grazing land was converted to agricultural land, which resulted in agricultural area that rose to 181,345.4 ha (55.79%) and grazing land to drop to 30,613.6 ha (9.42%). In Scenario D (Figure 27), 20% of shrub land was converted to agricultural land. Hence agricultural land increased to 177,474.2 ha (54.59%) and shrub land reduced to 15,128.8 ha (4.65%). In Scenario E (Figure 28), 20% of each of forest, grazing, and shrub lands were simultaneously converted to agricultural land. As the result, the area under agricultural land increased to 192,233.8 ha (59.14%) and that of forest, grazing, and shrub lands decreased to 28,424.8 ha, 30613.6 ha, and 15,128.8 ha, respectively.

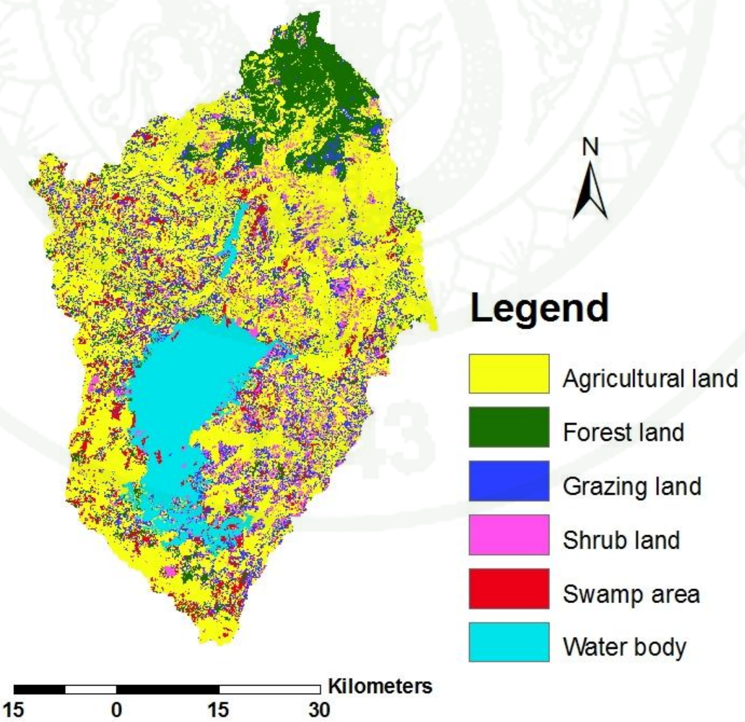

Figure 24 Land use/cover of the study area for base scenario (Scenario A).

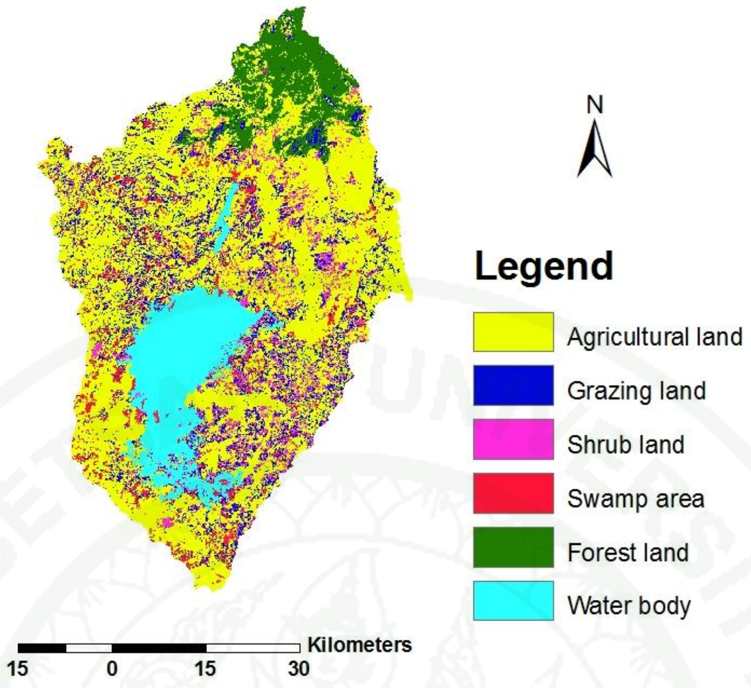

Figure 25 Land use/cover of the study area after 20% of forest lands are converted to agricultural land (Scenario B).

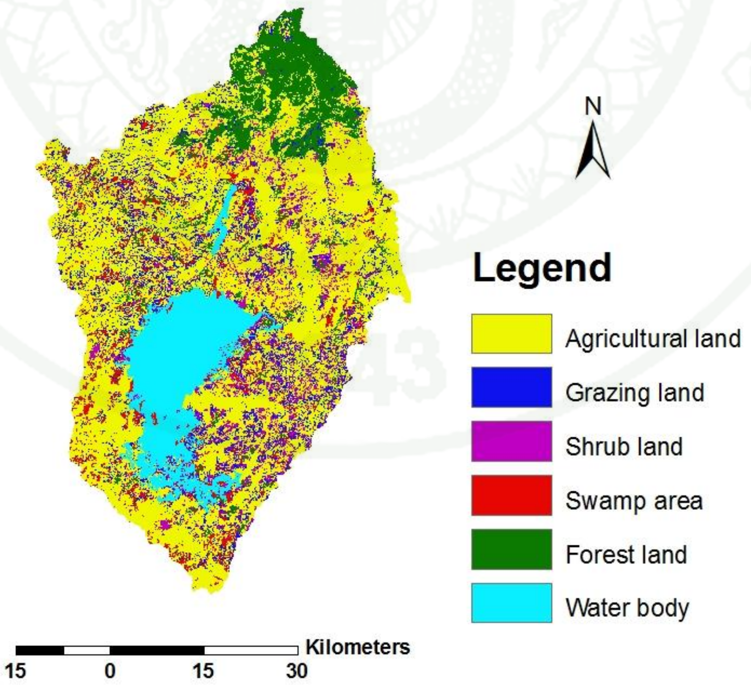

Figure 26 Land use/cover of the study area after 20% of grazing lands are converted to agricultural land (Scenario C).

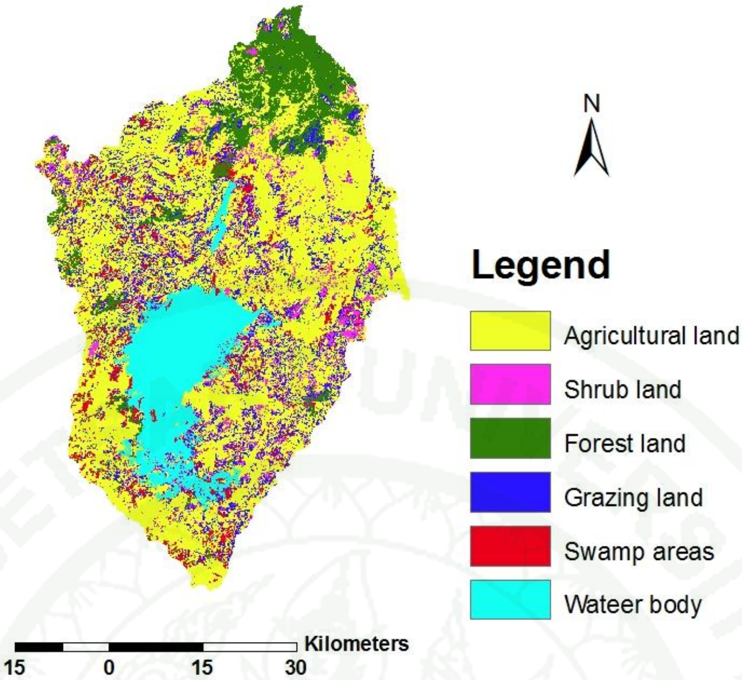

Figure 27 Land use/cover of the study area after 20% of shrub lands are converted to agricultural land (Scenario D).

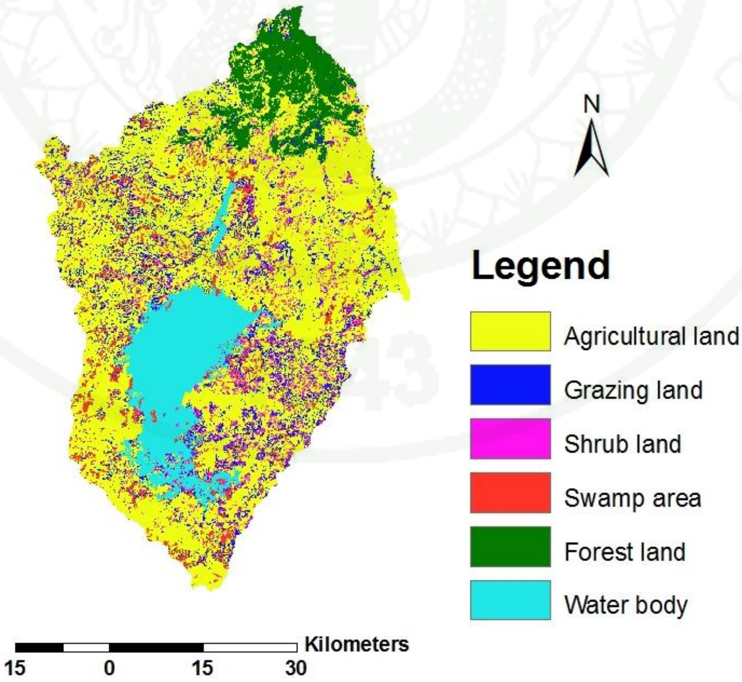

Figure 28 Land use/cover of the study area for land use scenario E.

Prediction of runoff and sediment yields

Model calibration

SWAT model was applied to predict the impacts of land use and management practices on the hydrological processes (especially on runoff and sediment yields) in Fincha watershed. The predicted and observed runoff volumes and sediment yields were plotted on monthly bases for comparison.

During calibration, the comparison between the simulated and observed runoff volumes under various land use change scenarios showed that there is good agreement between the predicted and measured average monthly runoff volumes (with R^2 values ranging from 0.82 to 0.84 and E_{NS} values ranging from 0.73 to 0.75). The adequacy of the model is further indicated by its clear response to extreme rainfall events resulting in high runoff volumes (Example in August 1994). The simulated and observed average monthly runoff volumes for the land use scenario E is shown on Figure 29. As it can be clearly shown on the scatter plot of the simulated and observed average monthly runoff volumes for the land use scenario E (Figure 30), the model tends to underestimate the predicted runoff volumes.

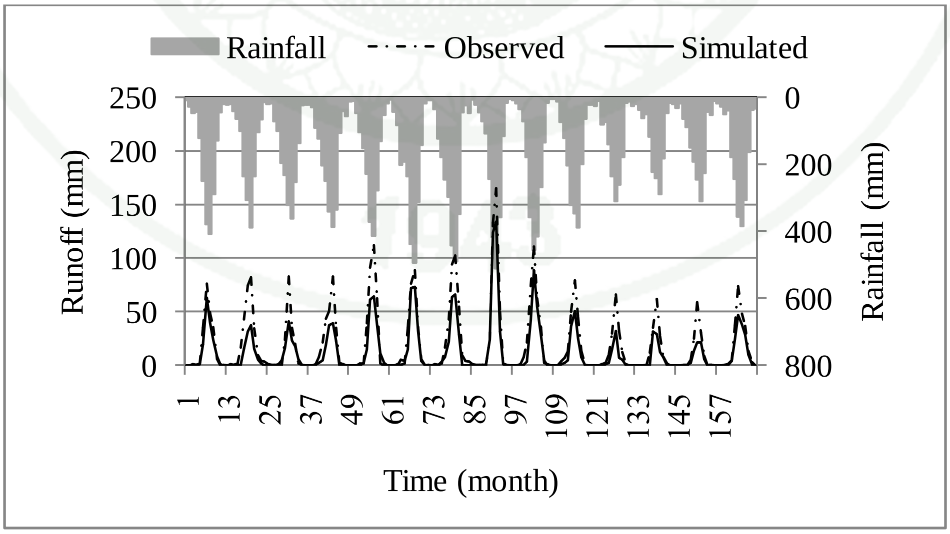

Figure 29 Average monthly simulated and observed runoff volumes under land use scenario E.

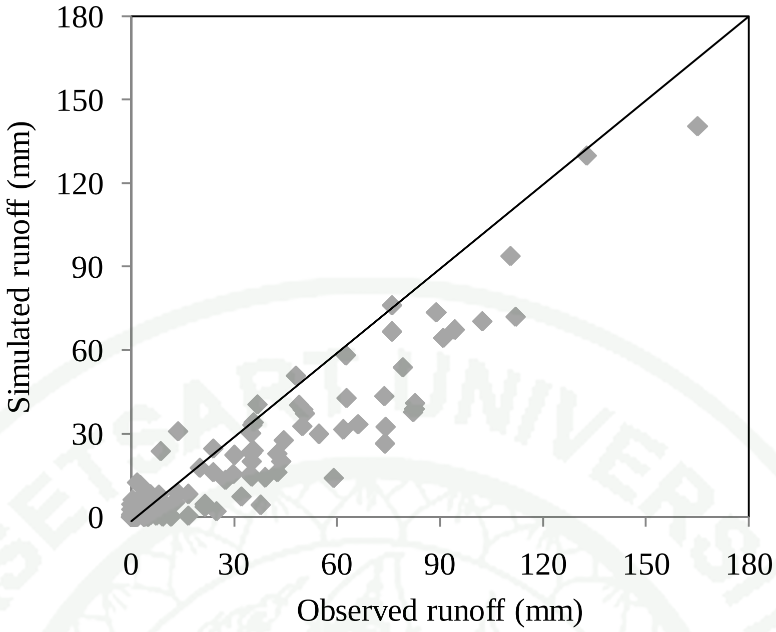

Figure 30 Scatter plot of the simulated vs observed runoff under land use scenario E.

Table 27 Statistical results for various land use scenarios.

Description	Runoff		Sediment yield	
	R^2	E_{NS}	R^2	E_{NS}
Scenario A	0.84	0.74	0.84	0.81
Scenario B	0.84	0.75	0.84	0.81
Scenario C	0.83	0.74	0.86	0.84
Scenario D	0.83	0.75	0.86	0.84
Scenario E	0.83	0.75	0.86	0.85

The simulated and observed average monthly runoff volumes for the land use scenario A, B, C, and D are shown on Appendix Figure 1, 3, 5, and 7, respectively. And the scatter plot of the simulated and observed average monthly runoff volumes for the respective land use scenarios are also shown on Appendix Figure 2, 4, 6, and 8. It is clearly indicated from the figures that in most instances the average monthly runoff volumes were underestimated by the model. Performance of the model in predicting both runoff volumes and sediment yields under various land use change scenarios is summarized in Table 27.

Sediment yield is also adequately predicted by the model and in general showed good agreement between the measured and simulated values (with R^2 values ranging from 0.84 to 0.86 and E_{NS} values ranging from 0.81 to 0.85) (Table 27). Figure 31 shows the simulated and observed average monthly sediment yields for the land use scenario E. The simulated and observed average monthly sediment yields for the land use scenario A, B, C and D are shown on Appendix Figure 9, 11, 13, and 15, respectively. And the scatter plot of the simulated and observed average monthly runoff volumes for the respective land use scenarios are shown on Appendix Figure 10, 12, 14, and 16. As it can be seen from the figures, although the average monthly sediment yields were adequately captured, the model tends to underestimate the values during some years and overestimate during some other years. The scatter plot of the observed versus simulated average monthly sediment yields for the land use scenario E shown on Figure 32 also confirmed that the predicted sediment yield values were underestimated by the model.

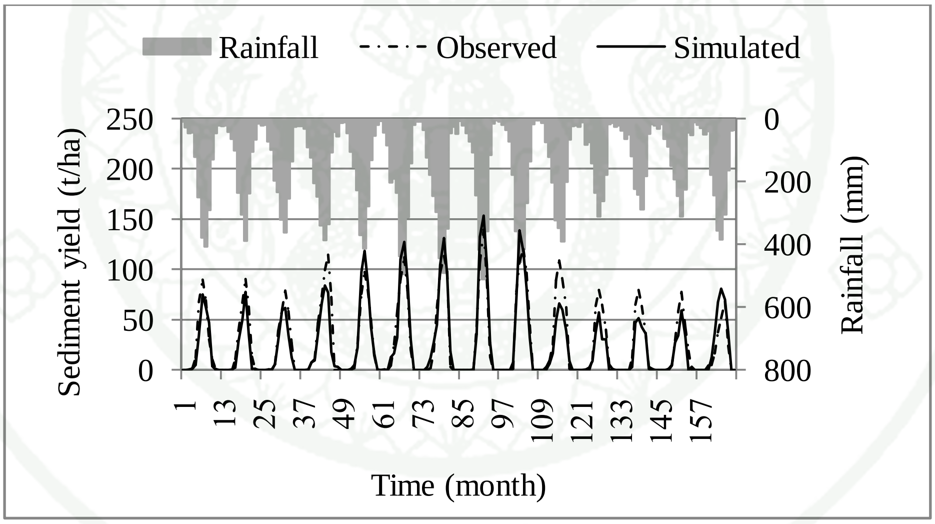

Figure 31 Average monthly simulated and observed sediment yield under land use scenario E.

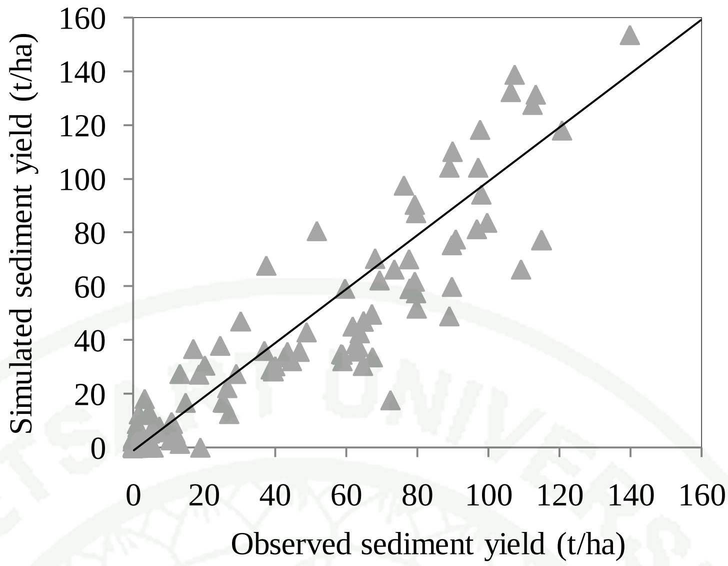

Figure 32 Scatter plot of the simulated vs observed sediment yields under land use scenario E.

The discrepancies between the simulated and observed average monthly sediment yield values may be attributed to the high deposition of sediments in the reservoir and channels and to the channel erosion during high flows. Nevertheless, the overall adequacy of the model in simulating runoff and sediment yields indicated its usefulness for predicting the effects of land use/cover change on the hydrological processes of a watershed.

Model validation

During validation period, there is close agreement between the observed and simulated average monthly runoff volumes with coefficient of determination (R^2) values ranging from 0.77 to 0.78 and Nash Sutcliffe efficiency (E_{NS}) values ranging from 0.76 to 0.78. It was also found that the simulated average monthly sediment yields agreed closely well with the measured average monthly sediment yields (with R^2 values ranging from 0.84 to 0.86 and E_{NS} values ranging from 0.52 to 0.71).

Effects of land use change on runoff and sediment yields

In order to evaluate the effect of land use/cover changes on the hydrological responses of the study watershed, the calibrated model was run to simulate runoff and sediment yields under various land use scenarios.

Runoff volumes

The simulated runoff volumes under various land use scenarios are presented in Table 28. Simulation results under various land use scenarios showed that runoff volumes increased by 19.20 mm (12.68%), 3.39 mm (2.24%), and 7.18 mm (4.74%), respectively when 20% of forest land, 20% of grazing land, and 20% of shrub lands are converted to agricultural land. Furthermore, the runoff volumes increased by 27.05 mm (17.86%) when 20% of each of forest, grazing, and shrub lands are simultaneously converted to agricultural land. The simulated average monthly runoff volumes under various land use scenarios are shown in Figure 33. And the simulated annual runoff volumes under various land use scenarios are shown in Appendix Figure 17.

Table 28 Simulated runoff volumes under various land use scenarios.

Land use scenario	Runoff (mm)	Difference	Change (%)
Scenario A	151.42		
Scenario B	170.62	19.20	12.68
Scenario C	154.81	3.39	2.24
Scenario D	158.60	7.18	4.74
Scenario E	178.47	27.05	17.86

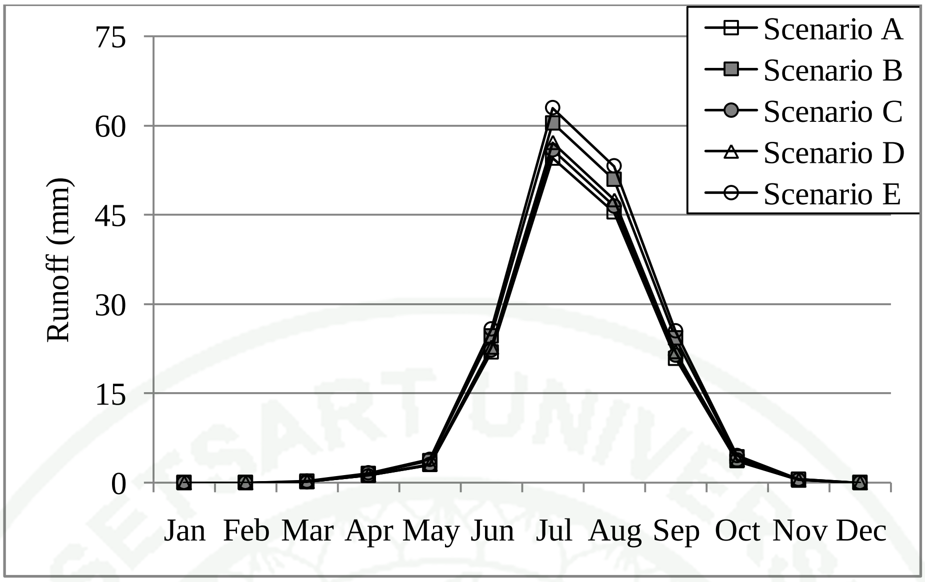

Figure 33 Simulated average monthly runoff volumes under various land use scenarios.

Sediment yield

Sediment yield is the amount of overland soil loss due to water erosion in the watershed. It reflects the integrated response of sediment generation processes and stream processes at watershed scale. The simulated sediment yields under various land use scenarios are presented in Table 29. Simulation results indicated that the sediment yields increased by 8.39 t/ha (16.20%), 1.07 t/ha (2.07%), and 1.97 t/ha (3.80%), respectively when 20% of forest land, 20% of grazing land , and 20% of shrub lands are converted to agricultural land. Moreover, sediment yields increased by 10.08 t/ha (19.46%) when 20% of each of forest, grazing, and shrub lands are simultaneously converted to agricultural land.

Figure 34 shows the simulated average monthly sediment yields under various land use scenarios. The simulated annual sediment yields under various land use scenarios are shown in Appendix Figure 18. Simulation of various land use scenarios clearly indicated that, as the result of the increase under the area of agricultural land and the subsequent decrease in the areas of forest, grazing and shrub lands the average annual and monthly runoff volumes and sediment yields increased.

Table 29 Simulated sediment yields under various land use scenarios.

Land use scenario	Sediment yield (t/ha)	Difference	Change (%)
Scenario A	51.80		
Scenario B	60.19	8.39	2.07
Scenario C	52.87	1.07	3.80
Scenario D	53.77	1.97	19.46
Scenario E	61.88	10.08	16.20

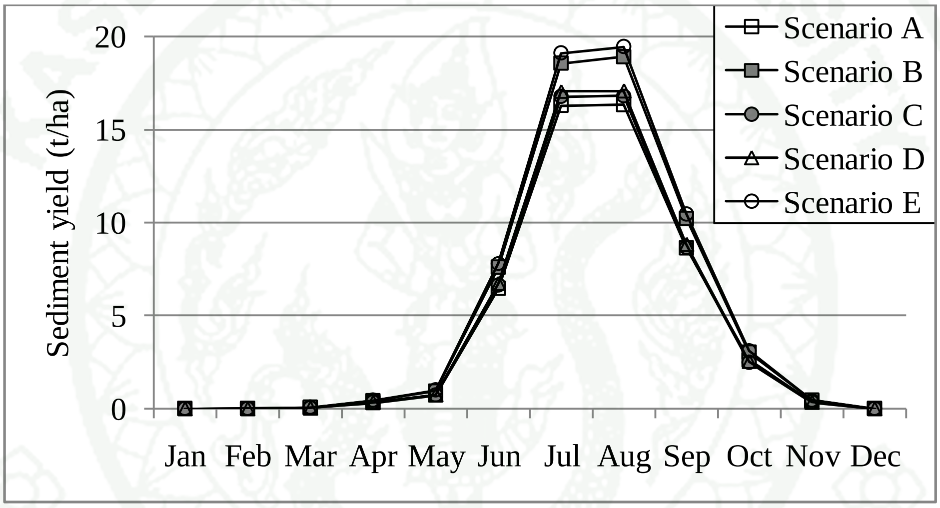

Figure 34 Simulated average monthly sediment yields under various land use scenarios.

As hydrologic responses of a watershed are influenced by the type and degree of land use/cover conditions, the strongest relative impact of land use change can be observed in the amount of runoff volumes and sediment yields generated. For example under scenario B (when 20% of forest lands are converted to agricultural land), runoff volumes and sediment yields increased from 151.42 to 170.62 mm and from 51.80 to 60.19 t/ha, respectively. Similarly under scenario E (when 20% of each of forest, grazing, and shrub lands are simultaneously converted to agricultural land), runoff volumes (Table 28) and sediment yields (Table 29) increased from 151.42 to 178.47 mm and from 51.80 to 61.88 t/ha, respectively.

Because the soils of agricultural lands are bare and easily susceptible to erosion when repeatedly tilled and left without a protective cover, they are less protected against raindrop impact shortly after sowing, when the plants do not cover the soil completely and thus runoff rate and transportation of soil particles increased. Such condition will cause significant soil erosion and sedimentation. It showed that hydrologic responses are an indicator of watershed conditions, and any change in land use/cover can affect the overall health and condition of the watershed.

Effects of land management practices on runoff and sediment yields

In order to have a clear picture of the impacts of management practices on the hydrological responses of the study watershed, the calibrated model was run to simulate runoff and sediment yields using two land management scenarios (with and without soil conservation interventions) under various land use scenarios.

Simulation of management practices clearly showed that under the base scenario (existing land use conditions), average monthly sediment yields decreased by 20.82 t/ha (40.19%) as the result of soil conservation interventions. The result also showed that due to soil conservation interventions monthly sediment yields decreased by 23.71 t/ha (39.39%), 20.97 t/ha (39.66%), and 21.35 t/ha (39.71%), respectively when 20% of forest land, 20% of grazing land, and 20% of shrub lands are converted to agricultural land. Likewise, when 20% of each of forest, grazing, and shrub lands are simultaneously converted to agricultural land average monthly sediment yields decreased by 24.41 t/ha (39.45%) as the result of soil conservation interventions (Table 31). However, average monthly runoff volumes remained almost unchanged when simulated with and without soil conservation interventions under various land use scenarios (Table 30). This result evidently showed that sediment yield is highly affected by management practices. On the other hand, runoff volume is less affected by management practices.

The comparison of the simulated average monthly sediment yields with and without soil conservation interventions for the land use scenario A, B, C, D, and E are shown on Figure 35, 36, 37, 38, and 39, respectively. For example under scenario B (when 20% of forest lands are converted to agricultural land), the average monthly sediment yields decreased from 60.19 to 36.48 t/ha (by 39.39%) as the result of soil conservation interventions. Similarly, under scenario E (when 20% of each of forest land, grazing land, and shrub lands are simultaneously converted to agricultural land), the average monthly sediment yields decreased from 61.88 to 37.47 t/ha (by 39.45%). (See also Table 31).

Table 30 Simulated runoff volumes with and without interventions.

	Runoff (mm)			
Land use scenario	Without interventions	With interventions	Difference	Change (%)
Scenario A	151.42	151.51	0.09	0.06
Scenario B	170.62	170.58	0.04	0.02
Scenario C	154.81	154.88	0.07	0.05
Scenario D	158.60	158.65	0.05	0.03
Scenario E	178.47	178.42	0.05	0.03

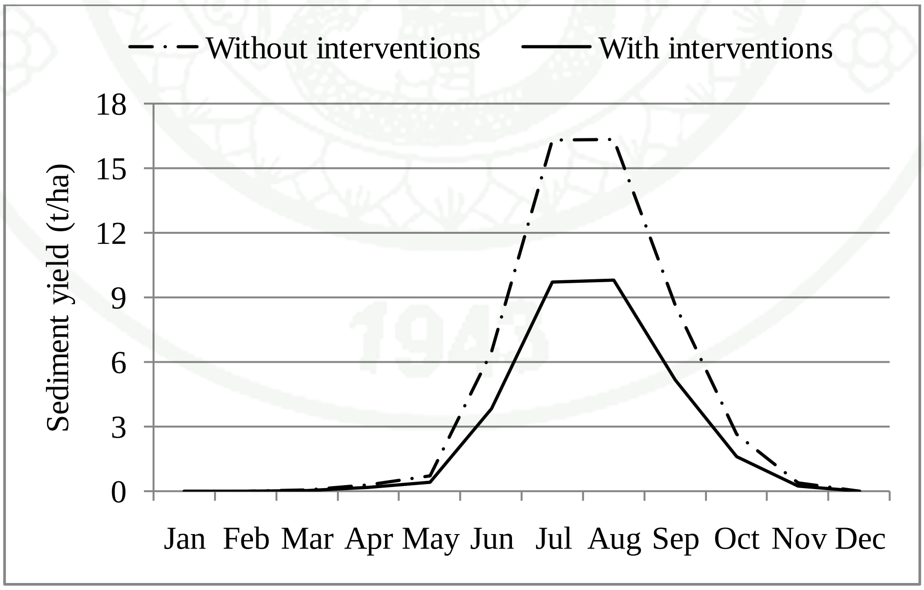

Figure 35 Simulated average monthly sediment yields with and without intervention under land use scenario A.

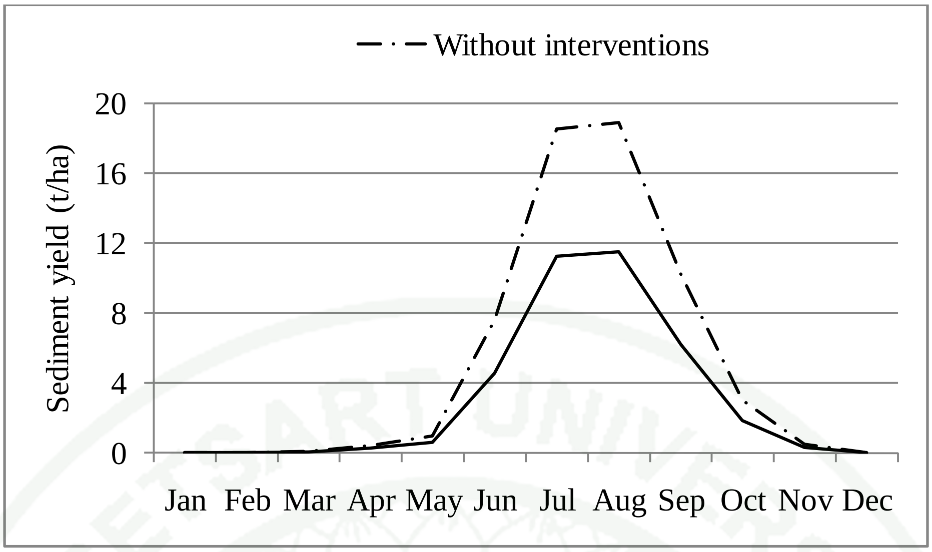

Figure 36 Simulated average monthly sediment yields with and without intervention under land use scenario B.

The difference in the simulated values of sediment yields during the simulation of management practices clearly indicated that the rate of soil erosion and the amount of soil particles transported from agricultural lands decreased with soil conservation interventions. It follows that appropriate land management practices such as strips of crops, strips of woodland, and hedgerows are highly effective at reducing overland flow by increasing subsurface storage and infiltration rates, thereby causing a significant reduction in surface runoff rate and sediment yields. Protection of the soil surface from the erosive forces of rainfall significantly reduces soil particle detachment by raindrop impact and sediments transported by concentrated overland flow along with a reduction of mechanical soil movement.

It is, therefore, apparent that changes in the type of vegetation, soil structure, surface topography and drainage associated with land management practices can significantly affect the intensity and spatial distribution of runoff generation, erosion and thereby sediment loads transported from the watershed. That means the runoff rate and the quantity of sediment yields generated from a watershed depends on the type of management it receives.

Table 31 Simulated sediment yields with and without interventions.

Land use scenario	Sediment yields (t/ha) Without interventions	With interventions	Difference	Change (%)
Scenario A	51.80	30.98	20.82	40.19
Scenario B	60.19	36.48	23.71	39.39
Scenario C	52.87	31.90	20.97	39.66
Scenario D	53.77	32.42	21.35	39.71
Scenario E	61.88	37.47	24.41	39.45

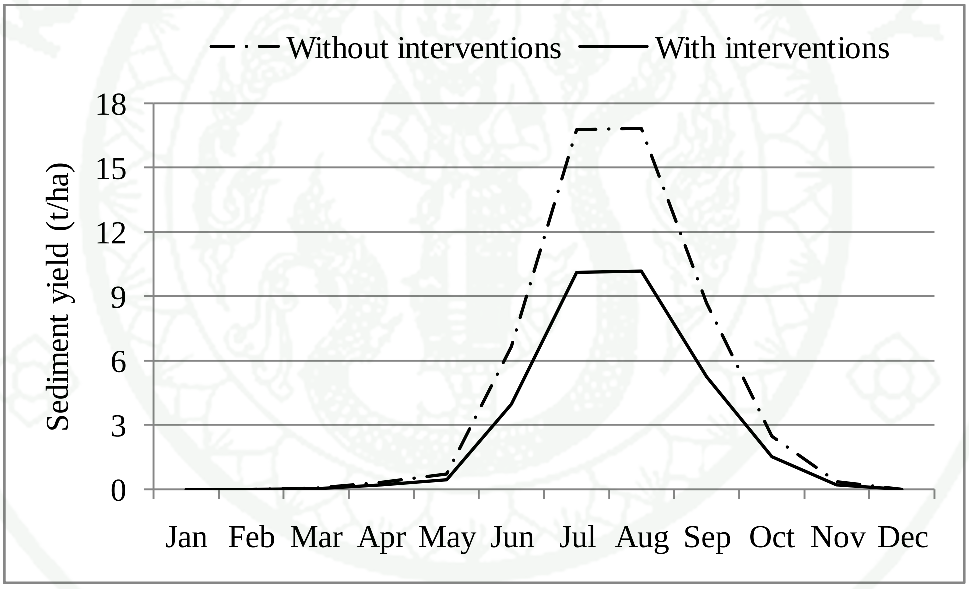

Figure 37 Simulated average monthly sediment yields with and without intervention under land use scenario C.

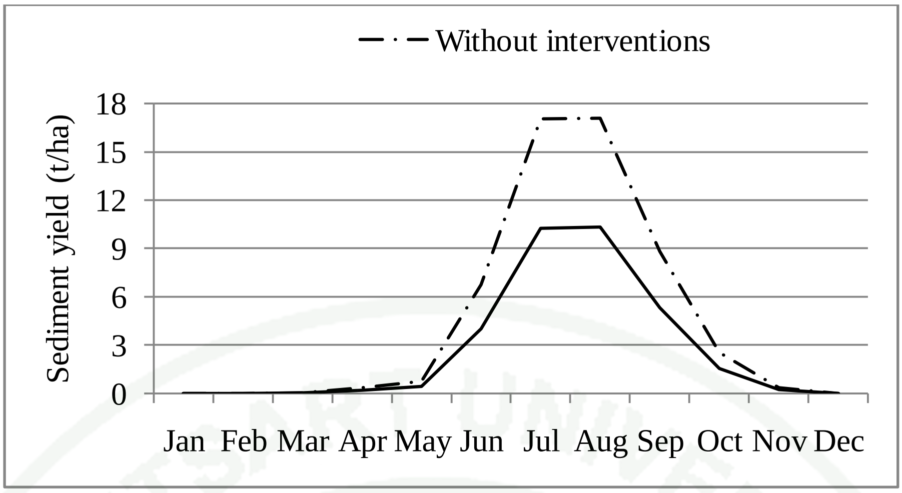

Figure 38 Simulated average monthly sediment yields with and without intervention under land use scenario D.

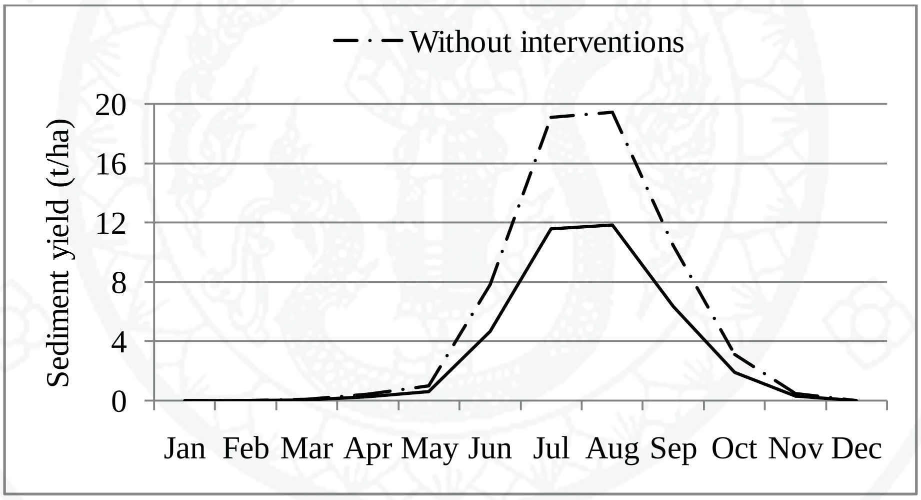

Figure 39 Simulated average monthly sediment yields with and without intervention under land use scenario E.

These results clearly demonstrated that both runoff and sediment yields are significantly affected by land use changes. On the other hand, the effect of management practices on sediment yields is high. However, its effect on runoff volume is less. This study has confirmed that the SWAT model can be considered as a useful tool for modeling the impacts of land use and management practices on runoff and sediment yields.

Current Situation of the Fincha Watershed

It is clear that the natural resources base (land, water and forest) of an area is fundamental to the survival and livelihood of the people living in that area. However, if these limited resources are under pressure due to some external factors, the net result will be unalterable. This is what is happening in many highland areas of Ethiopia in general, and in Fincha watershed in particular. Currently, Fincha watershed is facing rapid deforestation and degradation of land and water resources. The ever increasing demand for food have resulted in extensive forest clearing for agricultural use, exploitation of forests for fuel wood, fodder, and construction materials. In Fincha watershed, the main causes of soil erosion are the rapidly increasing human population, limited area of fertile soils on flat lands, deforestation, and excessive livestock population. Moreover, cultivation on steep slopes by clearing of vegetation has accelerated erosion in the highlands (Figure 40).

Figure 40 Clearing of vegetation from steep area. (Photo: July 2010, by Abdi)

The dissected terrain, the extensive areas with steep slopes, and the high intensity of rainfall lead to accelerated soil erosion once deforestation occurs. The gradual expansion of agricultural land from gently sloping land onto the steeper slopes of neighboring mountains on the one hand, and into the flat swampy plains of the plateau on the other accelerated soil erosion (Figure 41). Consequently, large areas of forest, grazing, and shrub lands have been converted to farm lands leading to sever land slide (Figure 42), soil erosion and sedimentation of rivers, streams, reservoir, and siltation of low land areas (Figure 43). Soil degradation in Fincha watershed can be seen as a direct result of expansion of agricultural lands.

Figure 41 Soil erosion observed in the study area. (Photo: July 2010, by Abdi)

At present, the majority of the watershed is under intensive cultivation of annual crops with poor farming system that encourage erosion. These include cultivation of cereal crops such as *teff* (Ergrotis tef) and wheat (*Triticum sativum*) which require the preparation of a fine tilth seedbed. Moreover, the socio-political situation, especially insecurity of land tenure has greatly discouraged farmers from investing in soil conservation practices.

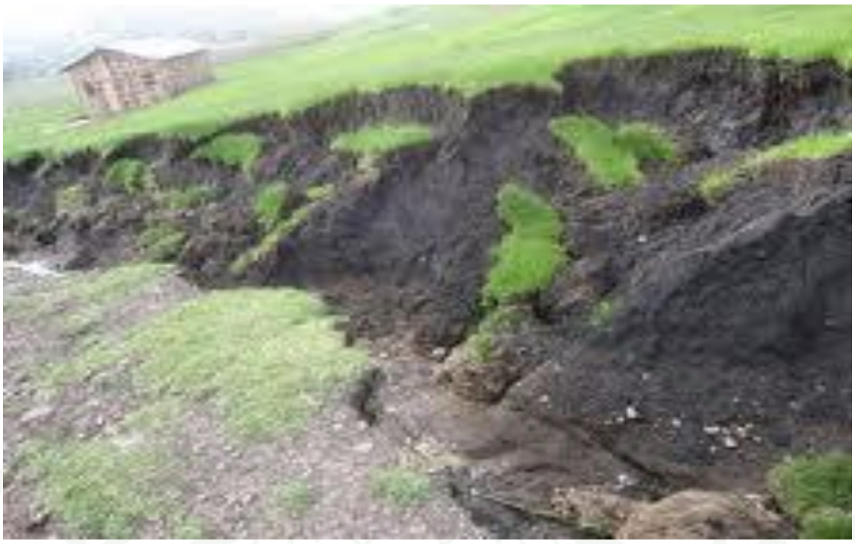

Figure 42 Land slide observed in the study area. (Photo: July 2010, by Abdi)

At present, soil erosion and its consequent effects are the most important problem in Fincha watershed and will continue to be the most severe threat to the area unless conservation-oriented land management practices are employed. The patterns of land use change and present status of soil erosion found in Fincha watershed will generate substantial soil erosion and in the long run aggravate the poverty of farmers living in the area.

The present status and rate of soil erosion in Fincha watershed call for immediate action to retard and reverse this degradation process. However, the ever increasing number of population, in comparison with the annual agricultural growth, will lead to even more intensive use of cultivable and pasture land to produce more food and feed the growing human and livestock populations. Therefore, it is clear that intensification of land use must be accompanied by technological innovations that will lead to increased productivity, while simultaneously conserving the soil resource. Soil erosion is thus the most immediate environmental problem facing the watershed. The loss of soil and the deterioration in fertility, moisture storage capacity, and the structure of the remaining soils all reduce the area’s agricultural productivity.

Figure 43 Sediment deposition at low land areas. (Photo: July 2010, by Abdi)

In Fincha watershed, land degradation and its consequent effects are a great threat for the future and hence require great effort and resources to ameliorate. The major causes of land degradation in the area are the rapid population increase, severe soil loss, deforestation, low vegetative cover and unbalanced crop and livestock production.

The balance between crop, livestock, and forest production is disturbed, and the farmer is forced to put more land into crop production. For environmentally and socially sustainable development, there is an urgent need to promote awareness and understanding of the interdependence of natural, socioeconomic, and political systems at local and national levels. Understanding the current status and causes of land degradation is very important. Therefore, there is an urgent need for developing integrated watershed management plan to retard and reverse this degradation process. This study reveals the important elements of land degradation in Fincha watershed and suggests possible solutions that may help to improve the situation.

CONCLUSSION AND RECOMMENDATION

Conclusion

The land use change of the Fincha watershed was analyzed from 1985 to 2005 using an integrated approach of satellite remote sensing, GIS, and Markov modeling. Moreover, the soil and water assessment tool (SWAT) model has been calibrated and validated on monthly basis to simulate the hydrological processes and predict the effects of land use change and management practices on runoff and sediment yields from the study watershed with an area of 3,251 km^2. From the results of the study the following conclusions were drawn:

1. The integration of satellite remote sensing, Geographical Information System (GIS), and Markov modeling has demonstrated its ability to provide comprehensive information on the direction, nature, rate, and location of land use changes. The analysis can serve as an indicator of the direction and magnitude of change in the future as well as a quantitative description of change in the past.

2. During the study period, agricultural land and water bodies have notably increased in area by as much as 60,606 ha and 19,184 ha, respectively. In contrast, the area of forest land, grazing land, swamp area, and shrub lands have decreased by 36,225 ha, 17,376 ha, 19,948 ha, and 6,240 ha, respectively.

3. During calibration and validation, SWAT model adequately predicted runoff and sediment yields with coefficient of determinations (R^2) ranging from 0.82 to 0.86 and Nash Sutcliffe Efficiencies (E_{NS}) ranging from 0.73 to 0.85.

4. Simulation of various land use scenarios clearly showed that average monthly runoff volumes increased by 19.20 mm, 3.39 mm, and 7.18 mm, respectively when 20% of forest, 20% of grazing and 20% of shrub lands are converted to agricultural land. The worst scenario is when 20% of each of forest, grazing, and shrub lands are simultaneously converted to agricultural land that resulted in an increase of average monthly runoff volumes by 27.05 mm.

5. Simulation of various land use scenarios also evidently indicated that average monthly sediment yields increased by 8.39, 1.07 and 1.97 t/ha, respectively when 20% of forest, 20% of grazing, and 20% of shrub lands are converted to agricultural land. More seriously, when 20% of each of forest, grazing, and shrub lands are simultaneously converted to agricultural land, the average monthly sediment yields increased by 10.08 t/ha.

6. Simulation of land management practices also clearly showed that while average monthly runoff volumes remained almost unchanged, average monthly sediment yields decreased by 20.82, 23.71, 20.93 and 21.35 t/ha, respectively as the result of soil conservation interventions under the base scenario, when 20% of forest, 20% of grazing, and 20% of shrub lands are converted to agricultural land. Furthermore, the average monthly sediment yields decreased by 24.41 t/ha when 20% of each of forest, grazing, and shrub lands are simultaneously converted to agricultural land due to interventions.

Recommendation

1) As the application of stochastic models to simulate dynamic systems such as land use and land cover changes in a developing nation is rare, much work needs to be done in order to develop an operational procedure that integrates the techniques of satellite remote sensing, GIS, and Markov modeling for monitoring and modeling land use and land cover changes.

2) This study has vividly demonstrated that the SWAT model can be considered as a useful tool for simulating the hydrological processes of a watershed and modeling the impacts of land use change and management practices on runoff and sediment yields; and thus, can be further extended for simulating other hydrological processes such as annual water yield, base flows, and stream flows under various scenarios.

3) As the SWAT model is capable of simulating the hydrological processes in a watershed, it can be further extended to similar watersheds in the country, particularly in the Blue Nile Basin of Ethiopia, where quantifying the total volume of runoff and

sediment yields generated from the basin is urgently required for better land and water resources planning and management purposes.

4) The simulated effects of the conversion of forest, grazing, and shrub lands to agricultural land clearly indicated an alarming situation under all the land use scenarios in general and under scenario E in particular. Therefore, we recommend that policies addressing this issue should be formulated both at the local and national level. Parallel to this, an intensive information and educational campaign about the consequences of expansion of crop lands on the expenses of forest, grazing, and shrub lands and ways of rehabilitating the watershed should be done. Finally, alternative livelihood opportunities for farmers living surrounding the Fincha Reservoir, and those living on the steep and mountainous areas within the watershed should be considered in policy implementation.

5) As land development is a continuous process, for the optimum use of the land and water resources of the area, it is recommended that soil and water conservation such as construction of various terraces, water ways, rehabilitation of degraded areas, and land management practices such as crop residuals, contour tillage, strip cropping on the contour etc should be considered.

LITERATURE CITED

Agarwal, C., M.G. Green, J.M. Grove, T.P. Evans, and C.M. Schweik. 2000. A Review and assessment of land use change models. Dynamics of space, time, and human choice. USDA Forest Service, VT, USA. 90pp.

Alansi, A.W., M.S.M. Amin, G. Abdul Halim, H.Z.M. Shafri, A.M. Thamer, A.R.M, Waleed, W. Aimrun, and M. H. Ezrin. 2009. The effect of development and land use change on rainfall-runoff and runoff-sediment relationships under humid tropical condition: case study of Bernam watershed Malaysia

Anderson, J.R., E. Hardy, J. Roach, and R. Witmer. 1976. Land Use and Land Cover Classification System for Use with Remote Sensing Sensor Data, Washington, DC:US. **Geological Survey Profession P**aper 964, 28pp.

Arabi, M., Govindaraju, R.S., Hantush, M.M., Engel, B.A. 2006. Role of watershed subdivision on modelling the effectiveness of Best Management Practices with SWAT. JAWRA 42 (2), 513–528.

Arabi M., J. Frakenberger, B.A. Engel, and J.G. Arnold. 2008. Representation of Agricultural management practices with SWAT. **Hydrol. Process**. 22(16): 3042 ‐ 3055.

Arnold, J.G., J.R. Williams and D.R. Maidment. 1995. Continuous-time water and sediment-routing model for large basins. **J. Hydraul. Eng**. 121(2): 171−183.

Arnold, J.G., R. Srinivason, R.R. Muttiah, J.R. Williams. 1998. Large Area Hydrologic Modeling and Assessment Part I: Model development. **J. Am. Water Resour. Assoc**. 34(1): 73−89.

Arnold, J.G., R. Srinivasan, T.S. Ramanarayanan, and M.D. Luzio. 1999. Water resources of the Texas Gulf Basin. **Water Sci. Technol**. 39(3): 121-133.

Arnold, J.G. and J.R. Williams. 1995. SWRRB—A watershed scale model for soil and water resources management. pp. 847-908. In V.P. Singh (ed). Computer models of watershed hydrology. Water Resources Publications.

Arnold, J.G. and N. Fohrer. 2005. SWAT2000: Current Capabilities and Research Opportunities in Applied Watershed Modeling. **Hydrol. Process**. 19 (3): 563 - 572.

Arnold, J.G. and P.M. Allen. 1999. Automated methods for estimating base flow and groundwater recharge from stream flow records. **J. Am. Water Resour. Assoc**. 35(2): 411 - 424.

Arvind, C.P. and M.S. Nathawat. 2006. Land Use Land Cover Mapping Through Digital Image Processing of Satellite Data – A case study from Panchkula, Ambala and Yamunanagar Districts, Haryana State, India

Assefa, K. 1994. Valuing environmental quality changes in Horro-Guduru: **Field survey report**. Ethiopia Electric Power Corporation, Addis Ababa, Ethiopia.

Bagnold, R.A. 1977. Bed load transport in natural rivers. **Water Resour. Res**. 13: 303-312.

Baker, W.L. 1989. A review of models of landscape change. **Landscape Ecology**. 2: 111–133.

Behera, S. and R.K. Panda. 2006. Evaluations of management alternatives for an agricultural watershed in a sub-humid subtropical region using a physical process model. **Agric. Ecosyst. Environ**. 113(1-4): 62 - 72.

Belay, T. 2000. Land use/land cover changes in the Derekolli catchment of the South Welo zone of Amhara region, Ethiopia. **EASSRR**. 17(1): 20.

Bell, E.J. 1974. Markov analysis of land use change: an application of stochastic processes to remotely sensed data. **Socio-Econ Planning Sci**. 8: 311–316.

Bell, E.J. and R.C. Hinojosa. 1977. Markov analysis of land use change: continuous time and stationary processes. **Socio-Econ Planning Sci**. 11: 13–17.

Bellot, J., A. Bonet, J.R. Sanchez, and E. Chirino. 2001. Likely effects of land use changes on the runoff and aquifer recharge in a semiarid landscape using a hydrological model. **Landscape and urban planning**. 55: 41-53.

Benaman, J., and C.A. Shoemaker. 2005. An analysis of high-flow sediment event data for evaluating model performance. **Hydrol. Process**. 19(3): 605-620.

Bezuayehu, T. 2006. People and dams: environmental and socio-economic impacts of Fincha'a hydropower dam, western Ethiopia. **Tropical Resour. Manag. paper** 75pp. Wageningen University and Research Center, Wageningen, The Netherlands.

Bezuayehu, T., A. Gezahegn, A. Yigezu, M.A. Jabbar, and D. Paulos. 2002. Nature and causes of land degradation in the Oromiya region: a review. **Socio-economic and policy Research working paper** 36. IRLI, Nirobi, Kenya, 82pp.

Bezuayehu, T., and G. Sterk. 2008. Land use changes induced by a hydropower reservoir in Fincha watershed, Ethiopia. **Mountain Res**. **Dev**. 28(1): 72-80.

Bicik, I., L. Jelecek and V. Stepanek. 2001. Land-use changes and their social driving forces in Czechia in the 19th and 20th centuries. **Land Use Policy**. 18 (2001): 65–73.

Binder, C., R.M. Boumans, and R. Costanza. 2003. Applying the Patuxent Landscape Unit Model to human dominated ecosystems: the case of agriculture. **Ecol. Model**. 159: 161-177.

Bingner, R.L. 1996. Runoff simulated from Goodwin Creek Watershed using SWAT. **Trans. ASAE.** 39(1): 85-90.

Binh, D.N., A.N. Tuan, and H.L. Huong. SWAT application coupled with web technology for soil erosion assessment in North western region of Vietnam. In: **International SWAT Conference**. August 4-6, 2010. Seoul, Korea.

Bisht, B.S. and P.C. Tiwari. 1996. Land use planning for sustainable development in Kumaun Lesser Himalaya study of the Gomti watershed. **J. Sustainable Dev. and World Ecology**. 3: 23-34.

Black, A., E. Strand, G.R. Wright, M.J. Scott, P. Morgan and C. Watson. 1998. Land use history at multiple scales: implications for conservation planning. **Landscape and Urban Planning**. 43: 49–63.

Bosch, J.M., and J.D. Hewlett. 1982. A review of catchment experiments to determine the effect of vegetation changes on water yield and evapotranspiration. **J. Hydrol**. 55: 3-23.

Bouraoui, F., S. Benabdallah, A. Jrad, and G. Bidoglio. 2005. Application of the SWAT model on the Medjerda River Basin (Tunisia). **Phys. Chem. Earth**. 30(8-10): 497-507.

Bourne, L.S. 1971. Physical adjustment processes and land use succession: a review and central city example. **Economic Geo**. 47: 1–15.

Bowling, L., P. Storck, and D.P. Lettenmaier. 2000. Hydrological effects of logging in western Washington, USA. **Water Resour. Res**. 36: 3223-3240.

Bracmort, K.S., M. Arabi, J. R. Frankenberger, B. A. Engel, and J. G. Arnold. 2006. Modeling long-term water quality impact of structural BMPs. **Trans. ASABE**. 49(2): 367-374.

Brandt, C. J. 1990. Simulation of the size distribution and erosivity of raindrops and throughfall drops. **Earth Surface Processes and Landforms**. 15: 687-698.

Brath, A., A. Montanari, and G. Moretti. 2006. Assessing the effects of land use change on flood frequency via hydrological simulation (with uncertainty). **J. Hydrol**. 324 (1-4): 141–153.

Brown, L.C., and T.O. Barnwell. 1987. The enhanced water quality models QUAL2E and QUAL2E-UNCAS documentation and user manual. EPA document EPA/600/3-87/007. USEPA, Athens. GA.

Bürgi, M. and E.W.B. Russell. 2001. Integrative methods to study landscape changes. **Land Use Policy**. 18: 9–16.

Burns, D., T. Vitvar, J. McDonnell, J. Hassett, J. Duncan, and C. Kendall. 2005. Effects of suburban development on runoff generation in the croton river basin, New York, USA. **J. Hydrol**. 311: 266-281.

Calder, I.R. 1992. Hydrologic effects of land use change. In Maidment, D.R. (ed.): **Handbook of Hydrology**. 13. I -13.5.

Campbell, J.B. 2007. **Introduction to Remote Sensing**, Fourth edition, The Guilford Press, New York, USA. 626pp.

Cao, W., W.B. Bowden, and T. Davie. 2008. Modeling impacts of land cover change on critical water resources in the Motueka river catchment, New Zealand. **Water Resourc. Manag.** 23 (1): 137-151.

Carlson,T.N. and S.G.A. Azofeifa. 1999. Satellite Remote Sensing of land Use changes in and around San Jose, Costa Rica. **Rem. Sens. Environ**. 70: 247–256.

Chaplot, V., Saleh, A., Jaynes, D.B., Arnold, J.G. 2004. Predicting water, sediment and NO3–N loads under scenarios of land-use and management practices in a flat watershed. **Water Air Soil Poll**. 154: 271–293.

Chekol, D. A., B. Tischbein, H. Eggers, and P. Vlek. 2007. Application of SWAT for Assessment of Spatial Distribution of Water Resources and Analyzing Impact of Different Land Management Practices on Soil Erosion in Upper Awash River Basin Watershed, **FWU Water Resour. Publications**. 6 (10): 110-117.

Chen, S., S. Zeng, and C. Xie. 2000. Remote sensing and GIS for urban growth analysis in China. **Photogramm. Eng. Rem. Sens**. 66: 593–598.

Chen, J.F. and X.B. Li. 2004. Simulation of hydrological response to land-cover changes, Chinese. **J. Appl. Ecology**. 15(5): 833-836.

Cheng, H., W. Ouyang, F. Hao, X. Ren, and S. Yang. 2006. The non-point source pollution in livestock-breeding areas of the Heihe River Basin in Yellow River. **Stoch. Environ. Res. Risk Assess**. 21 (3): 213-221.

Chow, V.T., D.R. Maidment, and L.W. Mays. 1988. **Applied hydrology**. McGraw-Hill, Inc., New York, NY. 570pp.

Chu, T.W., A. Shirmohammadi, H. Montas, and A. Sadeghi. 2004. Evaluation of the SWAT model's sediment and nutrient components in the Piedmont physiographic region of Maryland. **Trans. ASAE**. 47(5): 1523-1538.

Clarke, K.C., S. Hoppen, and L. Gaydos. 1997. A self-modifying cellular automaton model of historical urbanization in the San Francisco Bay area. Environment and Planning B: **Planning and Design**. 24: 247–261.

Clarke, K.C. and L.J. Gaydos. 1998. Loose-coupling a cellular automaton model and GIS: long-term urban growth prediction for San Francisco and Washington/Baltimore. **Int. J. GIS**. 12: 699–714.

Congalton, R., and K. Green. 1999. **Assessing the Accuracy of Remotely Sensed Data: Principles and Practices**. Lewis Publishers, Boca Raton, FL. 137pp.

Congalton, R.G. 1991. A Review of Assessing the accuracy of classifications of remotely sensed data. **Rem. Sens. Environ**. 37: 35-46.

Congalton, R.G. and R.A. Mead. 1983. A Quantitative Method to Test for Consistency in Photo-interpretation. **Photogramm. Eng. Rem. Sens**. 49 (1): 69–74.

Coppin, P. and M. Bauer. 1996. Digital Change Detection in Forest Ecosystems with Remote Sensing Imagery. **Rem. Sens. Reviews**. 13: 207-234.

Correia, P.T. 2000. Future development in Portuguese rural areas: how to manage agricultural support for landscape conservation? **Landscape and Urban Planning**. 50: 95–106.

Costa, M.H., A. Botta, J.A. Cardille. 2003. Effects of large-scale changes in land cover on the discharge of the Tocantins River, Southeastern Amazonia. **J Hydrol**. 283: 206–217.

Cotler, H, and M.P. Ortega-Larrocea. 2006. Effects of land use on soil erosion in a tropical dry forest ecosystem, Chamela watershed. **Catena**. 65: 107-117.

Cotter, A.S., I. Chaubey, T.A. Costello, T.S. Soerens, and M.A. Nelson. 2003. Water quality model output uncertainty as affected by spatial resolution of input data. **J. Am. Water Resour. Assoc**. 39(4): 977-986.

Crooks, S. and H. Davies. 2001. Assessment of land use change in the Thames catchment and its effect on the flood regime of the river. **Phys. Chem. Earth (B)**. 26 (7–8): 583–591.

CSA, 2008. Statistical Abstract 2007, Central Statistical Agency, Addis Ababa, Ethiopia, 178pp.

Dai, C., L. Tang, P. Jiang, and J. Lin. 1996. Satellite remote sensing for monitoring urban expansion and environmental remediation. In: **Population Dynamics and Management of Urban Environment**. pp. 9–16. Beijing: The 47th IAF Congress.

Das S., R.P. Ruda, B. Gharabaghi, P.K. Goel, A. Singh, and I. Ahmed. 2007. Comparing the performance of SWAT and AnnAGNPS model in a watershed in Ontario. ASABE publishing paper: 701P0207. ASABE, St. Joseph, MI.

Demers, M.N. 2005. **Fundamentals of Geographic Information Systems**, John Wiley & Sons, Inc., Newyork, USA. 468pp.

De Roo, A., M. Odijk, G. Schmuck, E. Koster, and A. Lucieer. 2001. Assessing the effects of land use changes on floods in the Meuse and Oder Catchment. Physics and Chemistry of the Earth, Part B: **J. Hydrol**. 26(8): 593-599.

Dimyati, M., K. Mizuno, S. Kobayashi, and T. Kitamura. 1995. An Analysis of Land Use Change Using the Combination of MSS Landsat and Land Use Map- A case study of Yogyakarta, Indonesia. **Int. J. Rem. Sens.** 17(5): 931- 944.

Dixon J.A., L.M. Talbot, and G.J. M. Le Moigne. 1989. Dams and their environment: considerations in World, 258pp.

Drewett, J.R. 1969. A stochastic model of the land conversion process. **Regional Studies**. 3: 269–280.

Dunne, T., and L.B. Leopold. 1978. **Water in environmental planning**, W.H. Freeman and Co., New York. 513pp.

Dwivedi, R.S., K. Sreenivas, and K.V. Ramana. 2005. Land-use/land-cover change analysis in part of Ethiopia using Landsat Thematic Mapper data. **Int. J. Rem. Sens**. 26 (7): 1285-1287.

EELPA (Ethiopian Electrical Light and Power Authority). 1994. Fincha reservoir water availability and management. Report made by ACRES Intern. Ltd, Canada, 52pp.

EFAP (Ethiopian Forestry Action Program). 1994. The Challenge for Development. Volume II. Final Report. Ministry of Natural Resources Development and Environmental Protection Addis Ababa, Ethiopia, 95pp.

Ehlers, M., M.A. Jadkowski, R.R. Howard, and D.E. Brostuen. 1990. Application of SPOT data for regional growth analysis and local planning. **Photogramm. Eng. Rem. Sens**. 56: 175–180.

Ella, V.B. 2005. Simulating soil erosion and sediment yield in small upland watersheds using the WEPP model. In: Coxhead and G.E. Shiverly eds., **Land use change in tropical watersheds: evidence, cause and remedies**. CABI publishing. Wallingford, Oxfordshire, UK. pp. 109 - 125.

El-Swaify, S.A. 2002. Impacts of land use change on soil erosion and water quality- A case study from Hawaii. In: **Technology and method of SWC**. Proceedings of 12th International Soil Conservation Organization conference, May 26-31, 2002 Beijing, China. 3: 267-270.

Elwell, H.A. 1994. Conservation Tillage for Sustainable Crop Production Systems, Consultancy Report. Institute of Agricultural Engineering, Harare, Zimbabwe.

Engman, E.T. 1983. Roughness coefficients for routing surface runoff. **ASCE. J. Irrig.Drainage Eng.** 112 (1): 39-52.

ERDAS Field Guide. 1999. Earth Resources Data Analysis System. ERDAS Inc. Atlanta, Georgia. 628pp.

Fan, F., Q. Weng, Y. Wang. 2007. Land use and land cover change in Guangzhou, China, from 1998 to 2003, based on Landsat TM/ETM+ imagery. **Sensors**. 7: 1323-1342.

FAO. 1998. **The Soil and Terrain Database for northeastern Africa**. FAO, Rome.

FAO. 2002. **Major Soils of the world. Land and Water Digital Media Series**. Food and Agricultural Organization of the United Nations. FAO, Rome.

FAO. 2005. **Digital Soil Map of the World and Derived Soil Properties of the World**. Food and Agricultural Organization of the United Nations. FAO, Rome.

Fohrer N., S. Haverkamp, K. Eckhardt, and H.G. Frede. 2001. Hydrologic Response to Land Use Changes on the Catchment Scale. **Phys. Chem. Earth (B**). 26 (7-8): 577-582.

Fohrer, N.S., and J.G. Arnold. 2005. Editors of SWAT 2000 Development and Application. **Hydrol. Process**. Special Issue. 19(3): 563-859.

Fu, B. and L. Chen. 2000. Agricultural land scape spatial analysis in the semi-arid hill area of the Loess Plateau, China. **J. Arid Environ**. 44: 291-303.

Gallart, F., and P. Llorens. 2001. Water Resources and Environmental change in Spain. A Key Issue for Sustainable Integrated Catchment management. **Cuadernos de Investigación Geográfica**. 27: 7-16.

Gassman, P.W., M.R. Reyes, C.H. Green, and J.G. Arnold. 2005. **SWAT Peer-Reviewed Literature:** A Review, 3rd International SWAT Conference. Pp 1-18 July 11-15, Zurich.

Gassman, P.W., M.R. Reyes, C.H. Green. 2007. The Soil and Water Assessment Tool: historical development, applications, and the future research directions. **Trans. ASABE**. 50(4): 1211–1250.

Geohegan, J., L.A. Wainger, and N.E. Bockstael. 1997. Spatial landscape indices in a hedonic framework: an ecological economics analysis using GIS. **Ecological Economics.** 23: 251–264.

Gete, Z. 2000. Landscape dynamics and soil erosion process modeling in the Northwestern Ethiopian highlands, (PhD dissertation), African studies series A16, Geographica bernensia, Berne, Switzerland.

Giertz, S., B. Junge, and B. Diekkruger. 2005. Assessing the effects of land use change on soil physical properties and hydrological processes in the sub-humid tropical environment of West Africa. **Phys. Chem. Earth (B**). 30: 485-496.

Gikas, G.D., T. Yiannakopoulou, and V.A. Tsihrintzis. 2005. Modeling of non-point source pollution in a Mediterranean drainage basin. **Environ. Model. Assess**. 11 (3): 219-233.

Gosain, A.K., S. Rao, and D.B. Ray. 2005. Vulnearability Assement of Climate Change Impact on Indian Water Resources using SWAT Model, 3rd International SWAT Conference, Pp 231-240. July 11-15, Zurich.

Green, W.H., G.A. Ampt. 1911. Studies on soil physics, I. The flow of air and water through soils. **J. Agric. Sci**. 4: 11-24.

Guerschman, J.P., J.M. Paruelo, C.D. Bela, M.C. Giallorenzi, F. Pacin. 2003. Land cover classification in the Argentine Pampas using multi-temporal Landsat TM data. **Int. J. Rem. Sens**. 24: 3381–3402.

Hao, F.H., X.S. Zhang, and Z.F. Yang. 2004. A distributed non-point source pollution model: Calibration and validation in the Yellow River Basin. **J. Environ. Sci**. 16(4): 646-650.

Harris, P.M. and S.J. Ventura. 1995. The integration of geographic data with remotely sensed imagery to improve classification in an urban area. **Photogramm. Eng. Rem. Sens**. 61: 993–998.

Hernandez, M., S.C. Miller, D.C. Goodrich, B.F. Goff, W.G. Kepner, C.M. Edmonds, and K.B. Jones. 2000. Modeling runoff response to land cover and rainfall spatial variability in semi-arid watersheds. **Environ. Monitoring Assess**. 64: 285-298.

Hershfield, D.M. 1961. Rainfall frequency atlas of the United States for durations from 30 minutes to 24 hours and return periods from 1 to 100 years. U.S. Dept. Commerce Tech. Paper No. 40.

Herweg, K., and E. Ludi. 1999. The performance of soil and water conservation measures-case studies from Ethiopia and Eritrea. **Catena**. 36: 99-114.

Heuvelmans, G., J.F. Garcio-Qujano, B. Muys, J. Feyen, and P. Coppin. 2005. Modelling the water balance with SWAT as part of the land use impact evaluation in a life cycle study of CO2 emission reduction scenarios. **Hydrol. Process**. 19(3): 729-748.

Hewlett, J.D. 1979. Increases in water yield after several types of forest cutting. **Introd. Assoc. Sci. Hydrol**. 6: 5-17.

Hibbert, A.R. 1967. Forest treatment effects on water yield. In: W.E. Sopper and H.W. Lull (Ed), Int. Syrup. **Forest Hydrology**, Pergamon, Oxford, 813pp.

Hollis G.E. 1975. The effect of urbanization on flood of different recurrence interval. **Water Resourc. Res**. 113: 431–435.

Hundecha, Y., and A. Bardossy. 2004. Modeling of the effect of land use changes on the runoff generation of a river basin through parameter regionalization of a watershed model. **J. Hydrol**. 292: 281-295.

Hurni, H. 1990. Degradation and conservation of soil resources in the Ethiopian highlands. **Mt. Res. Dev**. 8 (2-3): 123–130.

Hurni, H. 1993. Land degradation, famine and land resource scenarios in Ethiopia. In: World Soil Erosion and Conservation (ed. D. Pimentel) pp. 27–62. Cambridge University Press, Cambridge, UK.

Jacobs, J.H. and R. Srinivasan. 2005. Application of SWAT in Developing Countries using Readily Available Data. (3rd Int. SWAT Conference, July 11-15, Zurich).

Jayakrishnan, R., R. Srinivasan, C.Santhi, and J.G. Arnold. 2005. Advances in the application of the SWAT model for water resources management. **Hydrol. Process**. 19: 749-762.

Jahan, S. 1986. The determination of stability and similarity of Markovian land use change processes: a theoretical and empirical analysis. **Socio-Econ Planning Sci**. 20: 243–251.

Jensen, J.R., R.S. Narumalani, J.D. Althausen, and O. Weatherbee. 1993. An evaluation of CoastWatch change detection Protocol in South Carolina. **Photogramm. Eng. Rem. Sens**. 59(6):1039-1046.

Jensen, J.R. 1996. **Introductory Digital Image Processing: A Remote Sensing Perspective (2nd edn)**. Upper Saddle River, NJ: Prentice Hall.

Jha, M., P.W. Gassman, S. Secchi, R. Gu, and J. Arnold. 2004. Effect of watershed subdivision on SWAT flow, sediment, and nutrient predictions. **J. Am. Water Resour. Assoc**. 40(3): 811-825.

Jha, M.K., P.W. Gassman and J.G. Arnold. 2007. Water quality modeling for the Raccoon River watershed using SWAT. **Trans. ASAE**. 50(2): 479 – 493.

Jianchu, X., A. Xihui, and D. Xiqing. 2005. Exploring the spatial and temporal dynamics of land use in Xizhuang watershed of Yunnan, southwest China. **Int. J. Applied Earth Observation and Geo-information**. 7: 299-309.

Juckem, P.F., R.J. Hunt, M.P. Anderson, and D.M. Robertson. 2008. Effects of climate and land management change on streamflow in the driftless area of Wisconsin. **J. Hydrol**. 355: 123-130.

Karvonen, T., H. Koivusalo, and M. Jauhiainen. 1999. A hydrological model for predicting runoff from different land use areas. **J. Hydrol**. 217: 253-265.

Kasai, M., G.J. Brierley, M.J. Page, T. Marutani, and N.A. Trustrum. 2005. Impacts of land use change on patterns of sediment flux in Weraamaia catchment, New Zealand. **Catena**. 64: 27- 60.

Kaur, R., O. Singh, R. Srinivasan, S.N. Das, and K. Mishra. 2004. Comparison of a subjective and a physical approach for identification of priority areas for soil and water management: A case study of Nagwan watershed in Hazaribagh District of Jharkhand, India. **Environ. Model. Assess**. 9(2): 115-127.

Kebron, T. 2000. Land cover changes between 1958 and 1986 in Kalu district, South Wello, Ethiopia. **Mt. Res. Dev**. 20: 42-51.

Kim, H., and G. Elman. 1990. Normalization of Satellite Imagery. **Introd. J. Rem. Sens**. 11(8): 1331-1347.

Kirsch, K., A. Kirsch and J.G. Arnold. 2002. Predicting sediment and phosphorus yields in the Rock River basin using SWAT. **Trans. ASAE**. 45(6): 1757 – 1769.

Kosmas, C., N. Danalatos and L.H. Cammeraat. 1997. Effect of land use on runoff and soil erosion rates under Mediterranean conditions. **Catena**. 29: 45–59.

Krause, P., D.P. Boyle and F. Base. 2005. Comparison of different efficiency criteria for hydrological model assessment. **Adv. Geosci**. 5: 89 – 97.

Lambin, E.F. 2001. The cause of land use and land cover change: moving beyond the myths. **Global Environmental Change**. 11: 261-269.

Landis, J.D. 1994. The California urban future model: a new-generation of metropolitan simulation-models. **Environ. Planning B**. 21: 399–420

Langford, K.J. 1976. Change in yield of water following a bush fire in a forest of Eucalyptus regnans. **J. Hydrol**. 29: 87–114.

Le Bissonnais, Y., C. Montier, M. Jamagne, J. Daroussin, and D. King. 2001. Mapping Erosion risk for cultivated soil in France. **Catena**. 46: 207-220.

Liu, H. and Q. Zhou. 2004. Accuracy analysis of remote sensing change detection by rule-based rationality evaluation with post classification. **Introd. J. Rem. Sens**. 25(5):1037-1050.

Lørup, J.K., J.C. Refsgaard, and D. Mazvimavi. 1998. Assessing the effect of land use change on catchment runoff by combined use of statistical tests and hydrological modelling: Case studies from Zimbabwe. **J. Hydrol**. 205: 147-163.

Lu, D., P. Mausel, M. Batistella, E. Moran. 2005. Land-cover binary change detection methods for use in the moist tropical region of the Amazon: a comparative study. **Int. J. Rem. Sens**. 26 (1): 101-114.

Lu, X., and D.I. Higgitt. 1998. Recent changes of sediment yield in the upper Yangtze, china. **Environ. Manag**. 22: 697-709.

Lu, X., P. Ashmore, and J.F. Wang. 2003. Seasonal Water Discharge and Sediment Load Changes in the Upper Yangtze, China. **Mt. Res. Dev**. 23: 56-64. Lull (Editors), Int. Syrup. **Forest Hydrology**, Pergamon, Oxford, 813 pp.

Mapfumo, E., D.S. Chansyk, and W.D. Williams. 2005. Simulating daily soil water under foothills fescue grazing with the soil and water assessment tool model (Alberta, Canada). **Hydrol. Process**. 18: 2787-2800.

Mas, J.F. 1999. Monitoring land-cover changes: a comparison of change detection techniques. **Int. J. Rem. Sens**. 20 (1): 139-152.

Mas, J.F., A. Velazquez, J.R.D. Gallegos, R.M. Saucedo, C. Alcantare, G. Bocco, R. Castro, T. Fernandez, and A.P. Vega. 2004. Assessing land use/cover changes: a nationwide multi-date spatial database for Mexico. **Int. J. Applied Earth Observation and Geo-information.** 5: 249-261.

Meaille, R. and L. Wald. 1990. Using geographic information system and satellite imagery within a numerical simulation of regional urban growth. **Introd. J. GIS**. 4:445-456.

Mesfin, W. 1985. Northern Shewa and Wello. Background paper on development strategy for the problem of vulnerability to famine. FAO, Ethiopia.

Meyer, W.B. 1995. Past and Present Land-use and Land-cover in the U.S.A. Consequences. pp.24-33.

Meyer, W.B. and B.L. Turner. 1996. Land-use/land-cover change: Challenges for geographers. **Geo. Journal**. 39(3): 237-240.

Michael, A. 2004. Lessons learned from existing hydro schemes, Case study: Koka dam, First National Water Forum conference Proceeding Paper. Pp. 49-58. Ministry of Water Resources, Addis Ababa, Ethiopia.

Miller, S.N., W.G. Kepner, M.H. Mehaffey, M. Hernandez, R.C. Miller, D.C. Goodrich, K.K Devonald, D.T. Heggem, and W.P. Miller. 2002. Integrating landscape assessment and hydrologic modeling for land cover change analysis. **J. Am. Water Resour. Assoc**. 38(4): 915-929.

Molnar, D.K., and P.Y. Julien. 1998. Estimation of upland erosion using GIS. **Computer and Geosciences**. 24: 183-192.

Moraes, J.M., G.Q. Pellegrino, M.V. Ballester, L.A. Martinelli, R.L. Victoria and A.V. Krusche. 1998. Trends in Hydrological Parameters of a Southern Brazilian Watershed and its Relation to Human Induced Changes. **Water Resour. Manag**. 12: 295-311.

Moriasi, D.N., J.G. Arnold, M.W. Van Liew, R.L. Bingner, R.D. Harmel, and T.L. Veith. 2007. Model evaluation guidelines for systematic quantification of accuracy in watershed simulations. **Trans. ASAE**. 50 (3): 885 ‐ 900.

Moshen, A. 1999. Environmental Land Use Change Detection and Assessment Using Multi – temporal Satellite Imagery. Zanjan University.

MoWR (Ministry of Water Resources). 2002. **Ethiopian water sector strategy**. MoWR, Addis Ababa, pp247.

Muleta, M.K., and J.W. Nicklow. 2005. Decision support for watershed management using evolutionary algorithms. **J. Water Resour. Planning and Manag**. 131(1): 35-44.

Muller, R.M. and J. Middleton. 1994. A Markov model of land-use change dynamics in the Niagara region, Ontario, Canada. **Landscape Ecology**. 9: 151–157.

Munasinghe, and W. Shearer. 1995. Defining and measuring sustainability. The Biogeochemical Foundation. The United Nations University (UNU) and the World Bank, Washington, DC.

Mustard, R.S., L. Defries, T. Fisher, and E. Moran. 2005. Land use/cover change pathways and impacts. In: **Land change science: observing, monitoring, and understanding trajectories of change on the earth's surface**, Kluwer Academic Publishers, Dordrecht, The Netherlands, pp. 411–429.

Muttitanon, W. and N.K. Tilpathi. 2005. Land use/land cover changes in the coastal zone of Ban Don Bay, Thailand using Landsat 5 TM data. **Int. J. Rem. Sens**. 26 (11): 2311-2323.

Nash, J.E. and J.V. Sutcliffe. 1970. River flow forecasting through conceptual models, part I. A discussion of principles. **J. Hydrol**. 10 (3): 282 ‑ 290.

Nathaniel, R.A., V.B. Ella, M.A. Reys, R. Srinivasan, C. Heatwole, and T. Dillaha. 2009. Predicting the effects of land use on runoff and sediment yield in selected sub-watersheds of the Manupali River using ArcSWAT. In: **Soil and Water Assessment Tool (SWAT), Global Applications**: Special publication No. 4. World Association of Soil & Water Conservation, Bangkok, Pp. 253-266.

Natural Resources Conservation Service Soil Survey Staff. 1996. National soil survey handbook, title 430-VI. U.S. Government Printing Office, Washington, D.C.

Ndomba, P.M., F.W. Mtalo, and A. Killingtveit. 2008. SWAT model application in a data scarce tropical complex catchment in Tanzania. **J. Phys. Chem**.

Neitsch, S.L., J.G. Arnold, J.R. Kiniry, and J.R. Williams. 2005. **Soil and Water Assessment Tool: Theoretical Documentation**. Blackland Research center, Grassland, Soil and Water Research Laboratory, Agricultural Research Service: Temple, TX, 476pp.

Neitsch, S.L., J.G. Arnold, J.R. Kiniry, R. Srinivasan, and J.R. Williams. 2002. **Soil and Water Assessment Tool (SWAT) User's Manual, Version 2000**. Blackland Research center, Grassland, Soil and Water Research Laboratory, Agricultural Research Service: Temple, TX, 461pp.

Niehoff, D., U. Fritsch, and A. Bronstert. 2002. Land use impacts on storm runoff generation: scenarios of land use change and simulation of hydrological response in a meso-scale catchment in SW-German. **J. Hydrol**. 267: 80-93.

OADB (Oromiya Agriculture Development Bureau). 1996. **Land Resources and Socio-Economic Survey Report of Coomman Watershed**. OADB, Addis Ababa, Ethiopia, 72pp.

Ojima, D.S., K.A. Galvin and B.L. Turner. 1994. The global impact of land-use change. **Biosci**. 44: 300–304.

Olorunfemi, J.F. 1983. Monitoring Urban Land – Use in Developed Countries –An aerial photographic approach. **Environmental Int**. 9: 27 - 32.

Pandey, V.K., S.N. Panda, S. Sudhakar. 2005. Modelling of an agricultural watershed using Remote Sensing and a Geographic Information System. **Biosyst. Eng**. 90 (3): 331–347.

Parajuli, P.B., K.R. Mankin and P.L. Barnes. 2007. New methods in modeling source specific bacteria scale using SWAT. ASABE publication No. 701P0207. ASABE: St. Joseph, MI.

Pasricha, A. 1999. Watershed modeling using Geographical Information System. PhD. Thesis, Department of Civil Engineering, IIT Delhi.

Pikounis, M., E. Varanou, E. Baltas, A. Dassaklis, and M. Mimikou. 2003. Application of the SWAT model in the Pinios River Basin under different land-use scenarios. Global nest: **The Introd. Journ**. 5(2): 71-79.

Podwojewski, P., D. Orange, P. Jouquet, C. Valentin, V.T. Nguyen, J.L. Janeau, and D.T. Tran. 2008. Land-use impacts on surface runoff and soil detachment within agricultural sloping lands in Northern Vietnam. **Catena**. 74: 109-118.

Poesen, J., J. Nachtergaele, G. Verstraeten, and C. Valentin. 2003. Gully erosion and environmental change: importance and research needs. **Catena**. 50: 91-133.

Prenzel, B. 2004. Remote sensing-based quantification of land-cover and land-use change for planning. **Progress in Planning**. 61: 281–299.

Qi, C. and S. Grunwald. 2005. GIS-Based Hydrologic modeling in the Sandusky watershed using SWAT. **Trans. ASAE**. 48(1): 160 – 180.

Rajan, K.S., and R. Shibasaki. 1997a. Estimation of agricultural productivity and its application to modelling the expansion of agricultural land in Thailand. **J. Agric. Meteorology**. 52(5): 815-818.

Rajan, K.S., and R. Shibasaki. 1997b. National scale land use change modeling-issues and applications. In: **Proceedings of the 18th Asian conference on remote sensing**, Kuala Lumpur, Malaysia, pp. H-2.

Richards John A. and Xiuping Jia. 1999. **Remote Sensing Digital Image Analysis: An Introduction**: Third edition. Springer. 363pp.

Riebsame, W.E., W.B. Meyer, and B.L. Turner. 1994. Modeling Land-use and Cover as Part of Global Environmental Change. **Climate Change**. 28: pp. 45.

Ripl, W. 1995. Management of water cycle and energy flow for ecosystem control: the energy-transport-reaction (ETR) model. **Ecological Modeling**. 78: 61-76.

Ritler, A. 1997. Land use, forests and the landscape of Ethiopia, 1699-1865. An enquiry into the historical geography of central-northern Ethiopia. Soil conservation Research Pragramme and Centre for Development and Environment. Research Report 38, Switzerland.

Robinson, V.B. 1978. Information theory and sequences of land use: an application. **The Professional Geographer**. 30: 174–179.

Rode, M., B. Klauer, D. Petry, M. Volk, G. Wenk, and D. Wagenschein. 2008. Integrated nutrient transport modelling with respect to the implementation of the

European WFD: the Weiße Elster case study, Germany. **Water SA**. 34(4): 490–496.

Rogana, J. and D. Chen. 2004. Remote sensing technology for mapping and monitoring land use/cover change. **Progress in Planning**. 61: 301–325.

Rosenfield, G.H. and K. Fizpatrick-Lins. 1986. A Coefficient of Agreement as a Measure of Thematic Classification Accuracy. **Photogramm. Eng. Rem. Sens**. 52 (2): 223–227.

Rosenthal, W.D., and D.W. Hoffman. 1999. Hydrologic modeling/GIS as an aid in locating monitoring sites. **Trans. ASAE**. 42(6): 1591-1598.

Rubiano, J. 2000. Land Use Change in Tropical Hillsides: the Influence of Pattern on Process. **Advances in Environmental Monitoring & Modeling**. 1(1): 61-79.

Saleh, A., J.G. Arnold, P.W. Gassman, L.W. Hauck, W.D. Rosenthal, J.R. Williams, and A.M.S. McFarland. 2000. Application of SWAT for the upper north Bosque Watershed. **Trans. ASAE**. 43(5): 1077-1087.

Santhi, C., J.G. Arnold, J.R. Williams, W.A. Dugas, R. Srinivasan, and L. M. Hauck. 2001. Validation of the SWAT model on a large river basin with point and non-point sources. **J. Am. Water Resour. Assoc**. 37(5): 1169-1188.

Schmidt, G., and M. Volk. 2005. Effects of input data resolution on SWAT simulations-A Case study at the EMs River Basin (North Western Germany). 3rd International SWAT Conference, pp 241-250. July 11-15 Zurich.

Schreider, S.Y., A.J. Jakeman, R.A. Letcher, R.J. Nathan, B.P. Neal, and S.G. Beavis. 2002. Detecting changes in stream flow response to changes in non-climatic catchment conditions: farm dam development in the Murray–Darling basin. Aust. **J. Hydrol**. 262: 84-98.

Seto, K.C., C.E. Woodcock, C. Song, X. Huang, J. Lu, and R.K. Kaufmann. 2004. Monitoring land use change in the Pearl River Delta using Landsat TM. **Int. J. Rem. Sens**. 23 (10): 1985-2004.

Shanti, C., Arnold, J.G., Williams, J.R., Dugas, W.A., Srinivasan, R., Hauck, L.M. 2003. Validation of the SWAT model on a large river basin with point and nonpoint sources. **JAWRA**. 37 (5): 1169–1188.

Sharpley, A.N., and J.R. Williams. 1990. Erosion/productivity impact calculator, I. Model documentation. USDA-ARS Technical Bulletin, 1768.

Shi, P.J., Y. Yuan, J. Zheng, J.A. Wang, Y. Ge., and G.Y. Qiu. 2007. The effect of land use change on runoff in Shenzhen region, China. **Catena**. 69: 31-35.

Shimelis, S.G., R. Srinivasan, and B. Dargahi. 2008. Hydrological modeling in the lake Tana basin, Ethiopia using SWAT model. **The open Hydrol. J**. 2: 49-62.

Shoshany, M., P. Kutiel, and H. Lavee. 1994. Monitoring temporal vegetation cover changes in Mediterranean & Arid Ecosystems using a remote sensing technique: case study of the Judean Mountain and Desert. **J. Arid Environ**. 33: 9 - 21.

Sileshi, B. 2001. Investigation of water resources aimed at multi objective development with respect to limited data situation: The case of Abbaya- Chamo Basin Ethiopia, (PhD dissertation), Technical University of Dresden, Germany.

Singh, A. 1989. Digital Change Detection Techniques Using Remotely Sensed Data. **Int. J. Rem. Sens**. 10 (6): 989-1003.

Siriwardena, L., B.L. Finlayson, and T.A. McMahon. 2006. The impact of land use change on catchment hydrology in large catchments: The Comet River, Central Queensland, Australia. **J. Hydrol**. 326: 199-214.

Skole, D., and C. Tucker. 1993. Tropical deforestation and habitat fragmentation in the Amazon: satellite data from 1978 and 1988. **Science**. 1905-1910.

Slaymaker, O. 2003. The sediment budget as conceptual framework and management tool. **Hydrobiologia**. 494: 71-82.

Soil Conservation Service Engineering Division. 1986. **Urban hydrology for small watersheds**. U.S. Department of Agriculture, Technical Release, 55pp.

Soil Conservation Service (SCS). 1972. Section 4: **Hydrology in National Engineering Handbook**. Soil Conservation Service, 92pp.

Solomon, A. 1994. Land use dynamics, soil degradation and potential for sustainable use in Mettu area, Illubabor region, Ethiopia (PhD dissertation) African studies series A13, **Geographica bernensia**, Berne, Switzerland.

Spruill, C.A., S.R. Workman and J.L. Taraba. 2000. Simulation of daily and monthly stream discharge from small watersheds using the SWAT model. **Trans. ASAE**. 43(6): 1431 - 1439.

Srinivasan, R., T.S. Ramanarayanan, J.G. Arnold, and S.T. Bednarz. 1998. Large area hydrologic modeling and assessment, part II: Model application. **J. Am. Water Resourc. Assoc**. 34(1): 91-101.

Stednick, J.D. 1996. Monitoring the effects of timber harvest on annaual water yield. **J. Hydrol**. 176: 79-95.

Stehman, SV. 1997. Selecting and interpreting measures of thematic classification accuracy. **Rem. Sens. of Environ**. 62: 77–89

Steininger, M.K. 1996. Tropical secondary forest regrowth in the Amazon: age, area and change estimation with Thematic Mapper. **Int. J. Rem. Sens**. 17: 9–27.

Stewart, W.J. 1994. **Introduction to the Numerical Solution of Markov Chains**. Princeton, NJ: Princeton University Press, 539pp.

Swain, A. 1997. Ethiopia, the Sudan, and Egypt: The Nile River dispute. **J. Mod. Afr. Stud**. 35: 675 - 694.

Tadele, K. and G. Forch. 2007. Impact of land use/cover change on stream flow: a case study of Hare watershed, Ethiopia. **FWU Water Resources Publications**. 6: 80 - 84.

Taillefumier, F., and H. Piegay. 2003. Contemporary land use changes in Prealpine Mediterranean mountains: a multivariate GIS-based approach applied to two municipalities in the Southern French Prealps. **Catena**. 51: 267-296.

Teillet, P.M. 1986. Image Correction for Radiometric Effects in Remote Sensing. **Int. J. Rem. Sens**. 7 (12): 1637-1651.

Terry, C. 1995. Dams in the development context: economic, social and environmental aspects of large dams. In: Both Sides of the Dam. Symposium 'Het Waterbouwdispuut', 22 February 1995 (eds A. Blom, J. van Dalen, I. Ploegmakers & A. Verweij) pp. 8–12. Delft, The Netherlands.

Thomas, M.L., L.R. Logan, and NR. Fausey. 1992. Land use and management effects on nonpoint loading from Miamian soil. **J. Am. Soil sci. Society**. 56: 1871-1875.

Treitz, P.M., P.J. Howard, and P. Gong. 1992. Application of satellite and GIS technologies for land cover/use mapping at the rural-urban fringe: a case study. **Photogramm. Eng. Rem. Sens**. 58: 439–448.

Tripathi, M.P., R.K. Panda, and N.S. Raghuwanshi. 2005. Development of effective management plan for critical subwatersheds using SWAT model. **Hydrol. Process**. 19: 809–826.

Tripathi, M.P., N.S. Raghuwanshi, and G.P. Rao. 2006. Effect of watershed subdivision on simulation of water balance components. **Hydrol. Process**. 20(5): 1137-1156.

Turner, M.G., D.N. Wear, and R.O. Flamm. 1996. Land ownership and land-cover change in the southern Appalachian highlands and the Olympic peninsula. **Ecol. Appl**. 6: 1150–1172.

Turner, B.L., D. Skole, S. Sanderson, G. Fischer, L. Fresco, and R. Leemans. 1995. **Land Use/ Land Cover Change Science/Research Plan**. Publications IHDP Report series, Report number 07. 172pp.

Turner, B.L., R.H. Moss, and D.L. Skole. 1993. Relating land use and global land-cover change: a proposal for an IGBP core Project. IGBP report No. 5. 65pp.

Ulbricht, K.A. and W.D. Heckendorf. 1998. Satellite images for recognition of landscape and land use changes. **J. Photogramm. Rem. Sens**. 53: 235-243.

USDA-SCS, 1972. **National Engineering Hand Book**, Hydrology section 4, Chapter 4-10. Washington DC: US Dep. Agriculture, Soil Conservation Service, 92pp.

Vache, K.B., J.M. Eilers, M.V. Santelmann. 2002. Water quality modeling of alternative agricultural scenarios in U.S. Corn Belt. **JAWRA.** 38 (3): 773–787.

Valentin, C., J. Poesen, and Y. Li. 2005. Gully erosion: Impacts, factors and control. **Catena**. 63: 132-153.

Van Liew, M.W., and J. Garbrecht. 2003. Hydrologic simulation of the Little Washita River Experimental Watershed using SWAT. **J. Amer. Water Resour. Assoc**. 39(2): 413-426.

Verburg, P.H. and Y. Chen. 2000. Multiscale characterization of land-use patterns in China. **Ecosys**. 3: 369–385.

Verburg, P.H., G.H.J. Koning, K. Kok, A. Veldkamp, L.O. Fresco, and J. Bouma. 1999. Quantifying the spatial structure of land use change: an integrated approach. Wageningen Agricultural University, Netherlands.

Verstraeten, G., and I.P. Prosser. 2005. Modelling the impact of land use change and farm dam construction on the sediment delivery to river channels at the regional scale. A case study of the Murrumbidgee catchment, Australia. **Geophysical Res. Abstracts.** 7: 08029.

Volk, M., S. Liersch, G. Schmidt. 2009. Towards the implementation of the European Water Framework Directive? Lessons learned from water quality simulations in an agricultural watershed. **Land Use Policy.** 26 (3): 580–588.

Walling, D.E., and D. Fang. 2003. Recent trends in the suspended sediment loads of the world's rivers. **Global and Planetary Change**. 39: 111-126.

Wang S., S. Kang, L. Zhang, and F. Li. 2008. Modeling hydrological response to different land use and climate change scenarios in the Zamu River basin of northwest China. **Hydrol. Process**. 22: 2502 - 2510.

Wang, X., A.M., Melesse and W. Yang. 2006. Influences of potential evapotranspiration estimation methods on SWAT's hydrologic simulation in a northwestern Minnesota watershed. **Trans. ASABE**. 49(6): 1755 - 1771.

Wang, Y., W. Choi, and M.B. Deal. 2005. Long-Term Impacts of Land-Use Change on Non- Point Source Pollutant Loads for the St. Louis Metropolitan Area, USA. **Environ. Mangt**. 35(2): 194-205.

Watson, B.M., N. Coops., S. Selvalingam, and M. Ghafouri. 2005. Integration of 3-PG into SWAT to Simulate the Growth of Evergreen Forests. 3rd International SWAT Conference. July 11-15, Zurich.

Wear, D.N., M.G. Turner, and R.J. Naiman. 1998. Land cover along an urban-rural gradient: implications for water quality. **Ecol. Appl**. 8: 619–630.

Weber, A., N. Fohrer, and D. Moller. 2001. Long-term land use changes in a mesocale watershed due to socio-economic factors—Effects on landscape structures and functions. **Ecol. Model**. 140: 125-140.

Wei, W., L. Chen, B. Fu, Z. Huang, D. Wu, and L. Gui. 2007. The effect of land uses and rainfall regimes on runoff and soil erosion in the semi-arid loess hilly area, China. **J. Hydrol**. 335: 247-258.

Weng, Q. 2001. A remote sensing-GIS evaluation of urban expansion and its impact on surface temperature in the Zhujiang Delta, China. **Introd. J. Rem. Sens**. 64: 273-284.

Weng, Q. 2002. Land use change analysis in the Zhujiang Delta of China using satellite remote sensing, GIS and stochastic modelling. **J. Enviriron. Mangt**. 64: 273-284.

Westmoreland, S. and D.A. Stow. 1992. Category identification of changed land-use polygons in an integrated image processing/GIS. **Photogramm. Eng. Rem. Sens**. 58: 1593–1599.

White, K.L. and I. Chaubey. 2005. Sensitivity analysis, calibration, and validations for a multisite multivariable SWAT model. **J. Am. Water Resour. Assoc**. 41(5): 1077 ‐ 1089.

White, K.L, I. Chaubey, B.E. Haggard, and M.D. Matlock. 2004. Comparison of two methods of modeling monthly TP yield from a watershed. ASABE meeting paper No. 042162. ASABE, Joseph MI.

Williams, J.R. 1969. Flood routing with variable travel time or variable storage coefficients. **Trans. ASAE**. 12(1): 100-103.

Williams, J.R. and R.W. Hann. 1973. HYMO: Problem-oriented language for hydrologic modeling. User's manual. USDA, ARS-S-9.

Williams, J.R. 1975. Sediment Routing for Agricultural Watersheds. Water resources bulletin. 11 (5): 965-974.

Williams, J.R. 1980. SPNM, a model for predicting sediment, phosphorus, and nitrogen from agricultural basins. Water Resources Bulletin. 16: 843-848.

Williams, J.R. 1995. The EPIC model. In Singh VP. (ED). Computer models of watershed hydrology. Water resources publications, Highlands Ranch, CO. Chapter 25, 909 −1000.

Wischmeier, W.H., and D.D Smith. 1958. Rainfall energy and its relationship to soil loss. **Trans. Am. Geophysical Union**. 39: 285-291.

Wischmeier, W.H., and D.D. Smith. 1965. Predicting rainfall erosion losses from cropland east of the Rocky Mountains. **Agriculture handbook**, 282. USDA-ARS.

Wischmeier, W.H., and D.D. Smith. 1978. Predicting rainfall erosion losses. A guide to conservation planning. **Agriculture handbook**, 537, USDA-ARS.

Wischmeier, W.H., C.B. Johnson, and B.V. Cross. 1971. A soil erodibility monograph for farmland and construction sites. **J. Soil and Water Conserv**. 26:189-193.

Woldeamlak, B. 2003. Towards integrated watershed management in highland Ethiopia: the Chemoga watershed case study, (PhD dissertation), **Tropical resources Management papers** 44, Wageningen University, The Netherlands.

Wooldridge, S., J. Kalma, and G. Kuczera. 2001. Parameterisation of a simple semi-distributed model for assessing the impact of land use on hydrologic response. **J. Hydrol**. 254: 16-32.

Wu, Q., H.Q. Li, R.S. Wang, J. Paulussen, Y. He. M. Wang, B.H. Wang, and Z. Wang. 2006. Monitoring and predicting land use change in Beijing using remote sensing and GIS. **Landscape and Urban Planning**. 78: 322 - 333.

Xiaomei, Y. and L.Q.Y. Ronqing. 1999. Change Detection Based on Remote Sensing Information Model and its Application to Coastal Line of Yellow River Delta – Earth Observation Center, NASDA, China.

Xue-song, Z., H. Fang-bua, C. Hong-guang, and L. Dao-feng. 2003. Application of SWAT model in the upstream watershed of the Luohe River. **Chinese Geog. Sci**. 13 (4): 334-339.

Yeh, A.G.O. and Li, X. 1999. Economic development and agricultural land loss in the Pearl River Delta, China. **Habitat International**. 23: 373–390.

Yuan, F., K.E. Sawaya, B.C. Loeffelholz, and M.E. Bauer. 2005. Land cover classification and change analysis of the Twin Cities metropolitan areas by multitemporal Landsat remote sensing. **Rem. Sens. Environ**. 98: 317-328.

Yu, D.S., X.Z. Shi, H.J. Wang, X.Y. Zhang, and D.C. Weindorf. 2008. Function of soils in regulating rainwater in southern China: Impacts of land uses and soils. **Pedosphere**. 18(6): 717-730.

Zaho, W.W., B.J. Fu, Q.H. Meng, Q.J. Zhang, and Y.H. Zhang. 2004. Effects of land-use change on rainfall-runoff and runoff-sediment relations: a case study in Zichang watershed of loess plateau of china. **J. Environ. Sci**. 16(3): 436-442.

Zeray, L., J. Roehrig and D.A. Chekol. 2007. Climate change impact on Lake Ziway watershed water availability, Ethiopia. FWU Water Resources Publications. 6: 18 - 23.

Zsuzsanna, D., J. Bartholy, R. Pongracz, and Z. Barcza. 2005. Analysis of land-use/land-cover change in the Carpathian region based on remote sensing techniques. **Phy. Chem. Earth**. 30: 109-115.

APPENDICES

Appendix A

Tables

Appendix Table 1 Row tally matrix between 1985 to 1995 (in counts).

From (i) \ To (j)	Agricultural land	Forest land	Grazing land	Water body	Swamp	Shrub land	Total 1985
Agricultural land	847535	384982	78965	1000	4265	75514	1392261
Forest land	456681	211166	126830	5530	11517	71691	883415
Grazing land	351091	17087	184893	105138	5531	21316	685056
Water body	1813	0	25790	195668	26560	3856	253687
Swamp	6404	6070	128965	28759	249275	58628	478101
Shrub land	95790	55659	33214	46569	27083	51328	309643
Total 1995	1759314	674964	578657	382664	324231	282333	4002163

Appendix Table 2 Row tally matrix between 1995 to 2005 (in counts).

From (i) \ To (j)	Agricultural land	Forest land	Grazing land	Water body	Swamp	Shrub land	Total 1995
Agricultural land	1326912	275676	74639	992	5245	75850	1759314
Forest land	362256	110996	114834	5533	11524	69821	674964
Grazing land	351191	19083	94693	95138	5931	12621	578657
Water body	2513	0	22790	325968	26260	5133	382664
Swamp	6404	6070	128965	15759	149275	17758	324231
Shrub land	89130	25609	35206	46479	34273	51636	282333
Total 2005	2138406	437434	471127	489869	232508	232819	4002163

Appendix Table 3 Row tally matrix between 1985 to 2005 (in counts).

From (i) \ To (j)	Agricultural land	Forest land	Grazing land	Water body	Swamp	Shrub land	Total 1985
Agricultural land	1243411	17777	68739	11992	5245	45097	1392261
Forest land	416851	350896	26830	5530	11617	71691	883415
Grazing land	371091	17087	194693	95138	5631	1416	685056
Water body	4513	0	26790	211968	6560	3856	253687
Swamp	6750	6015	120861	108672	176372	59431	478101
Shrub land	95790	45659	33214	56569	27083	51328	309643
Total 2005	2138406	437434	471127	489869	232508	232819	4002163

Appendix Table 4 Transition probability matrix (P) between 1985 and 1995.

From (i) \ To (j)	Agricultural land	Forest land	Grazing land	Water body	Swamp	Shrub land
Agricultural land	0.6087	0.2765	0.0567	0.0007	0.0031	0.0542
Forest land	0.5169	0.2390	0.1436	0.0063	0.0130	0.0811
Grazing land	0.5125	0.0249	0.2699	0.1535	0.0081	0.0311
Water body	0.0071	0.0000	0.1017	0.7713	0.1047	0.0152
Swamp	0.0134	0.0127	0.2697	0.0602	0.5214	0.1226
Shrub land	0.3093	0.1797	0.1073	0.1504	0.0874	0.1657

Appendix Table 5 Transition probability matrix (P) between 1995 and 2005.

From (i) \ To (j)	Agricultural land	Forest land	Grazing land	Water body	Swamp	Shrub land
Agricultural land	0.7542	0.1567	0.0424	0.0005	0.0029	0.0431
Forest land	0.5367	0.1644	0.1701	0.0082	0.0171	0.1034
Grazing land	0.6069	0.0329	0.1636	0.1644	0.0102	0.0218
Water body	0.0066	0.0000	0.0595	0.8518	0.0686	0.0134
Swamp	0.0197	0.0187	0.3977	0.0486	0.4604	0.0547
Shrub land	0.3156	0.0907	0.1247	0.1646	0.1214	0.1829

Appendix Table 6 Transition probability matrix (P) between 1985 and 2005.

From (i) \ To (j)	Agricultural land	Forest land	Grazing land	Water body	Swamp	Shrub land
Agricultural land	0.8931	0.0128	0.0494	0.0086	0.0037	0.0324
Forest land	0.4718	0.3972	0.0304	0.0063	0.0131	0.0812
Grazing land	0.5417	0.0249	0.2842	0.1388	0.0082	0.0021
Water body	0.0178	0.0000	0.1056	0.8356	0.0258	0.0152
Swamp	0.0141	0.0126	0.2528	0.2273	0.3689	0.1243
Shrub land	0.3093	0.1475	0.1072	0.1827	0.0875	0.1657

Appendix Table 7 Statistical precipitation and temperature data (1985-2005) for Fincha station.

Description	Jan	Feb	Mar	Apr	May	Jun	Jul	Aug	Sep	Oct	Nov	Dec
PCP_MM	16	24.3	67.1	102.1	165	294	413	401	259	83	25	23
PCPSTD	0.8	1.36	2.51	4.17	4.84	7.9	9.6	7.78	5.6	3.2	1.4	1.3
PCPSKW	1.86	2.98	2.0	1.76	0.74	1.1	0.6	0.75	0.01	2.1	2.6	2.9
PR_W1	0.21	0.47	0.6	0.53	0.44	0.7	0.8	0.65	0.63	0.3	0.3	0.2
PR_W2	0.37	0.36	0.74	0.69	0.87	0.7	0.6	0.62	0.57	0.5	0.4	0.4
PCPD	3.09	3.95	8.09	9.0	13	16	15	16	13	9.0	4.8	3.4
TMPMX	28.4	29.2	29.5	29.2	29.1	27	24	22.6	24	26	26	27
TMPSTDMX	1.19	1.25	1.26	1.44	1.49	1.3	0.9	0.71	0.89	0.9	0.6	0.8
TMPMN	7.7	7.8	9.0	10.1	9.9	9.3	9.2	8.5	9.1	7.4	7.0	6.1
TMPSTDMN	1.05	0.93	0.96	0.82	0.76	0.6	0.7	0.68	0.6	1.0	1.2	1.5

Where:

PCP_MM: average monthly precipitation (mm)

PCPSTD: standard deviation

PCPSKW: skewness coefficient

PR_W1: probability of a wet day following a dry day

PR_W2: probability of a wet day following a wet day

PCPD: average number of days of precipitation in a month

TMPMX: mean daily maximum temperature for a month (^{o}C)

TMPSTDMX: st. deviation for daily max. temperature in month (^{o}C)

TMPMN: mean daily minimum temperature for a month (^{o}C)

TMPSTDMN: st. deviation for daily min. temperature in month (^{o}C)

Appendix Table 8 Statistical precipitation and temperature data (1985-2005) for Shambu station.

Description	Jan	Feb	Mar	Apr	May	Jun	Jul	Aug	Sep	Oct	Nov	Dec
PCP_MM	17	27	70	104	175	291	416	414	282	89	23	22
PCPSTD	0.8	1.5	2.6	4.24	4.92	7.98	9.64	7.7	5.27	3.2	1.4	1.0
PCPSKW	1.9	2.8	1.9	1.73	0.7	1.15	0.53	0.74	-0.15	2.3	3.5	1.7
PR_W1	0.2	0.5	0.6	0.57	0.47	0.73	0.83	0.71	0.68	0.4	0.3	0.2
PR_W2	0.4	0.4	0.7	0.7	0.86	0.73	0.63	0.62	0.57	0.5	0.4	0.4
PCPD	3.4	4.1	8.3	9.27	13.1	16.3	15.3	16.2	13.1	9.1	4.8	3.6
TMPMX	27	27	28	27.4	27.6	26.3	26	25.4	25.7	28	26	27
TMPSTDMX	1.8	1.9	1.7	2.39	2.03	1.81	2.49	2.21	1.96	2.2	1.7	2.1
TMPMN	7.1	7.7	8.0	7.2	6.5	6.4	5.8	5.9	6.2	6.3	6.9	7.6
TMPSTDMN	1.2	1.4	1.4	1.94	2.14	1.97	2.04	1.95	1.83	1.7	1.5	1.5

Where:

PCP_MM: average monthly precipitation (mm)

PCPSTD: standard deviation

PCPSKW: skewness coefficient

PR_W1: probability of a wet day following a dry day

PR_W2: probability of a wet day following a wet day

PCPD: average number of days of precipitation in a month

TMPMX: mean daily maximum temperature for a month (^oC)

TMPSTDMX: st. deviation for daily max. temperature in month (^oC)

TMPMN: mean daily minimum temperature for a month (^oC)

TMPSTDMN: st. deviation for daily min. temperature in month (^oC)

Appendix Table 9 Statistical precipitation and temperature data (1985-2005) for Hareto station.

Description	Jan	Feb	Mar	Apr	May	Jun	Jul	Aug	Sep	Oct	Nov	Dec
PCP_MM	15	29	64	122	173	250	413	415	280	106	37	27
PCPSTD	0.8	1.5	2.4	4.75	5.54	7.44	8.86	8.04	6.43	4.29	2.5	1.3
PCPSKW	2.0	2.3	1.8	1.42	1.5	1.38	0.6	0.8	0.58	1.97	3.7	2.5
PR_W1	0.2	0.5	0.6	0.54	0.45	0.7	0.78	0.67	0.65	0.34	0.3	0.2
PR_W2	0.4	0.4	0.7	0.69	0.86	0.72	0.63	0.61	0.57	0.53	0.4	0.4
PCPD	3.2	4.1	8.2	9.09	13.1	16.1	15.1	16.1	13.1	9.09	4.8	3.5
TMPMX	27	27	28	27.2	27.4	26.1	26.2	25.5	25.6	27.3	26	27
TMPSTDMX	1.8	1.9	1.6	2.37	2.01	1.79	2.51	2.22	1.94	2.11	1.7	2.1
TMPMN	7.3	7.9	8.4	7.6	6.9	6.7	5.9	6.0	6.3	6.5	7.2	7.8
TMPSTDMN	1.2	1.4	1.4	1.9	2.1	1.88	1.94	1.94	1.79	1.64	1.5	1.4

Where:

PCP_MM: average monthly precipitation (mm)

PCPSTD: standard deviation

PCPSKW: skewness coefficient

PR_W1: probability of a wet day following a dry day

PR_W2: probability of a wet day following a wet day

PCPD: average number of days of precipitation in a month

TMPMX: mean daily maximum temperature for a month (^oC)

TMPSTDMX: st. deviation for daily max. temperature in month (^oC)

TMPMN: mean daily minimum temperature for a month (^oC)

TMPSTDMN: st. deviation for daily min. temperature in month (^oC)

Appendix Table 10 Statistical precipitation and temperature data (1985-2005) for Gabate station.

Description	Jan	Feb	Mar	Apr	May	Jun	Jul	Aug	Sep	Oct	Nov	Dec
PCP_MM	13	24	67	132	171	278	418	424	250	64	26	25
PCPSTD	0.7	1.2	2.4	4.89	4.97	7.87	8.85	8.12	5.98	2.9	1.6	1.3
PCPSKW	2.2	1.6	2.0	1.5	1.18	1.29	0.48	0.63	0.1	2.4	3.4	2.6
PR_W1	0.2	0.5	0.6	0.54	0.45	0.7	0.76	0.66	0.66	0.3	0.3	0.2
PR_W2	0.4	0.4	0.7	0.69	0.86	0.73	0.62	0.61	0.56	0.5	0.4	0.4
PCPD	3.1	4.1	8.1	9.05	13.1	16.1	15.1	16.1	13.1	9	4.8	3.5
TMPMX	28	29	29	29.2	29.1	26.6	24.1	22.5	24.1	26	26	26
TMPSTDMX	1.2	1.2	1.2	1.44	1.49	1.27	0.93	0.7	0.9	0.9	0.6	0.8
TMPMN	7.9	8	9.1	10	9.9	9.3	9.3	8.5	9.1	7.4	7.1	6.3
TMPSTDMN	1.0	0.9	1.0	0.83	0.76	0.61	0.65	0.68	0.6	1.0	1.1	1.5

Where:

PCP_MM: average monthly precipitation (mm)

PCPSTD: standard deviation

PCPSKW: skewness coefficient

PR_W1: probability of a wet day following a dry day

PR_W2: probability of a wet day following a wet day

PCPD: average number of days of precipitation in a month

TMPMX: mean daily maximum temperature for a month (°C)

TMPSTDMX: st. deviation for daily max. temperature in month (°C)

TMPMN: mean daily minimum temperature for a month (°C)

TMPSTDMN: st. deviation for daily min. temperature in month (°C)

Appendix Table 11 Statistical precipitation and temperature data (1985-2005) for Kombolcha station.

Description	Jan	Feb	Mar	Apr	May	Jun	Jul	Aug	Sep	Oct	Nov	Dec
PCP_MM	12.2	16.1	65.4	95.2	179	259.6	407.1	388.5	269.0	107.7	32.4	26.3
PCPSTD	0.61	0.84	2.57	3.97	5.52	7.54	9.59	7.48	5.87	3.83	2.27	1.29
PCPSKW	1.53	1.67	1.72	1.53	1.14	1.22	0.62	0.87	0.43	2.01	4.22	2.76
PR_W1	0.19	0.45	0.57	0.50	0.41	0.62	0.67	0.58	0.57	0.30	0.23	0.17
PR_W2	0.40	0.36	0.75	0.70	0.88	0.73	0.63	0.62	0.57	0.53	0.36	0.38
PCPD	2.95	3.82	7.95	8.82	12.77	15.73	14.77	15.73	12.77	8.73	4.45	3.23
TMPMX	28.7	29.4	29.7	29.5	29.3	26.9	24.6	22.9	24.5	26.4	26.6	26.7
TMPSTDMX	1.22	1.27	1.28	1.46	1.51	1.3	0.99	0.73	0.93	0.99	0.7	0.8
TMPMN	8.0	7.9	9.3	10.2	10.1	9.5	9.4	8.9	9.3	7.7	7.5	6.4
TMPSTDMN	0.99	0.92	0.94	0.81	0.75	0.59	0.63	0.63	0.58	0.93	1.04	1.43

Where:

PCP_MM: average monthly precipitation (mm)

PCPSTD: standard deviation

PCPSKW: skewness coefficient

PR_W1: probability of a wet day following a dry day

PR_W2: probability of a wet day following a wet day

PCPD: average number of days of precipitation in a month

TMPMX: mean daily maximum temperature for a month (^{o}C)

TMPSTDMX: st. deviation for daily max. temperature in month (^{o}C)

TMPMN: mean daily minimum temperature for a month (^{o}C)

TMPSTDMN: st. deviation for daily min. temperature in month (^{o}C)

Appendix Table 12 Input data for Markov model based on the TP from 1985-1995.

0.960875	0.027652	0.005672	0.000072	0.000306	0.005424
0.051695	0.923903	0.014357	0.000626	0.001304	0.008115
0.051250	0.002494	0.926989	0.015347	0.000807	0.003112
0.000715	0.000000	0.010166	0.977130	0.010470	0.001520
0.001339	0.001270	0.026974	0.006015	0.952139	0.012263
0.030936	0.017975	0.010727	0.015040	0.008747	0.916577
0.347877	0.220734	0.171171	0.063387	0.119460	0.077368

Appendix Table 13 Input data for Markov model based on the TP from 1995-2005.

0.975422	0.015670	0.004243	0.000056	0.000298	0.004311
0.053670	0.916445	0.017013	0.000820	0.001707	0.010344
0.060691	0.003298	0.916364	0.016441	0.001025	0.002181
0.000657	0.000000	0.005956	0.985184	0.006862	0.001341
0.001975	0.001872	0.039776	0.004860	0.946040	0.005477
0.031569	0.009070	0.012470	0.016462	0.012139	0.918289
0.439590	0.168649	0.144586	0.095614	0.081014	0.070545

Appendix Table 14 Input data for Markov model based on the TP from 1985-2005.

0.994654	0.000638	0.002469	0.000431	0.000188	0.001620
0.023593	0.969860	0.001519	0.000313	0.000658	0.004058
0.027085	0.001247	0.964210	0.006944	0.000411	0.000103
0.000889	0.000000	0.005280	0.991777	0.001293	0.000760
0.000706	0.000629	0.012640	0.011365	0.968445	0.006215
0.015468	0.007373	0.005363	0.009135	0.004373	0.958288
0.347877	0.220734	0.171171	0.063387	0.119461	0.077370

Appendix B

Figures

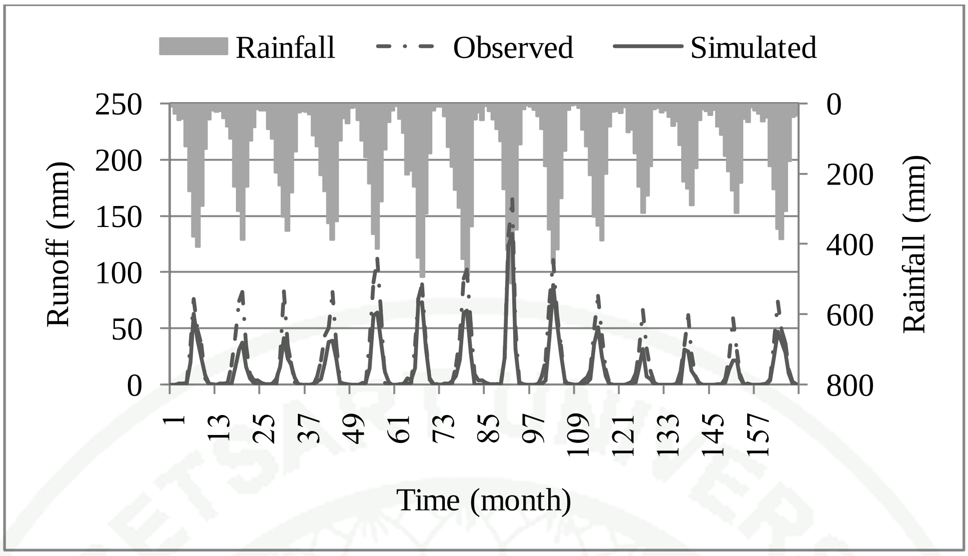

Appendix Figure 1 Simulated and observed average monthly runoff volumes under land use scenario A.

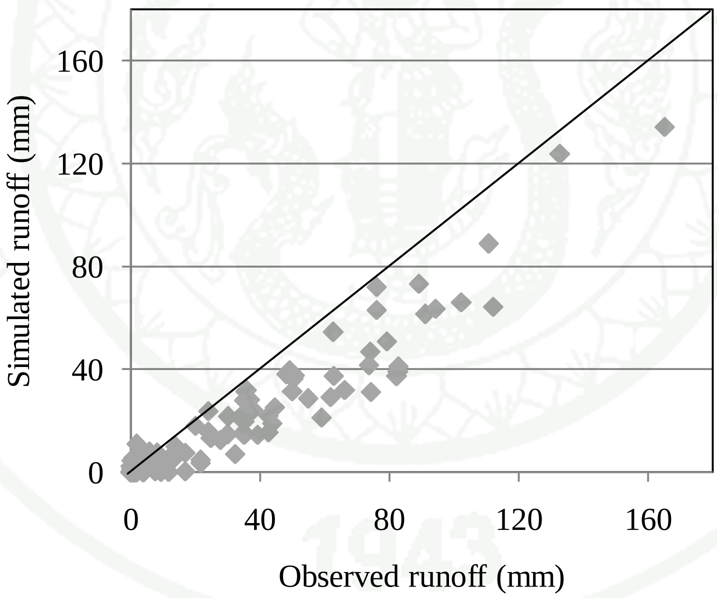

Appendix Figure 2 Scatter plot of the simulated vs observed average monthly runoff volumes under land use scenario A.

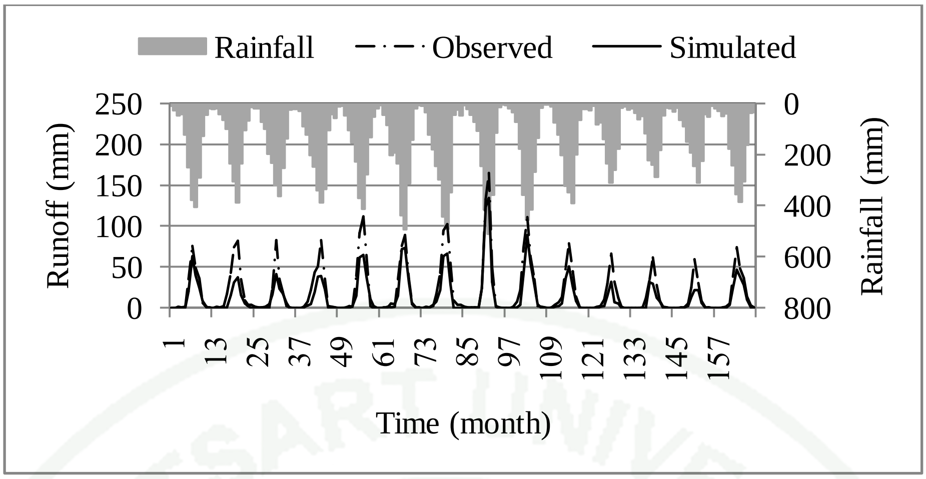

Appendix Figure 3 Simulated and observed average monthly runoff volumes under land use scenario B.

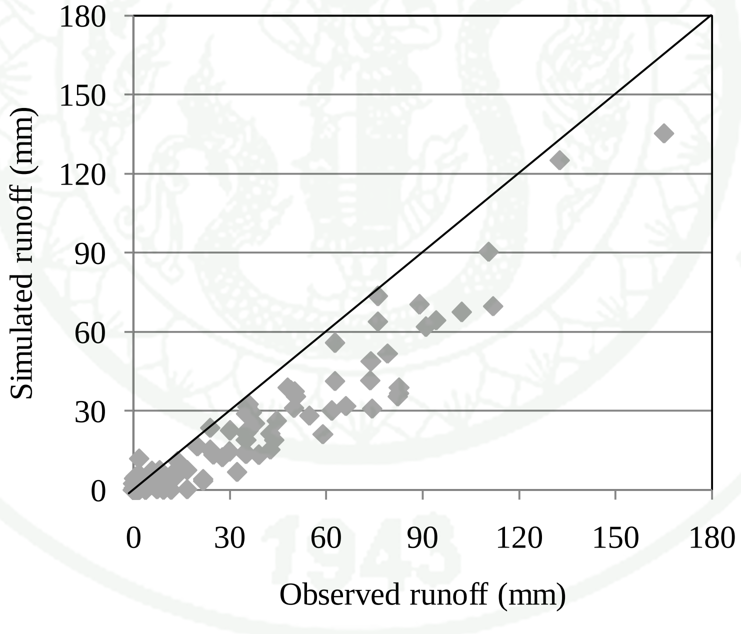

Appendix Figure 4 Scatter plot of the simulated vs observed average monthly runoff volumes under land use scenario B.

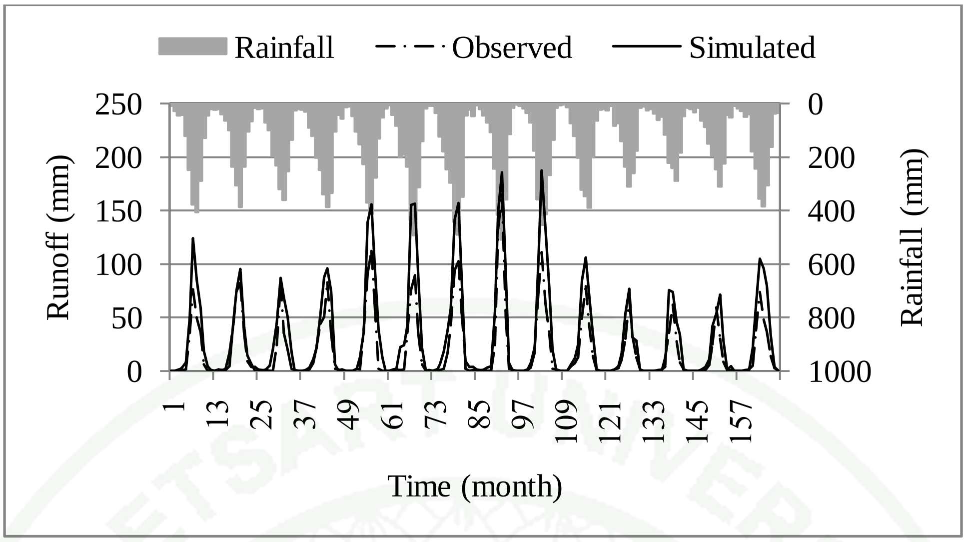

Appendix Figure 5 Simulated and observed average monthly runoff volumes under land use scenario C.

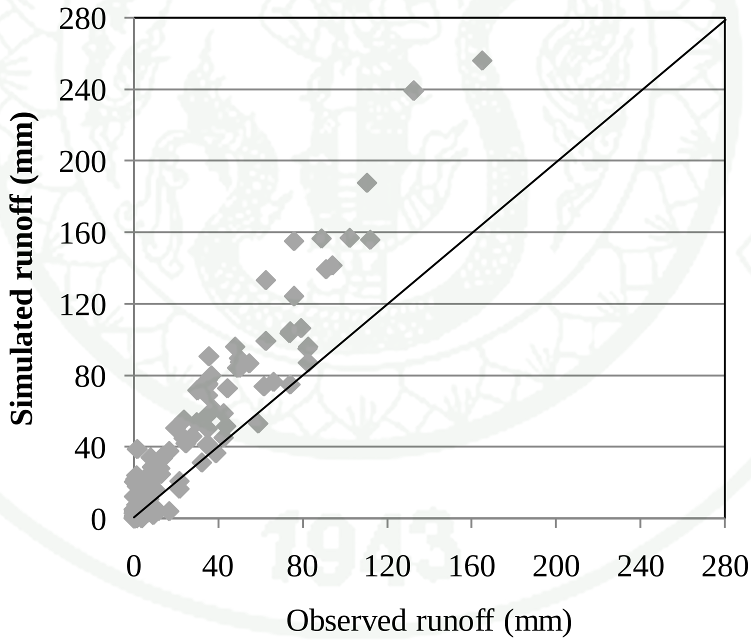

Appendix Figure 6 Scatter plot of the simulated vs observed average monthly runoff volumes under land use scenario C.

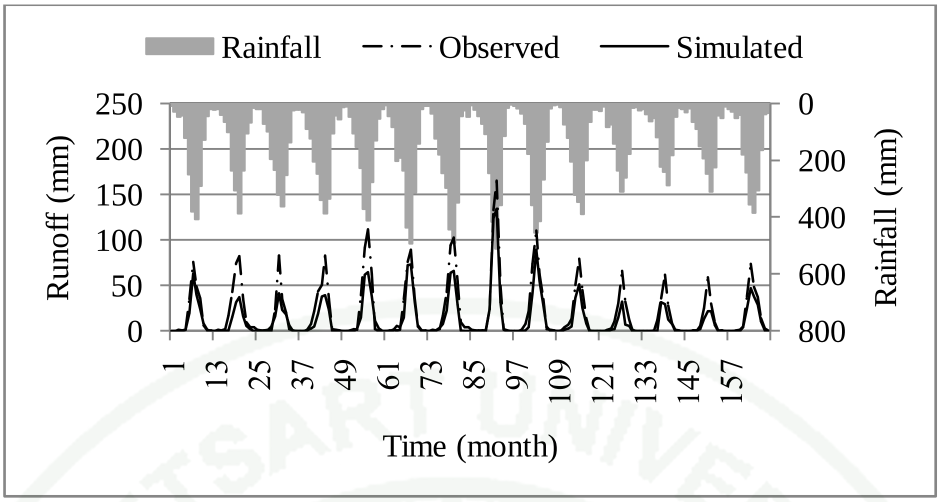

Appendix Figure 7 Simulated and observed average monthly runoff volumes under land use scenario D.

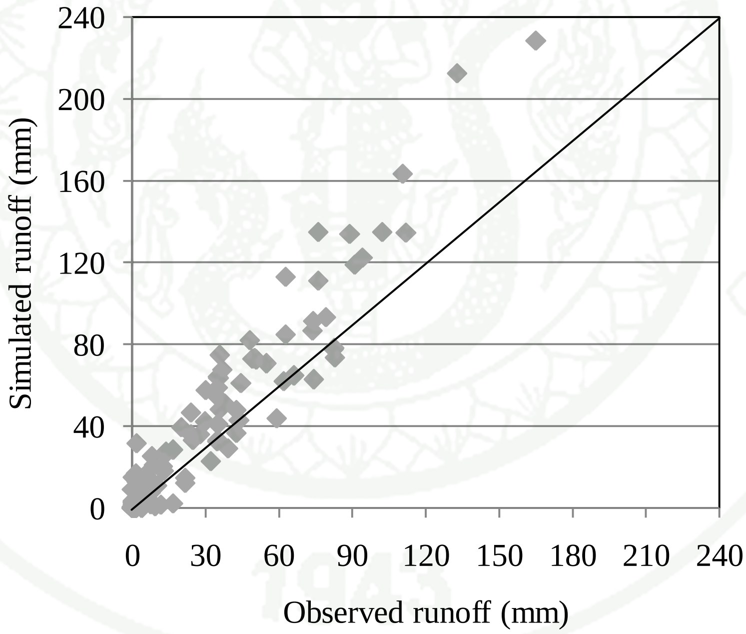

Appendix Figure 8 Scatter plot of the simulated vs observed average monthly runoff volumes under land use scenario D.

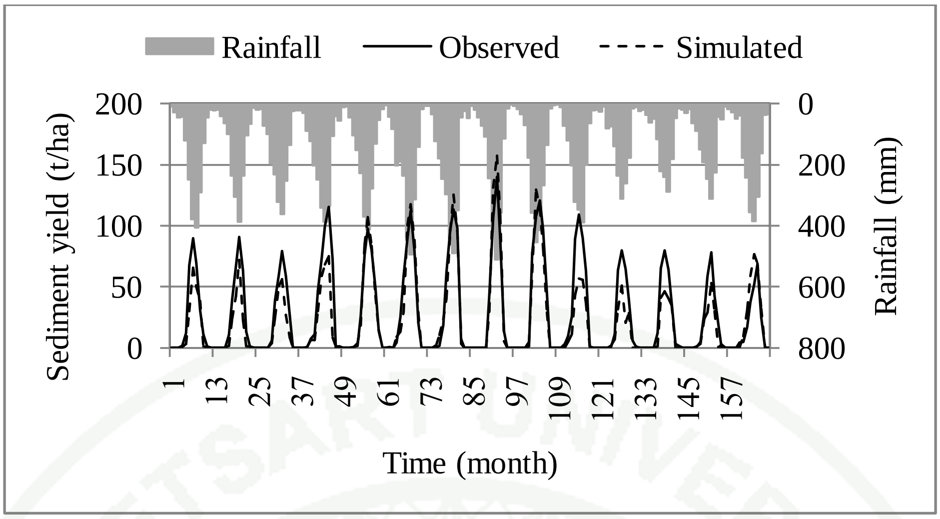

Appendix Figure 9 Simulated and observed average monthly sediment yields under land use scenario A.

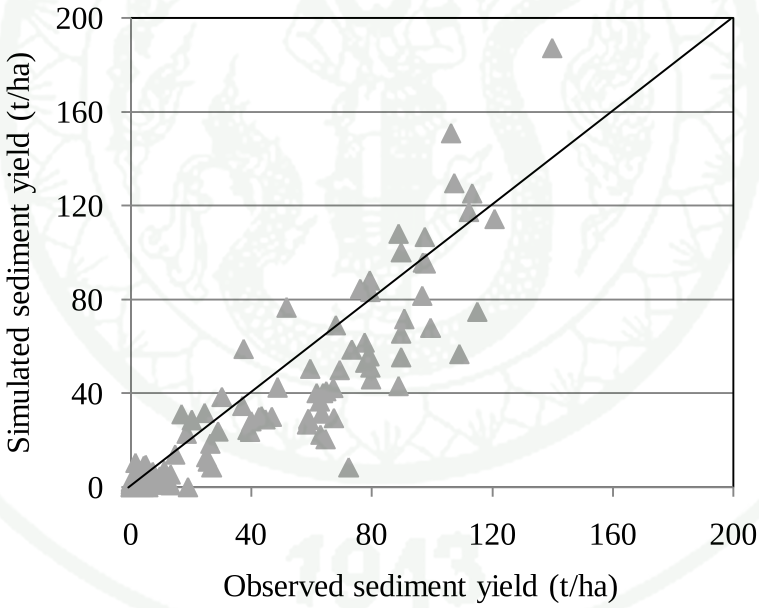

Appendix Figure 10 Scatter plot of the simulated vs observed average monthly sediment yields under land use scenario A.

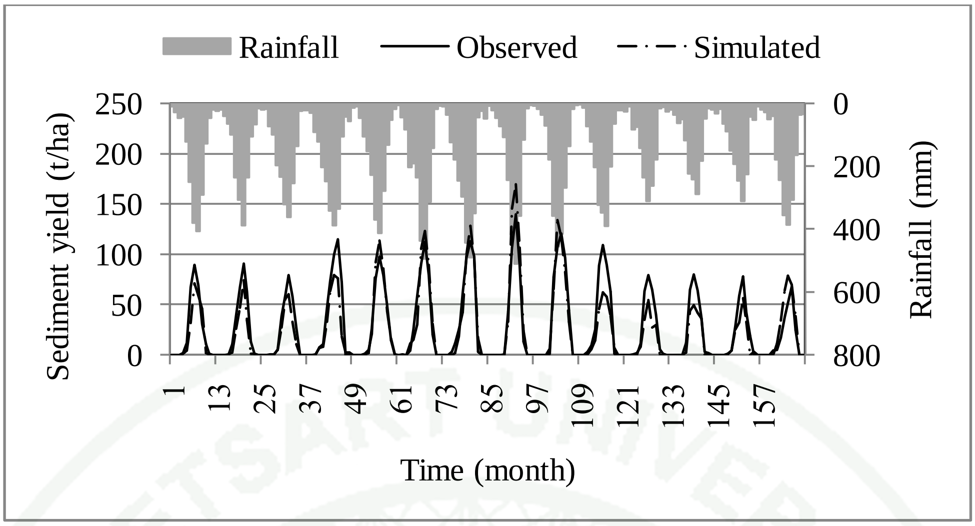

Appendix Figure 11 Simulated and observed average monthly sediment yields under land use scenario B.

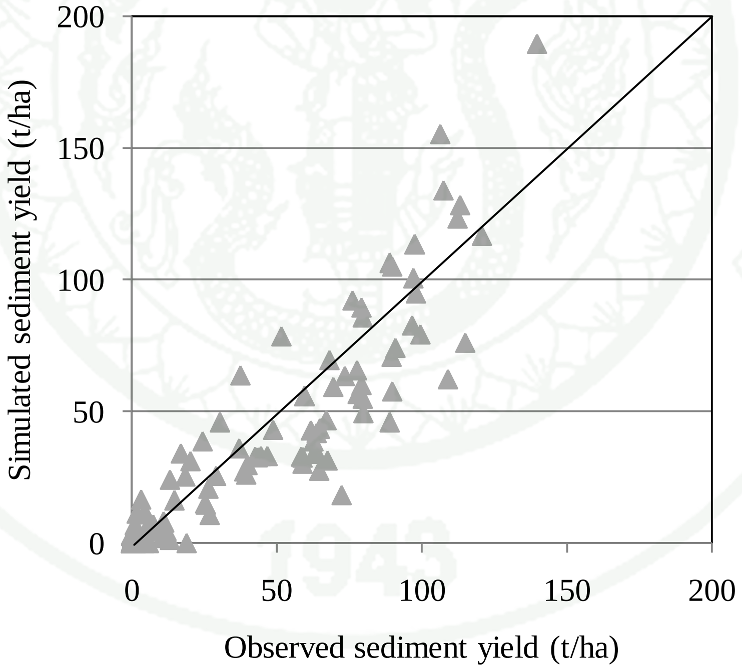

Appendix Figure 12 Scatter plot of the simulated and observed average monthly sediment yields under land use scenario B.

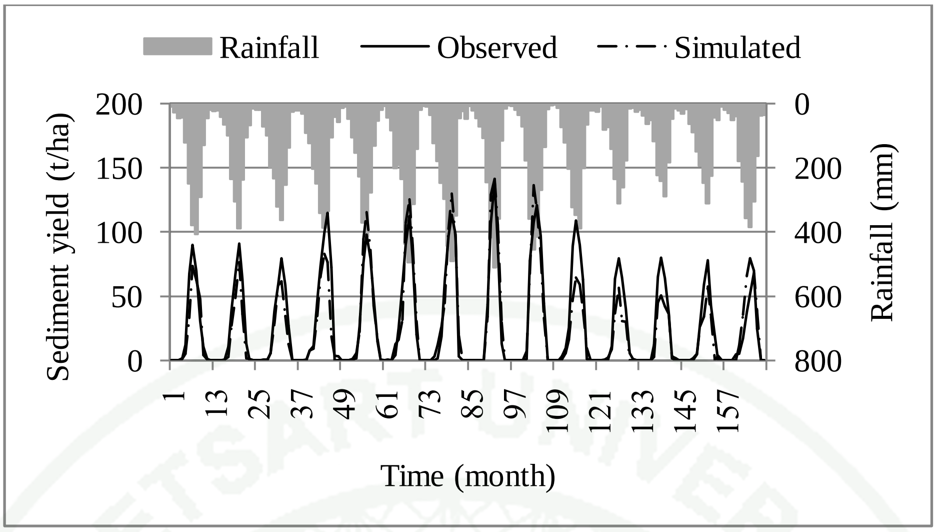

Appendix Figure 13 Simulated and observed average monthly sediment yields under land use scenario C.

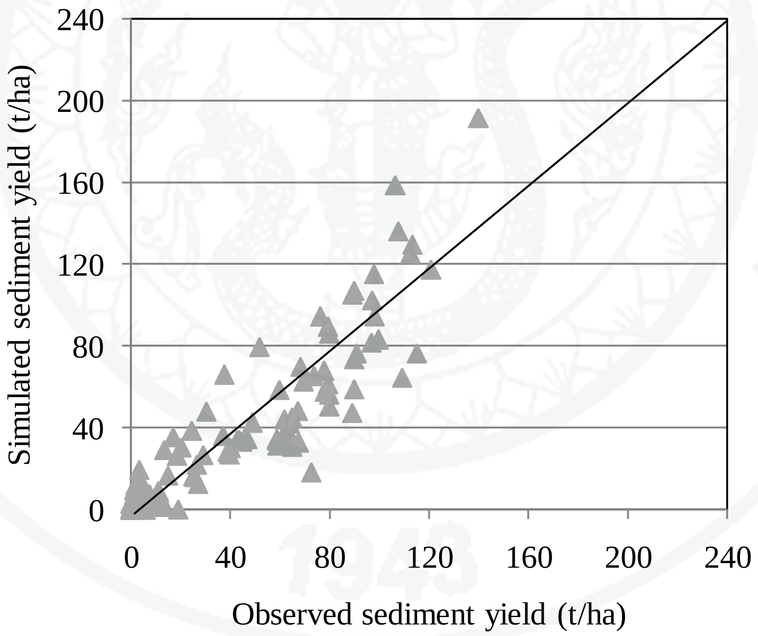

Appendix Figure 14 Scatter plot of the simulated vs observed average monthly sediment yields under land use scenario C.

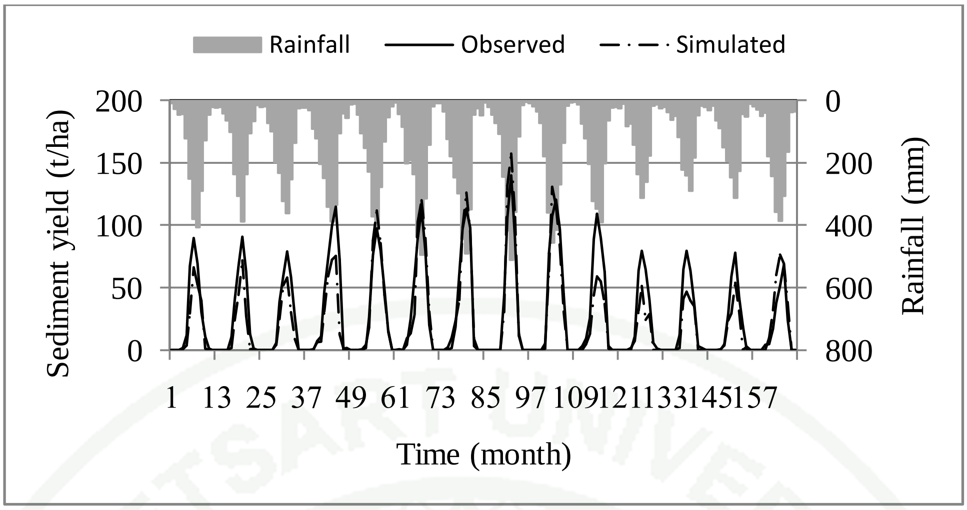

Appendix Figure 15 Simulated and observed average monthly sediment yields under land use scenario D.

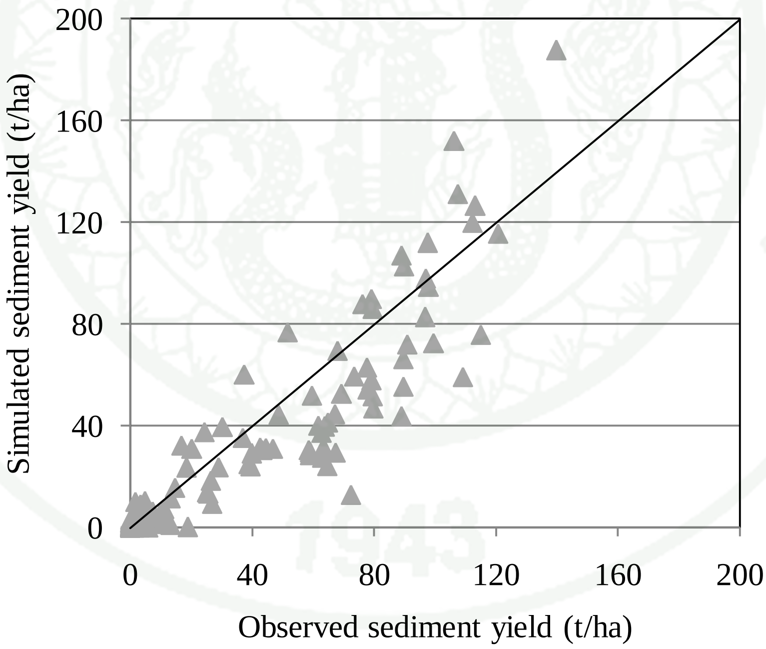

Appendix Figure 16 Scatter plot of the simulated vs observed average monthly sediment yields under land use scenario D.

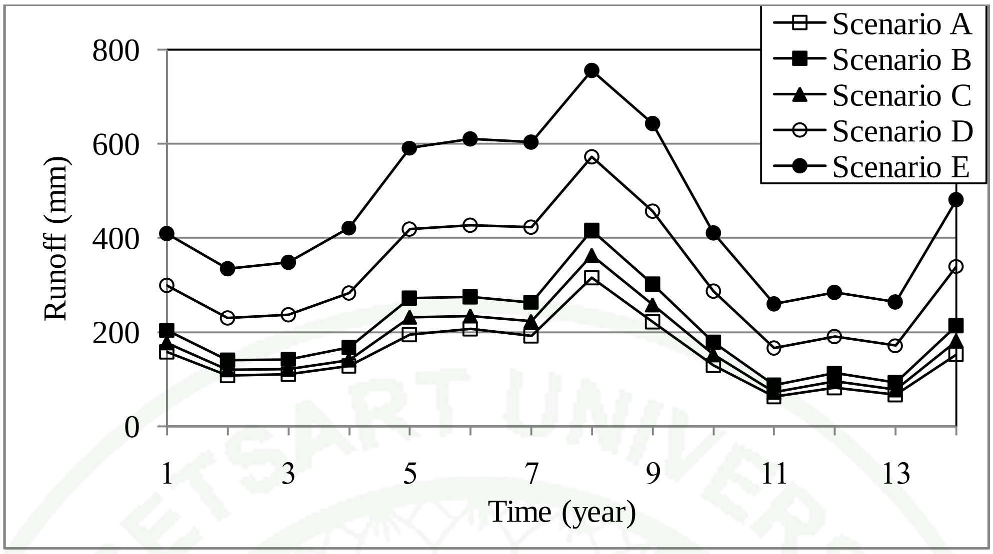

Appendix Figure 17 Simulated annual runoff volumes under various land use scenarios.

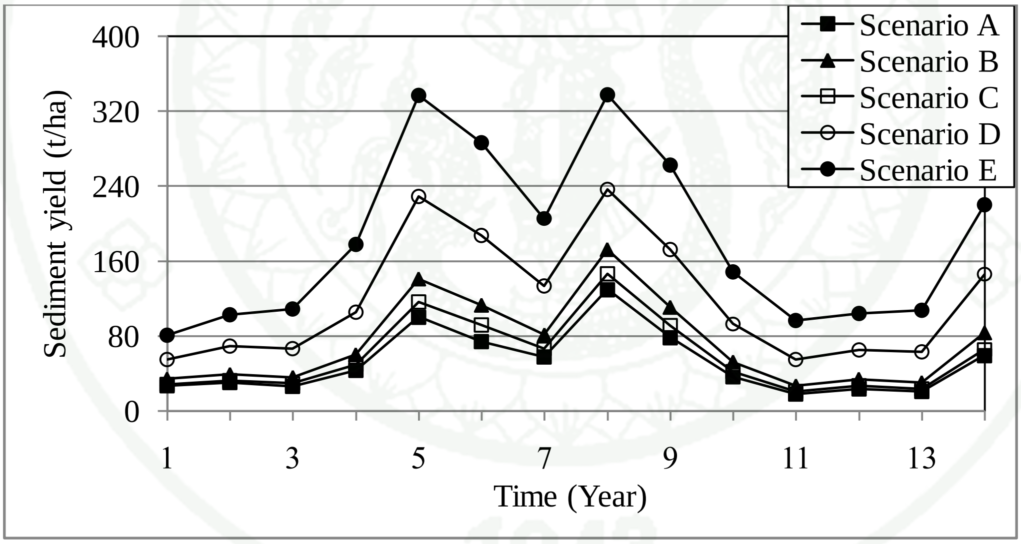

Appendix Figure 18 Simulated annual sediment yields under various land use scenarios.

CURRICULUM VITAE

NAME : Mr Abdi Boru Ayana

BIRT DATE : June 12, 1969

BIRTH PLACE : Wallagga, Ethiopia

EDUCATION :

YEAR	INISTITUTE	DEGREE/DIPILOMA
1991	Alemaya University of Agriculture	B.Sc. (Agricultural Engineering)
2000	Haryana Agricultural University	M.Sc. (Post Harvest Technology)

POSITION/TITLE : Soil and Water Conservation Expert

WORK PLACE : Oromia Bureau of Agriculture, Ethiopia

SCHOLARSHIP/AWARDS : Rural Capacity Building Project, Ministry of Agriculture, Ethiopia